

**The differential effect of fructose on metabolic risk factors**

By

**Kyla M. Walsh**

A thesis submitted to the School of Graduate Studies in partial fulfilment of the requirements for  
the degree of

Master of Science

Department of Biochemistry

Faculty of Science

Memorial University of Newfoundland

January 2<sup>nd</sup>, 2024

St. John's, Newfoundland and Labrador

## Abstract

High fructose intakes have previously been associated with dysregulation of carbohydrate and lipid metabolism within the liver. This dysregulation of metabolism can produce a distinctive phenotype that includes fatty liver, insulin resistance and dysregulated lipid transport. Although the association between fructose consumption and disease has yet to be elucidated, this phenotype is associated with metabolic-related diseases such as obesity, type 2 diabetes mellitus, and non-alcoholic fatty liver disease. Newly emerging research suggests that previous long-term exposure to fructose may result in metabolic adaptations to create a new steady state, thereby providing a protective effect against bolus doses of fructose. The objective of this study was to determine if previous exposure to fructose can alleviate symptoms of metabolic distress such as weight gain, high liver weight and blood metabolomics. To achieve this objective, adult sex-balanced C57Bl/6J mice consumed a high-fat, high-sugar, hypercaloric diet consisting of either 0%, 10%, or 20% of total calories from fructose. In the preliminary study, the 20% fructose group returned to chow diet after 2-weeks to examine if metabolic adaptations are possible after a short time interval. Prior to necropsy, 0.5 g/kg U-C<sup>13</sup>-fructose (stable isotope) and 0.5 g/kg glucose were orally gavaged. After 30 minutes, the mice were sacrificed by heart puncture and all samples were collected and flash frozen. Previous fructose exposure was associated with a higher enrichment of glucose from <sup>13</sup>C-fructose, specifically in females. Other sex-related differences were also present including liver weight, fatty acid profile, and triacylglycerol content, suggesting that oral fructose alters metabolic outcomes in a sex-dependent manner in mice.

## Acknowledgements

I would like to thank my co-supervisors Dr. Scott Harding and Dr. Robert Bertolo as well as my committee member Dr. Janet Brunton for their ongoing support and guidance throughout both my graduate and undergraduate degrees.

Additionally, I would like to extend my appreciation to a few of the many individuals that took time out of their busy schedules to help me throughout this project. Julia White and Dalshini Kirupanathan – thank you for your tremendous advice and support that always led me in the right direction. Hannah Murphy and Keisha Roche – thank you for the countless hours you spent prepping and running samples with me and for always making the lab a fun place to be. Zack Clancy – thank you for keeping me sane and supporting me throughout both of our degrees together. Melissa MacKay – as my roommate and “bubble buddy”, thank you for stepping in to help complete necropsies so that I could continue my project while staying within the current pandemic restrictions. In addition, thank you to all members of the Harding Lab and the Brunton/Bertolo Lab who extended their knowledge and expertise to me throughout the entirety of my degree.

Finally, to my parents, sister, dogs, roommates, and friends who provided the emotional support required to finish a challenging degree with the unparalleled added stress of a pandemic – I truly could not have done this without all of you.

# Table of Contents

Abstract.....	ii
Table of Contents.....	iv
List of Tables.....	viii
List of Figures.....	ix
<b>1. Introduction.....</b>	<b>1</b>
1.1. Fructose and Fructose Consumption.....	1
1.1.1. Sugar Consumption and the Western Diet.....	1
1.1.2. Free Sugars.....	2
1.1.2.1. Monosaccharides: Fructose and Glucose.....	2
1.1.2.2. Sucrose and HFCS.....	3
1.2. Fructose Metabolism.....	4
1.2.1. Fructose is Converted to Glycolytic Intermediates.....	4
1.2.2. Transport into the Cell.....	8
1.2.3. Fructose Metabolism in the Gut.....	9
1.2.4. Carbohydrate Metabolism in the Liver.....	10
1.2.4.1. Glucose Metabolism in the Liver.....	10
1.2.4.2. Fructose Metabolism in the Liver.....	12
1.2.5. Fructose and Lipid Handling.....	13
1.2.6. Fructose as a Factor in Metabolic Diseases.....	14
1.2.6.1. Fructose and CVD.....	15
1.2.6.1. Fructose and NAFLD.....	16

1.2.6.2.	Fructose and T2DM .....	17
1.3.	Rationale, Hypothesis and Objectives .....	18
<b>2.</b>	<b>Materials and Methods.....</b>	<b>21</b>
2.1.	Animal Ordering and Housing.....	21
2.2.	Diet and Dietary Treatment Groups.....	22
2.2.1.	Dietary Treatment Groups .....	23
2.2.2.	Dietary Intakes .....	24
2.2.3.	Body Weight Measurements.....	24
2.3.	Isotope Gavage and Necropsy Preparation.....	25
2.4.	Necropsy .....	27
2.5.	Laboratory Analytical Procedures .....	28
2.5.2.	Glucose Concentrations – Glucose Oxidase.....	28
2.5.3.	Glucose and Fructose Concentration and Isotopic Enrichment by Gas Chromatography – Mass Spectrometry .....	30
2.5.4.	Lipid Analysis.....	32
2.5.4.1.	Fatty Acid Profile and Quantification by Gas Chromatography – Flame Ionization Detection.....	32
2.5.4.2.	Cholesterol Lipoprotein Quantification by Spectrophotometric Assay.....	34
2.5.4.3.	triacylglycerol Quantification by Spectrophotometric Assay.....	35
2.5.4.4.	High Density Lipoprotein Quantification by Spectrophotometric Assay.....	36
2.5.5.	Cardiac Histology .....	38
2.6.	Statistics .....	38

<b>3. Results .....</b>	<b>40</b>
3.1. Fructose Energy Study 1 .....	40
3.1.1. Effect of Diet on Body Weight Gain .....	40
3.1.2. Effect of Diet on Liver Weight .....	42
3.1.3. Validation of Glucometer by Glucose Oxidase Method.....	45
3.1.1. Effect of Diet on Blood Glucose Concentrations .....	47
3.1.2. Effect of Diet on Lipid Quantification and Profile .....	49
3.1.2.1. Fatty Acid Profile.....	49
3.1.2.2. Cholesterol Lipoprotein Quantification .....	54
3.1.2.3. Triacylglycerol Quantification.....	56
3.1.2.4. HDL Cholesterol Quantification.....	58
3.1.2.5. Non-HDL Cholesterol Quantification.....	60
3.2. Fructose Energy Study 2.....	62
3.2.1. Effect of Diet on Dietary Intake.....	62
3.2.2. Effect of Diet on Body Weight Gain .....	64
3.2.3. Effect of Added Sugars on Glucose and Fructose Metabolism .....	66
3.2.3.1. Glucometer.....	66
3.2.3.2. Glucose Oxidase .....	68
3.2.3.3. Isotopic Enrichment by GC-MS .....	70
3.2.4. Effect of Diet on Lipid Profile .....	74
3.2.4.1. Effect of Diet on Liver Weight .....	74
3.2.4.2. Fatty Acid Profile.....	77
3.2.4.3. Fatty Acid Quantification .....	80

3.2.4.4.	Triacylglycerol Quantification.....	85
3.2.4.5.	Cholesterol Lipoprotein Quantification .....	87
3.2.4.6.	HDL Quantification .....	89
3.2.4.7.	Non-HDL Quantification.....	91
3.2.5.	Effect of Diet on Cardiac Pathology.....	93
<b>4.</b>	<b>Discussion .....</b>	<b>95</b>
4.1.	The Effect Fructose on Sugar Metabolism .....	95
4.2.	The Effect of Fructose on Blood Glucose Concentrations .....	96
4.3.	The Effect of Fructose on Body Weight and Liver Weight Gain.....	98
4.4.	The Effect of Fructose on Total Lipid Quantification and Profile.....	99
4.5.	The Effect of Fructose on Plasma Cholesterol Quantification and Profile.....	100
4.6.	The Effect of Fructose on Cardiac Pathology and Atherosclerosis .....	100
4.7.	Conclusion and Future Directions .....	101
<b>5.</b>	<b>References.....</b>	<b>103</b>
<b>6.</b>	<b>Appendices.....</b>	<b>110</b>

## **List of Tables**

Table 3.1 Quantification of fatty acids in liver tissue in FE2 mice .....	81
Table 3.2 Fatty acid percent composition of RBC membranes of FE2 mice .....	83

## List of Figures

Figure 1.1 A schematic showing the Hawthorn and Fischer Projections of (A) Glucose, (B) Galactose, and (C) Fructose.....	2
Figure 1.2 Schematic indicating the major metabolic pathways of carbohydrates and flux of dietary glucose and fructose (Sun & Empie, 2012) .....	7
Figure 1.3 Glucose is converted to glucose-6-phosphate .....	11
Figure 1.4 A schematic showing the fate of glucose in the liver (Adeva-Andany et al., 2016)...	11
Figure 2.1 Visual representation of the gavage and necropsy procedure .....	26
Figure 3.1 Effect of sex by diet on body weight gain – FE1 .....	41
Figure 3.2 Effect of diet on liver weight of FE1 mice .....	43
Figure 3.3 Effect of diet on adjusted liver weight of FE1 mice.....	44
Figure 3.4 Validation of glucometer method by glucose oxidase method .....	46
Figure 3.5 Effect of diet on blood glucose by glucose oxidase method in FE1 mice.....	48
Figure 3.6 Effect of diet on liver lipid profile of FE1 mice.....	<b>Error! Bookmark not defined.</b>
Figure 3.7 Effect of diet on RBC lipid profile of FE1 mice .....	<b>Error! Bookmark not defined.</b>
Figure 3.8 Effect of diet on heart tissue lipid profile of FE1 mice	<b>Error! Bookmark not defined.</b>
Figure 3.9 Effect of diet on mean total plasma cholesterol of FE1 mice.....	55
Figure 3.10 Effect of diet on mean plasma TAG concentrations of FE1 mice.....	57
Figure 3.11 Effect of diet on mean plasma non-HDL cholesterol concentrations of FE1 mice...	61
Figure 3.12 Effect of sex by diet on dietary intake in FE2 mice .....	63
Figure 3.13 Effect of sex by diet on body weight gain in FE2 mice .....	65
Figure 3.14 Effect of diet on blood glucose concentration at various time points in FE2 mice...	67

Figure 3.15 Effect of sex by diet on blood glucose concentrations by glucometer method at various time points in FE2 mice .....	<b>Error! Bookmark not defined.</b>
Figure 3.16 Effect of diet on blood glucose by glucose oxidase method in FE2 mice.....	69
Figure 3.17 Effect of diet on mean fructose TTR for various ions at T = 30 minutes in FE2 mice .....	72
Figure 3.18 Effect of diet on mean glucose TTR for various ions at T = 30 minutes in FE2 mice .....	73
Figure 3.19 Effect of diet on liver weight of FE2 mice .....	75
Figure 3.20 Effect of diet on adjusted liver weight of FE2 mice.....	76
Figure 3.21 Effect of diet on RBC lipid profile of FE2 mice .....	78
Figure 3.22 Effect of diet on liver lipid profile of FE2 mice .....	79
Figure 3.23 Effect of diet on mean plasma TAG concentrations of FE2 mice.....	86
Figure 3.24 Effect of diet on mean total plasma cholesterol of FE2 mice.....	88
Figure 3.25 Effect of diet on mean plasma c-HDL cholesterol concentrations of FE2 mice .....	90
Figure 3.26 Effect of diet on mean plasma non-HDL cholesterol concentrations of FE2 mice...	92
Figure 3.27 Effect of diet on cardiac pathology of FE2 mice.....	94

## **List of Appendices**

Appendix I: Composition of standard chow diet (NC1770956)

Appendix II: Composition of mineral mix #210050

Appendix III: Composition of vitamin mix #310081

Appendix IV: Composition of 0% fructose diet

Appendix V: Composition of 10% fructose diet

Appendix VI: Composition of 20% fructose diet

Appendix VII: Average food consumption per day by sex and dietary treatment in FE1

Appendix VIII: Glucose standard curve formed by plotting known glucose standards against corrected absorbance readings at 340 nm.

Appendix IX: Cholesterol standard curve formed by plotting known cholesterol standards against corrected absorbance readings at 505 nm.

Appendix X: triacylglycerol standard curve formed by plotting known triacylglycerol standards against corrected absorbance readings at 505 nm.

Appendix XI: HDL standard curve formed by plotting known HDL standards against corrected absorbance readings at 600 nm.

Appendix XII: Additional data demonstrating sex differences

Appendix XIII: Isotopomer analysis of fragments formed by carbon-carbon bond cleavage of D-glucose-MOA and D-fructose-MOA as demonstrated by Wahjudi et al.

Appendix XIV: Mass spectra fragmentation pattern of (A) D-glucose-MOA and (B) D-fructose-MOA as demonstrated by Wahjudi et al.

## List of Abbreviations

ANOVA	Analysis of variance
ATP	Adenosine triphosphate
BW	Body weight
CCHS	Canadian Community Health Survey
CV	Coefficient of variation
CVD	Cardiovascular disease
DHAP	Dihydroxyacetone phosphate
DIO	Diet induced obesity
DNL	<i>De novo</i> lipogenesis
F-1-P	Fructose-1-phosphate
F-6-P	Fructose-6-phosphate
FA	Fatty acid
FAMEs	Fatty acid methyl ester
FE1	Fructose energy study 1
FE2	Fructose energy study 2
G-3-P	Glucose-3-phosphate
G-6-P	Glucose-6-phosphate
GC-FID	Gas chromatography flame-ionization detection
GC-MS	Gas chromatography mass spectrometry
GLUT2	Glucose transporter 2
GLUT4	Glucose transporter 4
GLUT5	Glucose transporter 5

HDL	High density lipoprotein
HFCS	High fructose corn syrup
HP	Heart puncture
IV	Intravenous
LDL	Low density lipoprotein
MUFAs	Monounsaturated fatty acids
n-3 PUFAs	Omega-3 polyunsaturated fatty acids
n-6 PUFAs	Omega-6 polyunsaturated fatty acids
MOX	Methoxylamine hydrochloride
NAFL	Non-alcoholic fatty liver
NAFLD	Non-alcoholic fatty liver disease
NASH	Non-alcoholic steatohepatitis
PFK-1	Phosphofructokinase-1
PUFAs	Polyunsaturated fatty acids
RBCs	Red blood cells
SFAs	Saturated fatty acids
SGLT-1	Sodium-glucose transport protein-1
TAG	<b>Triacylglycerol</b>
TCA	Tricarboxylic acid
TTR	Tracer/tracee ratio
T2DM	Type 2 Diabetes Mellitus
VLDL	Very low density lipoprotein

# 1. Introduction

## 1.1. Fructose and Fructose Consumption

### 1.1.1. Sugar Consumption and the Western Diet

In North America, an obesity epidemic is occurring due to the combination of poor dietary patterns and lack of exercise. Commonly referred to as the “Western diet”, these dietary patterns are characterized by high intakes of saturated fats, processed meats, refined grains, alcohol, salt, refined sugar and high fructose corn syrup (HFCS), and low intakes of fruits and vegetables (Bray et al., 2004; Brisbois et al., 2014; Marriott et al., 2009)

Historically, sugar was primarily consumed through natural sources, such as fruit and honey, but has since shifted towards highly processed refined forms derived from sugar cane or sugar beet (Bray et al., 2004). Several variations of these sugar sweeteners are currently heavily used within the food and beverage industry. Although glucose is consumed in the highest quantities, consumption of fructose has rapidly increased after its introduction into the food and beverage industry in the 1970s (White, 2008). In the last 30 years, worldwide dietary sugar consumption has continued to increase, far surpassing the recommended intake of 5% to a maximum of 10% of total calories per day. According to a cross-sectional study using data from the most recent Canadian Community Health Survey (CCHS) in 2015, older adolescents (14-18 years of age) evaluated to be in the highest quintile of sugar intakes consumed a staggering 38% of their daily caloric intake as sugar – and added sugar represented over half of this value at 52% (Chiavaroli et al., 2022). Today, the average North American consumes nearly 20% of their calories as sugar, and fructose comprises approximately half of these intakes – primarily as sucrose and HFCS (Marriott et al., 2009).

### 1.1.2. Free Sugars

The World Health Organization uses the term free sugars to describe all monosaccharides and disaccharides added to foods by the manufacturer, cook, or consumer, plus sugars naturally present in honey, syrups, and fruit juices (Geneva: World Health Organization, 2015).

Monosaccharides and disaccharides are two additional umbrella terms used in this definition that classify simple carbohydrates based on their structural formula.

#### 1.1.2.1. Monosaccharides: Fructose and Glucose

There are three monosaccharides commonly found in food: galactose, glucose, and fructose. All three of these monosaccharides share the same chemical formula ( $C_6H_{12}O_6$ ) but differ in structural formula.

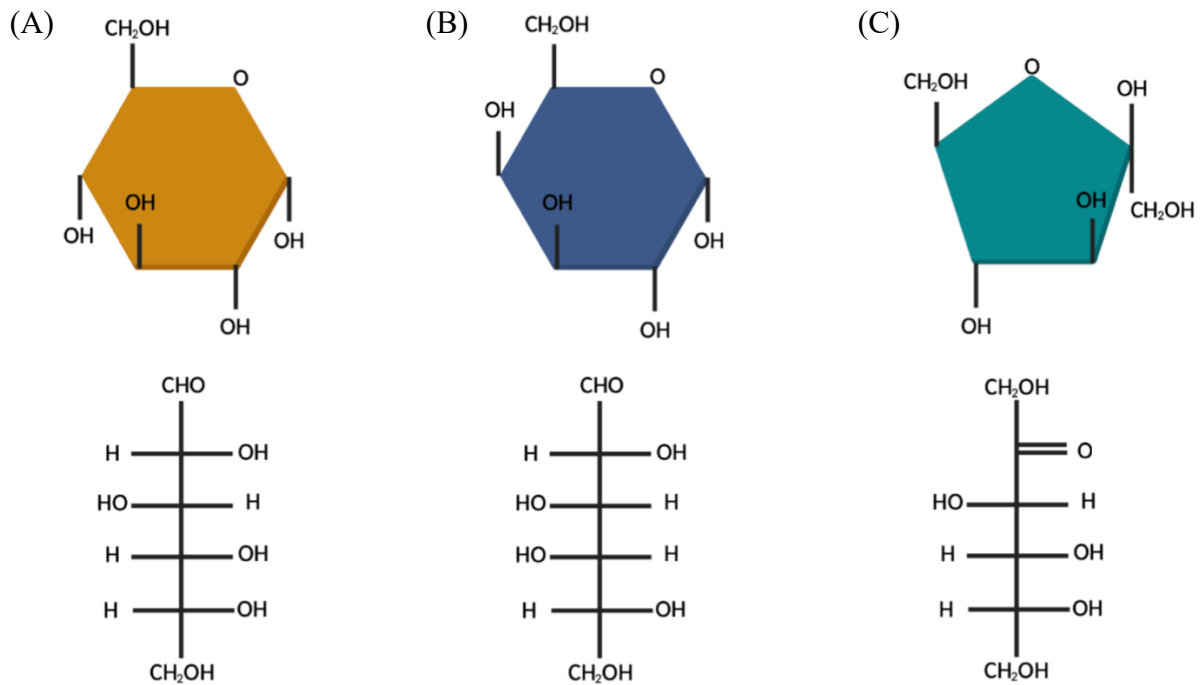


**Figure 1.1** A schematic showing the Haworth and Fischer Projections of (A) Glucose, (B) Galactose, and (C) Fructose.

Galactose is derived from lactose and is almost exclusively found in milk and dairy products. Therefore, due to a generally low consumption of milk in the adult population, galactose is consumed in low quantities in comparison to fructose and glucose. Fructose – often referred to as fruit sugar – is naturally found in sweet fruits, as well as honey and agave, and is unique from the other monosaccharides due to its ketohexose structure. Differing from glucose and galactose, fructose is a 6-carbon monosaccharide that forms a 5-membered ring; this ring-structure is unstable making fructose 8-10 times more reactive than glucose in the Maillard reaction (Gugliucci, 2017; Suárez et al., 1989). Due to this instability, no natural sources are exclusively comprised of fructose; honey is the most abundant source at 30-40% fructose content (Kirs et al., 2011). Most fructose consumed today is therefore acquired through industrial processes. Glucose is not only the most abundant monosaccharide found naturally in our food supply, but also comprises the majority of the free sugars circulating through the bloodstream of higher-level organisms – including humans. Contrasting fructose, glucose is an aldohexose sugar that forms a 6-membered ring. The structural differences between these two monosaccharides result in distinct metabolic differences that remain unclear. Although glucose metabolism is thoroughly studied and well understood, the on-going controversy surrounding the potential relationship between fructose consumption and onset of metabolic disease remains unclear. Fructose is rarely found as the sole sugar source in processed foods, and this poses a challenge when attempting to study the potential detrimental effects of this monosaccharide.

#### **1.1.2.2. Sucrose and HFCS**

Fructose is commonly consumed alongside glucose as either sucrose or HFCS. Sucrose, more commonly known as table sugar, is a disaccharide comprised of glucose and fructose units

that are linked together by a glycosidic bond. Due to this linkage, sucrose is always comprised of 50% glucose and 50% fructose. Various forms of HFCS are also comprised of glucose and fructose, but the sugars in HFCS are present as two separate monosaccharide units (White, 2008). The lack of a bond allows for the creation of different variations of HFCS based on the ratio of glucose and fructose units present. Given the name, HFCS is often misperceived by the consumer as containing high quantities of fructose. Not only is the composition very similar to the 50:50 ratio found in sucrose, but some versions actually contain less than 50% fructose. Due to the relative perceived sweetness of fructose being higher than glucose, the ratio of these monosaccharides can be altered to create different variations of HFCS with different sweetness profiles (Colonna et al., 2006; Helstad, 2019). The two most common forms of HFCS currently used within the food industry are HFCS-42 and HFCS-55, which contain 42% and 55% fructose respectively with the remaining composition being comprised of glucose (Ferraris et al., 2018).

After the introduction of HFCS into the food supply in the 1970s, the prevalence of obesity and fructose consumption began increasing at parallel rates, suggesting a potential association. However, as discussed in section 1.2.6 of this chapter, the current literature on the association between fructose and cardiometabolic risk factors remains contradictory as a direct link between HFCS intakes and disease risk has not yet been elucidated.

## **1.2. Fructose Metabolism**

### **1.2.1. Fructose is Converted to Glycolytic Intermediates**

Although glucose is the monosaccharide most associated with energy production in the body, fructose is also an important source of fuel. Due to the absence of a specific catalytic

pathway for fructose, the metabolism of this monosaccharide relies on being funnelled into the pathway dedicated to glucose metabolism: the glycolytic pathway.

The glycolytic pathway, commonly referred to as glycolysis, is a two-part energy-conversion pathway that occurs in the cytoplasm of eukaryotic cells. This pathway has multiple fates depending on the energy balance in the body; one glucose molecule can be catabolized to produce two pyruvate molecules, later leading to the production of adenosine triphosphate (ATP) through the tricarboxylic acid (TCA) cycle; alternatively, the carbons from glucose may be used to generate either fatty acids (FA) or amino acids. Stage 1 consists of four steps, whereby glucose is phosphorylated, isomerized, and phosphorylated a second time, ending in the cleavage of fructose-1,6-bisphosphate into two trioses: dihydroxyacetone phosphate (DHAP) and glyceraldehyde-3-phosphate (G-3-P). Steps one and three, catalyzed by the enzymes hexokinase and phosphofructokinase-1 (PFK-1) respectively, are integral in this part of the pathway as they require an investment of energy in the form of ATP. Due to the irreversible nature of these enzymes, they act as points of regulation and serve as control sites within glycolysis. Although fructose uses the glycolytic pathway, there are key metabolic differences including the possible evasion from PFK-1.

Fructose can enter glycolysis at two points (Figure 1.2). Fructose metabolised in extrahepatic tissues, specifically adipose or muscle, is phosphorylated directly by hexokinase to form fructose-6-phosphate (F-6-P) – a glycolytic intermediate. However, entering the pathway at the third intermediate still requires PFK-1, the most important control site in the mammalian glycolytic pathway, and therefore still allows for tight regulation. The extrahepatic tissue contribution is negligible when compared to the hepatic contribution. In the liver, a major site of fructose metabolism, this tight regulation is lost as fructose can bypass the PFK-1 catalyzed

reaction by entering glycolysis at the last step of Stage 1 as either DHAP or G-3-P (from glyceraldehyde). This lack of regulation leads to an excess of specific intermediates including glucose, acetyl-CoA, glycerate, and lactate, which may be a critical link to the association between excess fructose consumption and metabolic related disorders (Jang et al., 2018; Sun et al., 2012).

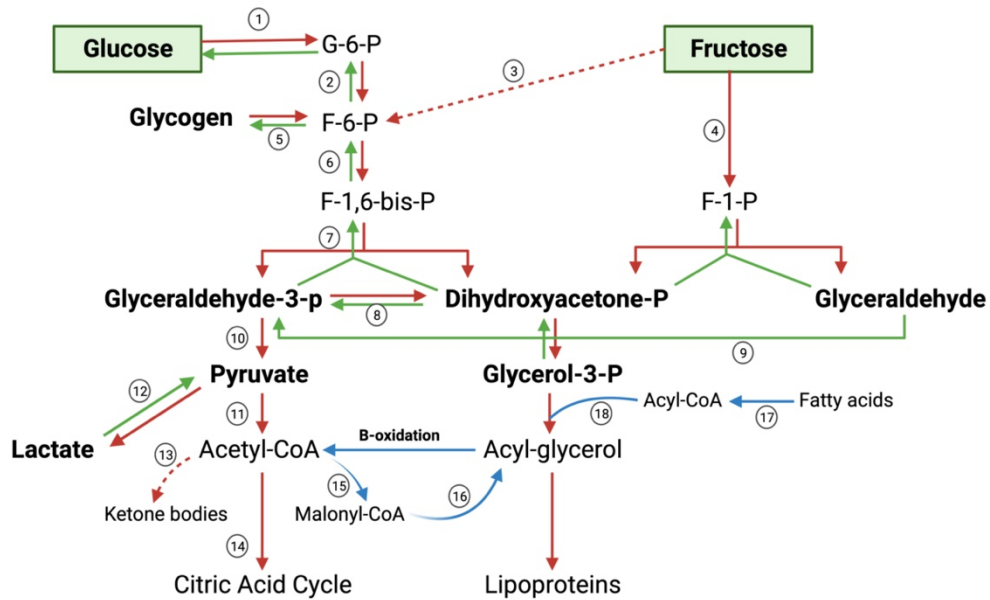


**Figure 1.2 Schematic indicating the major metabolic pathways of carbohydrates and flux of dietary glucose and fructose (Sun & Empie, 2012)**

P = phosphate. For enzymes numbered in circles: 1 = hexokinase/glucokinase or Glucose-6 phosphatase, 2 = phosphoglucose isomerase, 3 = hexokinase, 4 = fructokinase, 5 = glycogen synthase or phosphorylase, 6 = phosphofructokinase, 7 = aldolase, 8 = triose phosphate isomerase, 9 = triose kinase, 10 = several enzymes including pyruvate kinase, 11 = pyruvate dehydrogenase complex, 12 = lactate dehydrogenase, 13 = ketothiolase and other 3 enzymes, 14 = enzyme group relates to citric acid cycle, 15 = acetyl CoA carboxylase, 16 = multienzyme complexes, 17 = acyl CoA synthase, 18 = glycerol-phosphate acyl transferase and triacylglycerol synthase complex. The dashed-line and arrow represents minor pathways or will not occur under a healthy condition or ordinary sugar consumption. Green lines indicate reversible points of the pathway depending on energy state and blue lines indicate alternative intermediates that feed into or out of the glycolytic pathway. The compound names in **bold** would be major metabolic intermediates or end products of glucose or fructose metabolism. (Adapted from Sun et al., 2012)

### 1.2.2. Transport into the Cell

Another notable difference between glucose and fructose metabolism is the method of entry into the cell. Depending on the tissue or organ as well as the blood glucose concentration in the body, these monosaccharides rely on different transporters to enter and exit cells. Glucose, but not fructose, relies on glucose transporter four (GLUT4) to enter insulin-dependent tissues, including adipocytes and skeletal muscles (Chen, Cheung, Feng, Tanner, & Frommer, 2015). In hepatocytes, glucose utilizes sodium-glucose transporter 1 (SGLT1) or glucose transporter 2 (GLUT2) to enter the cell from portal circulation and is later released from the cell via GLUT2 transporters into systemic circulation. SGLT1 is a highly regulated transporter due to the requirement of energy; SGLT1 symporter utilizes active transport to move one glucose and two sodium molecules into the cell, whereby the sodium later exits the cell in exchange for potassium by a  $\text{Na}^+/\text{K}^+$  ATPase pump. When large quantities of glucose are consumed, the SGLT1 protein becomes saturated, and a release of insulin triggers the translocation of GLUT2 to the apical membrane. Therefore, high glucose load results in larger quantities of glucose to enter the cell from portal circulation through GLUT2 by means of facilitated diffusion. When insulin levels peak, translocated GLUT2 returns to storage vesicles and SGLT1 once again becomes the main transporter of glucose into the cell. Although fructose relies on the same GLUT2 protein to be released into systemic circulation, fructose uses glucose transporter five (GLUT5) to enter the cell in both hepatic and non-hepatic tissues (Ferraris et al., 2018).

Contradictory to its name, GLUT5 exclusively transports fructose into the cell from portal circulation. Although GLUT5 is located in several locations within the body including the kidney, brain, skeletal muscle, and adipose tissue – it is primarily expressed in the small intestine (Ferraris et al., 2018). Opposing the previous assumption that fructose is metabolized primarily

in the liver, high concentrations of GLUT5 in the small intestine led researchers to discover that the small intestine plays a large role in fructose metabolism (Ferraris et al., 2018; Jang et al., 2018).

### **1.2.3. Fructose Metabolism in the Gut**

Although the investigation of fructose and fructose metabolism began in the 1970's, most of the research published until recently relied on the assumption that the liver was the only major metabolism site for fructose. Because of this, several experiments utilized intravenous (IV) catheterization as the route of entry, thereby allowing fructose to bypass the gut and enter directly into portal circulation. Unlike glucose, fructose cannot be readily metabolized by most cells in the body; initial metabolism is limited to the small intestine, liver, and kidney (Ferraris et al., 2018).

A recent study in the rat model by Tappy et al. (2018, 2019) suggested that small oral doses of fructose (<0.5 g/kg BW) could be handled almost entirely by the small intestine, resulting in metabolites such as lactate and glucose to be released into portal circulation. A second study in the mouse model by Jang et al. (2018) reiterated these findings; they demonstrated that up to 90% of a low fructose dose (<1 g/kg BW) could be cleared by the small intestine, resulting in only trace amounts of fructose but high concentrations of fructose-derived metabolites including glucose, lactate, and glycerate in portal circulation. To our knowledge, the isotope tracer study by Jang et al. (2018) was the first of its kind to quantify the magnitude of fructose metabolism in the gut following the consumption of a realistic dose of fructose in the presence of glucose through the oral route. When labelled fructose with unlabelled glucose was administered by gavage (as a contrast to labelled glucose with unlabelled fructose), the resulting

labelled glycerate concentrations were 80-fold higher and labelled glucose – predominantly with a M+3 labelling pattern – quickly exceeded labelled fructose concentrations in the portal vein. The labelling pattern also reinforced that, similarly to what has been demonstrated in the liver, fructose preferably splits into two trioses by the gut and combines with an additional three-carbon units to form the M+3 glucose that is subsequently measured in portal circulation (Jang et al., 2018; Sun et al., 2012). However, as fructose dose increased, fructose concentrations in the portal circulation also increased in a dose-dependent manner. These findings suggest that the small intestine displays a protective shielding effect on the liver, but this protection can be overwhelmed with higher intakes, resulting in a dose-dependent spillover of fructose into the liver (Jang et al., 2018).

#### **1.2.4. Carbohydrate Metabolism in the Liver**

##### **1.2.4.1. Glucose Metabolism in the Liver**

The liver is a major site of metabolism in the body and is responsible for the degradation of all three macronutrients and the storage or release of their corresponding metabolites. The role of the liver in glucose metabolism in humans is well understood and tightly regulated; through the exogenous route, post-prandial glucose absorbed in the small intestine passes through the bloodstream via the portal vein into hepatocytes where it is taken up by GLUT2 and initially converted to glucose-6-phosphate (G-6-P) by glucokinase – a liver specific hexokinase (Figure 1.3).

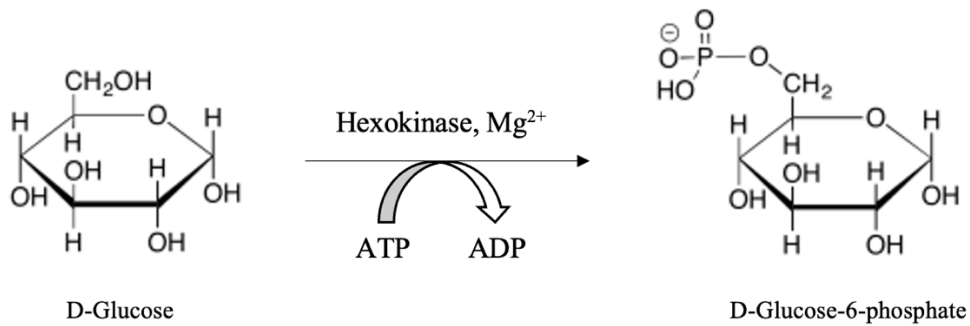


**Figure 1.3 Glucose is converted to glucose-6-phosphate**

ATP = Adenosine triphosphate, ADP = Adenosine diphosphate, Mg<sup>2+</sup> = Magnesium (II) ion

G-6-P can subsequently continue through the glycolytic pathway to produce pyruvate, or can be diverted to another fate, including: glycogen synthesis, the hexosamine pathway, the pentose phosphate pathway, oxidative routes, or fatty acid synthesis (Figure 1.4) if present in excess (Adeva et al., 2016).

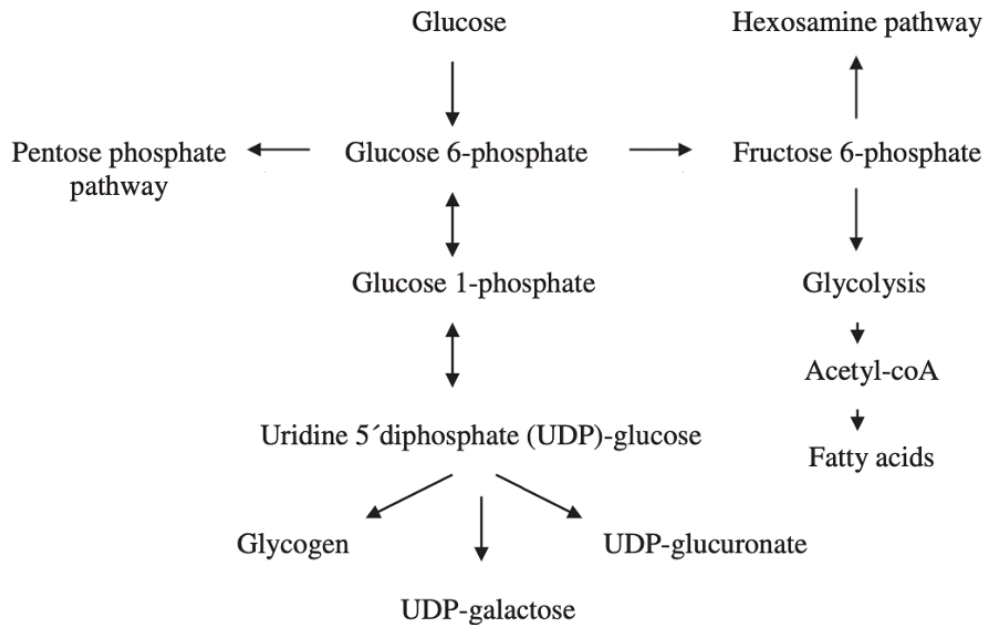


**Figure 1.4 A schematic showing the fate of glucose in the liver (Adeva-Andany et al., 2016)**

The liver can also perform up to 80% of endogenous glucose production in the prandial period; the liver can produce glucose through either the breakdown of stored glycogen, known as glycogenolysis, or perform gluconeogenesis using glucose precursors such as alanine, lactate, or glycerol (Sharabi et al., 2015). Evidently the liver plays a critical role in maintaining a tight regulation of blood glucose concentrations in both the prandial and post-prandial periods.

#### **1.2.4.2. Fructose Metabolism in the Liver**

Similarly to glucose, fructose that remains intact after being released from the enterocytes of the small intestine enters the hepatocytes passively through GLUT2 (Tappy, et al., 2010), but there are three significant differences that impact the regulation for the metabolism of these monosaccharides.

Once in the hepatocyte, fructose is rapidly converted to fructose-1-phosphate (F-1-P) by enzyme fructokinase; this enzyme is characterized by a low  $K_m$  value with high specificity for fructose. The enzyme specificity is a critical difference between glucose and fructose metabolism as glucokinase has a much higher  $K_m$  value for glucose, therefore the phosphorylation rate of glucose is slower as it is dependent on blood glucose concentrations – a key point of regulation (Ferraris et al., 2018). Additionally, because glucose has two points of regulation in glycolysis, fructose evades both steps 1 and 3 by entering the glycolytic pathway as a triose; F-1-P is readily cleaved by aldolase B to form triose phosphates, DHAP, or G-3-P (Figure 1.2). Furthermore, fructolytic enzymes are not inhibited by their products. Consequently, this lack of inhibition allows nearly all remaining dietary fructose to enter the hepatocyte and continue metabolism to form triose-phosphates (Campos et al., 2016). As metabolism progresses, the fate of fructose is reliant on which triose it is metabolized into.

Fructose converted to G-3-P will continue through Part 2 of glycolysis (Figure 1.2) to form pyruvate and subsequently form acetyl-CoA, which can enter the TCA cycle and result in the production of ATP; however, when TCA intermediates accumulate, these intermediates can revert to acetyl-CoA to be stored through the process of endogenous fatty acid synthesis as shown in Figure 1.2 (Samir et al., 2016). Alternatively, fructose converted to DHAP can form glycerol phosphate, leading to FA synthesis. Although the fate of fructose and the driving factors are not fully elucidated, the formation of lipogenic substrates from both trioses pose a possible link between differences in lipid handling through fructose versus glucose consumption, potentially resulting in increased disease risk.

#### **1.2.5. Fructose and Lipid Handling**

The discrepancies between glucose and fructose metabolism have been identified as a risk factor for increased **triacylglycerol** (TAG) concentrations and atherogenic lipid profile, potentially leading to a link with disease onset. Both monosaccharides utilize the same metabolic pathways, but high concentrations of fructose derived trioses in the liver stimulate disposal pathways, including *de novo* lipogenesis (DNL), and thereby lead to greater FA/TAG synthesis and VLDL-TAG secretion when compared to glucose (Campos et al., 2016; Tappy, 2018). While DNL was originally considered to be negligible in the disposal of dietary fructose and only a minor contributor to hepatic liver content, more recent studies indicate that DNL can contribute upwards of 26% of liver lipids in obese humans (Lambert et al., 2001; Samir et al., 2016). A common finding across human trials is the demonstration of very high fructose intakes leading to increased fasting and post-prandial TAG concentrations (Wang et al., 2014; Zhang et al., 2013); furthermore, high fasting and post-prandial TAG concentrations are associated with decreased

high-density lipoprotein (HDL) concentrations and/or increased total cholesterol concentrations. Campos et al. (2016); suggest that the increased TAG concentrations are achieved through the stimulation of DNL and very low density lipoprotein (VLDL) secretion; however, it appears that the lipid profile can be altered similarly through the use of glucose and high-fat content. These findings call into question if fructose is the driving factor in dyslipidemia, or if it is simply the additional calories contributed by fructose that pose a risk. Investigation into the studies that show a link between fructose consumption and dyslipidemia identified that the parameters often involved unrealistic and isolated doses of fructose and were limited to males, further questioning if fructose affects the lipid profile under realistic conditions.

#### **1.2.6. Fructose as a Factor in Metabolic Diseases**

In Canada, chronic diseases account for 89% of all deaths and consuming a healthy diet can prevent up to 80% of Type 2 Diabetes Mellitus (T2DM) and cardiovascular disease (CVD) cases, as well as 40% of cancers (Liu et al., 2020; WHO, 2015).

Fructose consumption has previously been linked with the development of obesity, fatty liver, and insulin resistance, which are all risk factors that promote diseased states associated with CVD, T2DM, and NAFLD. Inconsistencies in human and animal data suggest that additional factors, in combination with fructose intake, are required for the development of disease risk factors. For example, hypercaloric intake consistently emerges as a criterion required for the development of cardiometabolic related diseases associated with fructose. Athletes represent a valuable cohort of individuals who consume liberal quantities of fructose while maintaining an isocaloric or hypocaloric diet without the development of deleterious effects (Egli et al., 2013; Pereira et al., 2017; Tappy et al., 2019). Although a hypercaloric diet appears to be a

co-requisite with fructose for the development of risk factors such as obesity, hypercaloric diets irrespective of fructose content can result in obesity due to the storage of excess energy as fat. Whether fructose drives lipid production and subsequent weight gain differentially than glucose remains contradictory.

#### **1.2.6.1. Fructose and CVD**

When investigating lipid-handling in females versus males, there appears to be clear sex-specific differences. Although CVD was once thought to be a disease of the male heart, further research has revealed that it is more common in females, but it presents differently and often goes undiagnosed or untreated (Agarwala et al., 2020; Appelman et al., 2014). While women do experience a high prevalence of CVD, they are more likely to experience stroke and less likely to develop coronary heart disease (CHD) than males – CHD often being the more lethal diagnosis. The lower prevalence of CHD in females is thought to be related estrogen, as higher concentrations of this hormone appear to be protective against the development of dyslipidemia present in individuals diagnosed with both CHD and diabetes – a common comorbidity (Godsland, 1996). It could be speculated that this protection involves the ability for females to partition FA towards ketone bodies which can then be used as an alternate source of fuel, subsequently reducing the formation of very low-density lipoproteins (VLDL). Males have a lessened ability to form ketone bodies, so they shift toward the upregulation of VLDL, thereby increasing their risk for developing diseases such as NAFLD (Marinou et al., 2011).

### **1.2.6.1. Fructose and NAFLD**

NAFLD is a manifestation of a metabolic disease in the liver defined by the American Association for the Study of Liver Diseases as the presence of hepatic steatosis (excessive hepatic liver fat accumulation) without the presence of other risk factors including alcohol consumption, heredity disorders, or use of steatogenic medications. NAFLD can be further categorized into non-alcoholic fatty liver (NAFL) and non-alcoholic steatohepatitis (NASH), dependent on evidence of hepatocellular injury (NASH) or a lack of inflammation present (NAFL) (Chalasani et al., 2012). Although the pathogenesis is multifactorial, most patients diagnosed with NAFLD possess one or more comorbidities such as obesity, T2DM, or dyslipidemia. There are also epidemiological risk factors including sex: NAFLD appears to be a sexual dimorphic disease in both human and animal studies as females display an innate protection, likely from estrogen, against onset of the disease (Ballestri et al., 2017). In the presence of decreased estrogen levels – including postmenopausal women and women experiencing estrogen deficiency – individuals experience fat redistribution, resulting in an increase in visceral fat associated with the development and progression of NAFLD in both mice and human studies; this risk is subsequently reduced when individuals are placed on hormonal therapy, furthering exhibiting the link between lipid handling, NAFLD, and the protective effects of estrogen (Klair et al., 2016; Smith et al., 2017; Yang et al., 2014). However, NAFLD is a multifaceted disease highly dependent on sex, genetics, and lifestyle factors and warrants further investigation.

### **1.2.6.2. Fructose and T2DM**

Glucose is insulin-dependent whereby insulin is secreted upon ingestion to trigger the absorption and utilization of glucose and stabilize blood sugar concentrations. Due to the metabolic nature of fructose and the lack of insulin signalling, this monosaccharide is considered insulin independent; the lack of insulin response actually led to the recommendation of fructose as a sugar replacement for glucose for diabetic control after entering the market in the 1970s. (Mehnert, 1976). Although fructose alone cannot elicit an insulin response, fructose is consumed in combination with glucose which is insulin dependent. Additionally, as previously discussed, fructose is converted to triose-phosphates that have differing fates, including the formation of glucose. Fructose, unlike glucose, can therefore bypass the key regulatory enzymes and subsequently produce large quantities of glucose, lactate, pyruvate, and other glycolytic intermediates that consequently elicit an insulin response.

Fructose consumption has often been related to a lack of satiety in human and animal models. Due to an initial lack of insulin release upon fructose ingestion, an insulin-regulated hormone known as leptin is impacted. In normal fed conditions in the presence of glucose, insulin is first secreted from pancreatic beta cells to regulate and clear plasma glucose, which in turn signals the release of leptin – a hormone that regulates satiety and elicits the feeling of fullness. Without feeling satiated, the ingestion of fructose may promote a chain reaction of over eating and a hypercaloric state, leading to the development of obesity which is a comorbidity and risk factor for other cardiometabolic risk factors: including T2DM (Basciano et al., 2005; Elliott et al., 2002).

### 1.3. Rationale, Hypothesis and Objectives

Sugar consumption, specifically fructose, is suggested to be a potential contributor to the obesity epidemic occurring in North America. Far surpassing the recommended intakes of 5%, the average North American consumes nearly 20% of their calories as sugar, and fructose comprises approximately half of these intakes (Chiavaroli et al., 2022; Marriott et al., 2009; White, 2008). Although there are many similarities between glucose and fructose, fructose has the unique ability to evade key regulatory steps in glycolysis by first metabolizing into DHAP and G-3P (from glyceraldehyde), and then entering the pathway as trioses (Sun et al., 2012). Moreover, fructose uses GLUT5 – a transporter unique to fructose – rather than GLUT2 to enter the cell on the apical membrane. The evasion of key regulatory steps in combination with utilizing a unique transporter suggests that the ingestion of fructose may lead to uncontrolled metabolism and produce an accumulation of glycolytic and lipogenic intermediates that subsequently contribute to obesity and other cardiometabolic risk factors (Campos et al., 2016; Ferraris et al., 2018; Tappy, 2018).

An accumulation of lipogenic intermediates seen in fructose but not glucose, such as acetyl-CoA, is thought to be a link between fructose and dyslipidemia due to driving FA/TAG synthesis and VLDL-TAG secretion. However, it is unclear if it is fructose or simply the additional calories consumed through fructose as studies feeding glucose paired with high-fat content also induce dyslipidemia and obesity.

Although fructose has been widely studied, existing literature remains contradictory as previous studies utilize IV to administer fructose based on the previous assumption that fructose is primarily metabolized in the liver. Recent isotope tracer studies have disproved this assumption, finding that small oral doses of fructose can be metabolized nearly exclusively by

the small intestine, and only larger doses that overwhelm this pathway are metabolized in the liver (Jang et al., 2018; Tappy, 2018). Additionally, the current literature utilizes unrealistic and isolated doses of fructose. Recent findings suggest that fructose does lead to phenotypic changes associated with cardiometabolic risk, but these changes only occur in hypercaloric conditions (Jang et al., 2018; Jensen et al., 2018). Further research is required to examine if realistic doses of fructose paired with glucose (to mimic sucrose and HFCS) lead to an increased risk of developing cardiometabolic risk factors including weight gain, fatty liver, insulin resistance, and dyslipidemia.

Newly emerging research suggests that previous long-term exposure to fructose may result in metabolic adaptations to create a new steady state, thereby providing a protective effect against bolus doses of fructose. This protective effect appears to be heightened in females due to an increased ability to partition FA towards the production of ketone bodies, rather than an upregulation in VLDL (Godsland, 1996; Marinou et al., 2011).

We hypothesized that prolonged fructose feeding, only when combined with a hypercaloric diet, will result in deleterious cardiometabolic outcomes in mice, including: weight gain, liver weight gain, increased TAG content and total cholesterol, and increased post-prandial blood glucose concentrations compared to a non-fructose control. Additionally, we hypothesized that prolonged exposure to fructose will have a protective effect, leading to a heightened ability to convert fructose into glucose in mice.

Objectives:

01. To quantify both weight gain and liver weight gain.
02. To examine the lipid profile and quantify the total TAG content, total cholesterol, and HDL/non-HDL cholesterol in the liver, RBCs and heart tissue.
03. To determine if previous exposure to fructose alters the metabolism of a bolus dose of fructose and glucose through isotope tracers.

## 2. Materials and Methods

### 2.1. Animal Ordering and Housing

Prior to conducting the true study, a smaller preliminary pilot study was conducted to learn and perfect the surgical techniques and assess the diets on a smaller scale – the two studies were labelled as Fructose Energy Study 1 (FE1) and Fructose Energy Study 2 (FE2). Both FE1 and FE2 studies were conducted using the C57BL/6J mouse model because this strain is susceptible to developing diet-induced obesity (DIO) (Alexander et al., 2006; Buettner et al., 2007; Surwit et al., 1995). All animal procedures in this study were approved by the Institutional Animal Care Committee at Memorial University of Newfoundland and followed the guidelines set by the Canadian Council on Animal Care. Due to FE1 being a pilot study, only eighteen mice were utilized and divided by sex and then into one of three dietary interventions (n=3). In the FE2 study, fifty-four mice were balanced by sex and dietary treatment group (n=9).

For the FE1 study, 18 mice (12-weeks old) were received from The Jackson Laboratory and were initially housed in groups of three by dietary treatment group to increase enrichment. However, fighting and barbering occurred during group housing, resulting in separation to single housing after the acclimation period. All mice were kept in the Biotechnology Animal Care Facility at Memorial University of Newfoundland, St. John's, NL, Canada. The room provided 12 h light and dark cycles and a maintained temperature of 23 °C. For housing, Sealsafe Plus GM500 cages were used with a DGM rack (Techniplast) which provided uniform airflow and filtration to all cages. Each cage contained: a food hopper, water bottle, bedding, nesting material, a wooden block, a hanging binder ring, and a house for added enrichment. All mice were immediately placed on standard chow diet (Appendix I) that was provided *ad libitum*. After

the 3-day acclimation to single-housing, initial body weights were recorded and subsequently measured twice weekly throughout the entirety of the study.

For the FE2 study, fifty-four, 3-week-old mice were received from The Jackson Laboratory. Younger mice were ordered with an attempt of reducing aggression towards the study personnel – this was found to be effective. Mice were individually housed upon arrival, and the cages were located in the same room of the Biotechnology Animal Care Facility as FE1 under the same conditions. Each cage contained the same materials as FE1, but with the addition of a ceramic feeding bowl when the dietary treatments were implemented. The food bowl resulted in less food waste as the mice tended to shred and play with the experimental diets when placed in the overhead-hopper. After the 3-day acclimation period, initial body weights were recorded and subsequently measured twice weekly throughout the entirety of the study. Prior to starting the treatment, all mice were divided by sex and then randomized into treatment groups by weight to ensure the groups were balanced. One mouse (mouse number FE2-F9) was euthanized by the on-site veterinarian due to acquiring severe dermatitis that was not responding to topical treatment; fifty-three mice completed this study.

## **2.2. Diet and Dietary Treatment Groups**

Teklad Global 18% protein rodent diet (product number T.2018.15; Appendix I), containing all essential micro- and macronutrients, was utilized from post-wean until 15- (FE1) and 18-weeks of age (FE2); this chow maintenance period allowed the mice to become weight stable prior to starting the experiment. All three experimental diets (DYET#104809-104811) were purchased and produced by Dyets, Inc. These diets were modified versions of the 1993 American Institute of Nutrition Growth Rodent Diet (AIN-93G) that were customized to contain

only trace amounts of sucrose, glucose, and fructose for the purpose of this study. The mineral and vitamin mixes, #210025 (Appendix II) and #310025 (Appendix III) respectively, were also modified by replacing fructose with dextrose. The macronutrient composition of all dietary treatments consisted of 17% protein, 41% fat, and 42% carbohydrate – the source of carbohydrate being the only macronutrient that varied in composition. All diets were divided into 1 kg bags and stored on-site in a freezer (-18°C) to maintain freshness.

Due to fructose intake and metabolism being the focus of this study, the carbohydrate portion of this diet varied amongst treatment groups. The three treatment groups in this study were 0%, 10% and 20% of total calories from fructose. To achieve differing fructose content while maintaining isocaloric carbohydrate content, sucrose – a fructose containing disaccharide – and fructose in the base DIO diet were replaced with a combination of cornstarch and maltodextrin. The carbohydrate portion of the 0% fructose diet therefore consisted of all cornstarch and maltodextrin (Appendix IV) and then fructose was substituted appropriately to achieve 10% and 20% of total calories from fructose (Appendix V; Appendix VI).

### **2.2.1. Dietary Treatment Groups**

After the grow out period, the mice were equally divided into six groups (FE1 n=3, FE2 n=9); mice were divided by sex, weight balanced, and randomly placed into one of the three dietary treatment groups. In FE1, the 20% fructose formulation was too soft and unable to hold shape due to a manufacturing error. Because of the resulting consistency, there was not enough viable diet to complete the 6-week intervention and this group was reverted to chow diet for 11-weeks – henceforth this group is referred to as chow- $\partial$ .

In FE1, all mice dietary treatments were started on the same day. Due to the large number of animals in FE2, only one mouse from each of the six groups was started per day; this ensured that the necropsies would be staggered with 6-mice/day over nine days. All food was provided *ad libitum*; as previously mentioned, food hoppers and ceramic dishes were used in FE1 and glass food dishes were introduced in FE2 to minimize food waste. For FE1, the 0% and 10% groups remained on their specified dietary treatment for six weeks, whereas the chow- $\delta$  mice were placed on 20% for two weeks followed by chow for 11 weeks. All mice in FE2 remained on their specified dietary treatment for a total of 18-weeks.

### **2.2.2. Dietary Intakes**

Initial dietary intakes were recorded to ensure sufficient quantities of food were provided to maintain *ad libitum* feeding and then a second time at week 3 to further determine the specific intakes by group. Food consumption was measured by weight differences, accounting for cage waste, over a 3-day period (Appendix VII).

### **2.2.3. Body Weight Measurements**

Initial body weights were taken and recorded after the 3-day acclimation period and subsequently measured twice weekly throughout the chow maintenance period. As mentioned above, treatment start dates were staggered over nine days for FE2, so each mouse was weighed on their first day of treatment as a baseline measurement. Throughout the entire study, all mice were weighed twice weekly.

### 2.3. Isotope Gavage and Necropsy Preparation

The following procedures were completed for both FE1 and FE2. After completing the dietary intervention, the diet was removed from the cages 12 hours prior to necropsy to achieve a fasted state. The following morning, a cage containing a single mouse was brought into the procedure room and the mouse was weighed. Using the weight of the mouse, the quantity of isotope was calculated to achieve a dose of 0.5 g/kg D-[U-<sup>13</sup>C]-fructose and 0.5 g/kg unlabelled glucose. Once calculated, the required volume of each sugar was drawn into a 1 mL syringe with a 25G x 5/8 needle (BD PrecisionGlide). The needle was then discarded and replaced by a straight 20G x 25 mm gavage tip (Instech Laboratories, Inc) and set aside; this gavage needle was selected after measuring the length between the mouth of the mouse to the sternum.

A diagram of the necropsy procedure is outlined in Figure 2.1. To begin, the mouse was scruffed and placed into an aerated 10 mL Falcon tube, allowing one leg to remain outside of the tube. Holding carefully onto the tail and foot, hair removal cream was rubbed onto the leg using a cotton swab stick to expose the vein – this was more effective than shaving the area. After 60 seconds (no longer or it may burn the skin), the hair removal cream and subsequent fur was wiped off using a cotton swap and saline. An alcohol wipe was used to disinfect the exposed skin and a thin layer of Vaseline was applied to allow the blood to aggregate in a bubble for easier collection. While applying slight pressure to the leg, a 26G x 5/8 needle was used to prick the vein, and the saphenous blood was collected using a Microvette containing EDTA (Sarstedt AG & Co. KG, Germany). The blood sample was immediately placed on ice and the mouse was placed back into its cage: this was the baseline blood sample. After completing the blood sample, the same mouse was scruffed for gavage. Holding the scruffed mouse perpendicular to the surgical table, the dominant hand was used to pick up the gavage syringe, containing the

previously prepared solution and rub the tip in DietGel (ClearH<sub>2</sub>O) to entice the mouse. The ball of the needle was slowly placed into the side of the mouth and down into the esophagus. Once in position, the solution was slowly gavaged into the mouse and a timer was started. The mouse was placed back into its cage and observed for one minute to ensure proper delivery of the sugars. After 15 minutes had elapsed, the mouse was scruffed for a third time and the second saphenous blood sample was collected from the opposite leg. The mouse was placed in the induction chamber with oxygen and after 10 minutes in the chamber – 25 minutes after the gavage – the isoflurane was turned on causing the mouse to lose consciousness. Once unconscious, the mouse was transferred to the surgical table and a face mask providing the isoflurane and oxygen was placed over the mouth and nose in preparation for the necropsy.

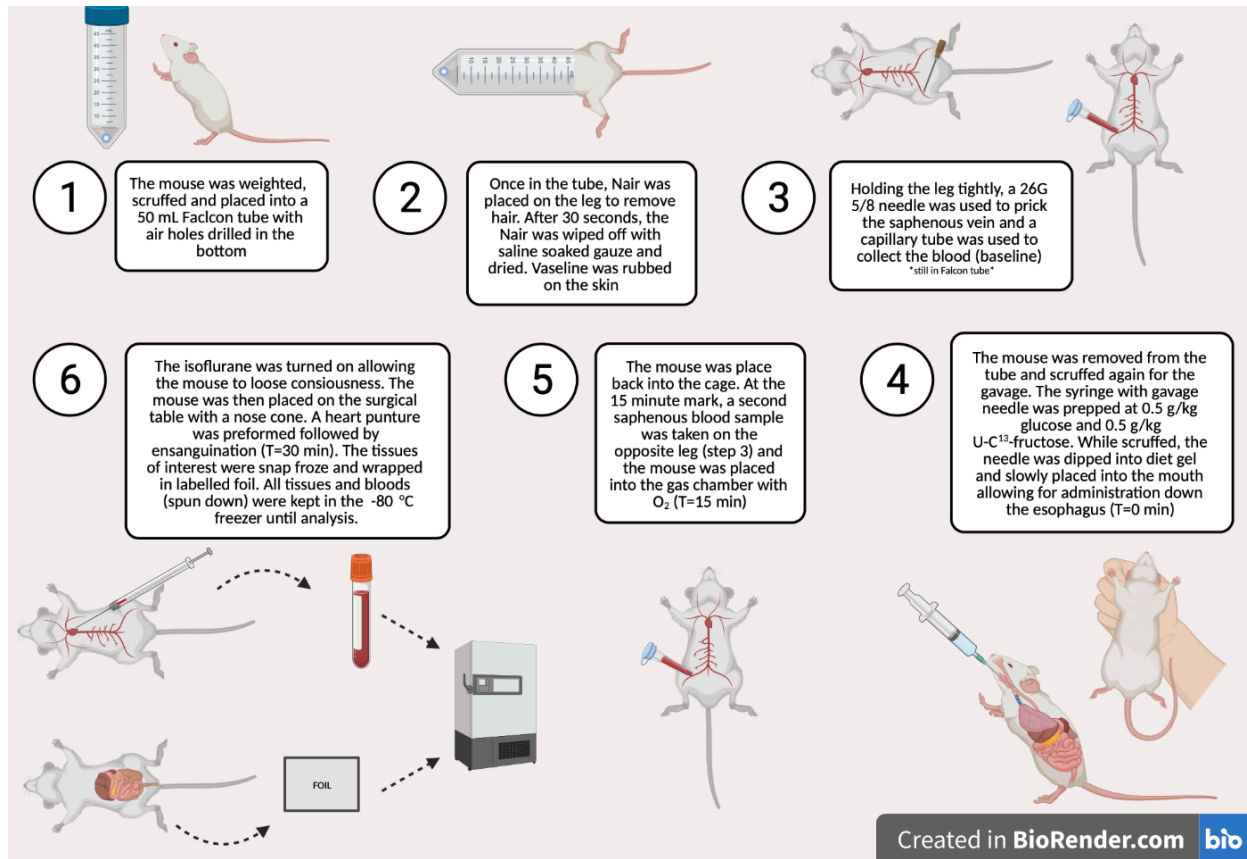


**Figure 2.1 Visual representation of the gavage and necropsy procedure**

## 2.4. Necropsy

After confirming the animal was in the surgical plane of anaesthesia by completing a toe pinch, a 1 mL syringe with a 25G x 5/8 needle was used to perform a heart puncture: this occurred 30 minutes post sugar gavage. With the non-dominant hand, the thumb and third finger were placed on the underarms to allow the ribs to lift. The index finger was then used to locate the sternum, and using the dominant hand, the needle was pushed in just under the ribs and slightly to the left to reach the heart. To ensure correct placement, the stopper is slightly pulled back until blood enters the syringe. Once in the heart, up to 1 mL of blood (or as much as possible) was drawn from the heart, placed in an Eppendorf with EDTA, and placed on ice. Using surgical scissors, the abdominal and chest cavities were opened revealing the organs. Following exsanguination, the heart was first removed to confirm the animal was dead. The remaining tissues were removed in the following order: small intestine, large intestine, stomach, liver, hind limb muscles (Soleus, Gastrocnemius, Extensor Digitorum Longus), renal fat pad, visceral fat pad, kidneys. All tissues were snap frozen with liquid nitrogen and placed in sample bags, with the exception of the right kidney which was placed in formalin. The liver was the only tissue that was weighed during removal. The end time was recorded, and the carcass was placed into a biohazard bag for disposal. This procedure was continued until all necropsies for the day were complete.

## **2.5. Laboratory Analytical Procedures**

### **2.5.1. Glucose Concentrations – Glucometer**

A glucose meter, or glucometer, with blood glucose test strips (Contour Next, Ascensia Diabetes Care Canada Inc.) was used throughout the necropsy procedure to take direct blood glucose readings at three time points. These devices are able to quickly determine the concentration of glucose in a sample due to the chemical reaction that occurs between the blood droplet and chemicals located on the test strip. Glucose is first converted to gluconic acid by the enzyme glucose oxidase, and then further converted to ferrocyanide by the presence of ferricyanide. Once reacted, the electrode present in the test strip oxidizes the ferricyanide present, resulting in a quantifiable electrical current that is proportional to the concentration of glucose present.

During the two saphenous bleeds – baseline and 15-minutes post-gavage – a new test strip was placed in the glucometer and the sample collected directly from the vein prick. For the HP sample – 30-minutes post-gavage – the test strip was filled after the blood collection via syringe. All glucose readings were recorded for each animal in a spreadsheet and this method was later validated by a plate assay.

### **2.5.2. Glucose Concentrations – Glucose Oxidase**

Plasma from the heart punctures in both FE1 and FE2 studies were used to analyze blood glucose concentrations 30 minutes post gavage; a smaller sample size of baseline and 15-minute samples were also selected at random and tested by glucose oxidase to validate the glucometer readings. To quantify, a glucose-SL assay kit (Sekure Chemistry, Sekisui Diagnostics PEI Inc.) was used followed by plate reader spectrophotometry. This method was used as the

concentration of the samples were expected to fall within the identified reportable range of 0.6 to 600 mg/dL (0.03 to 33.3 mmol/L).

To verify the assay, the recommended DC-Cal multi analyte calibrator standards were prepared by completing a serial dilution of stock solution (Pointe Scientific) with deionized water to achieve the following concentrations: 25, 50, 75, 100, 125 and 151 mg/dL. To test that the concentration range of the standard was appropriate, using a 96-well plate, 2  $\mu$ L of each standard was pipetted into a well followed by 200  $\mu$ L of glucose reagent (recommended sample to reagent ratio of 1:100). Plasma samples from three different animals were also tested (one from each dietary treatment group). Once completed, the plate was covered in foil and placed in the incubator at 37°C with agitation for 10 minutes. A SynergyMx plate reader (BioTek) was used to read the microplate at the recommended wavelength of 340 nm. The wavelength values for each standard were plotted against the known concentration and produced a linear standard curve with  $R^2 = 0.9978$  (Appendix VIII). Due to the absorbance of the samples falling outside of the standard curve, a second test plate was run and analyzed with the samples diluted to a concentration of 1:1 and 2:3 (plasma to deionized water). Moving forward, all samples were run at a plasma to deionized water dilution of 2:3, in duplicate, and the above method was continued until all samples were completed. The coefficient of variance (CV) was calculated for each duplicate: if the CV% was greater than ten, the sample was rerun. When the data set was complete, all plates were discarded, and any remaining reagent was placed in the fridge for storage.

### **2.5.3. Glucose and Fructose Concentration and Isotopic Enrichment by Gas Chromatography – Mass Spectrometry**

A method previously described by Wanjudi et al. (2010) was modified and used to measure plasma glucose, fructose, and D-[U-<sup>13</sup>C]-fructose at all three time points by gas chromatography – mass spectrometry (GC-MS) analysis.

To begin, plasma was pipetted into a labelled Eppendorf; due to small collection volumes, 50 µL of plasma was utilized for HP samples and only 20 µL of plasma was utilized for the saphenous samples. In the same Eppendorf, 300 µL barium hydroxide (0.3 M) and 300 µL zinc sulfate (0.3 M) were added and placed on a dry heat block at 60°C for 15 minutes. The samples were centrifuged at 2000 x g for 5 minutes to precipitate the proteins, and the supernatant was collected and transferred to a glass 2 mL GC vial (silicone screw cap liner/PTFE, ThermoScientific). To accelerate the drying process, the vials were then placed in a centrifugal evaporator (Eppendorf) at room temperature. Once dried, 100 µL methoxyamine hydrochloride (MOX) dissolved in pyridine (0.18 M) was added to each vial, capped, and incubated on a dry heat block at 70°C for 60 minutes to achieve derivatization. The vials were removed from the heat block for approximately 15 minutes to cool, followed by the addition of 100 µL acetic anhydride. Each vial was capped and placed back on the heat block for an additional 60 minutes at a reduced temperature of 45°C. The caps were then removed and set aside, and the vials were placed back into the centrifugal evaporator for the second drying period. Once dried, the sample was resuspended in 50 µL ethyl acetate, capped, and placed in the fridge. Due to the small volume, on the day of analysis, the 50 µL of sample in ethyl acetate was extracted by pipette and placed into a 150 µL insert (Agilent Technologies) and returned to the GC vial.

After the sample preparation was complete, the vials were placed on the GC-MS. Two microlitres was injected into an Agilent 6890 GC-5973 MS with an Agilent Technologies capillary column (30.0 m x 0.250 mm, 0.25  $\mu$ L film thickness, DB-5MS) by auto-sampler. Helium was the gas carrier used with a flow rate of 1 mL/min. To quantify the derivatized samples by GC-MS, data was collected in EI mode. Due to a small sample volume, glucose and fructose quantification was run concurrently and each run was performed with a splitless ratio. The inlet temperature was set to 200°C. The column temperature was held at 180°C for 20 minutes, initially ramping up 5°C/min to reach 215°C, followed by a second ramp up of 25°C/min to achieve a final temperature of 310°C. Analysis was performed in scan mode; due to similar retention times for the two monosaccharides, ion pairs with significant overlap were not selected.

In total, five specific ion pairs were monitored between glucose and fructose based on the literature (Appendices XII-XIII). For glucose, the three ions investigated were 131 m/z ([1, 2-<sup>13</sup>C<sub>2</sub>] D-glucose), 289 m/z ([3, 4, 5, 6-<sup>13</sup>C<sub>4</sub>] D-glucose), and 187 m/z ([3, 4, 5, 6-<sup>13</sup>C<sub>4</sub>] D-glucose: further cleavage of acetate and ketone groups) with the corresponding enriched ion pairs 133 m/z (M+2), 293 m/z (M+4), and 191 m/z (M+4). For fructose, the two ions investigated were 203 m/z ([1, 2, 3-<sup>13</sup>C<sub>3</sub>] D-fructose) and 101 m/z ([1, 2, 3-<sup>13</sup>C<sub>3</sub>] D-fructose: further cleavage of acetate and ketone groups) with the corresponding enriched ion pairs 206 m/z (M+3) and 104 m/z (M+3). Due to the absence of an internal standard, calculation of the TTR was the key objective rather than exact quantification of glucose and fructose plasma concentrations.

## **2.5.4. Lipid Analysis**

### **2.5.4.1. Fatty Acid Profile and Quantification by Gas Chromatography – Flame Ionization Detection**

Samples were prepared for gas chromatography – flame ionization detection (GC-FID) analysis via a butanol-methanol lipid extraction method modified from Löfgren and colleagues (Löfgren et al., 2012). Liver and RBCs from both studies as well as heart tissue from FE1 mice were run under this protocol. To start, 50 mg of sample was weighed on an analytical balance and transferred into a disposable test tube. For an internal standard, 100  $\mu$ L of C17 was added to the sample. To achieve the first-phase extraction, 1800  $\mu$ L of butanol/methanol (3:1, v/v) was added to the test tube and a mechanical homogenizer was used to homogenize the sample and then vortexed on high for one minute. For second-phase extraction, 1800  $\mu$ L heptane/ethyl acetate (3:1, v/v) was added and the solution was vortexed for one minute. To induce the phase separation, 1800  $\mu$ L 1% acetic acid was added and once again vortexed for one minute. The test tube was then centrifuged at 2000 x g for 10 minutes. Once separated, the upper organic layer was collected via Pasteur pipette and placed into a 100 mL screw top vial. To repeat this process, an additional 1 mL of heptane/ethyl acetate was added to the solution, centrifuged at 2000 x g for 10 minutes, and the top layer was collected and added to the previous organic layer: this step was completed a second time if required. With the combined organic layers, the screw top vials were placed on a nitrogen evaporator (Organomation Associates, Inc.) until dried down and the disposable tubes with the remaining bottom layers were discarded.

To begin the second phase of the extraction protocol, the dried down lipid residue was resuspended in 1 mL of hexane and vortexed. To form the fatty acid methyl esters (FAMES), 1 mL of methylation reagent (1% sulfuric acid in methanol) was added to the solution and the cap

was screwed tightly onto the vial – Plumber’s tape was used to achieve a tight seal. The vials were placed on the dry block heater (Fisher Scientific) for 1 hour at 70°C. After an hour, the vials were cooled and 3 mL of 5% Na<sub>2</sub>CO<sub>2</sub> was added to the solution. To extract the FAMES, 2 mL hexane was added, vortexed for one minute, and centrifuged at 2000 x g for 10 minutes. Once separated, the top hexane layer was removed and transferred to a new disposable test tube. This process was repeated one to two more times by adding an additional 2 mL of hexane each time. The combined hexane layers placed on the nitrogen evaporator until dried down. The sample was resuspended in 1 mL of hexane and vortexed for one minute. Due to the high concentration, 200 µL of the final volume was transferred into a 2 ml GC vial (silicone screw cap line/PTFE, Thermo Scientific) with an additional 1.5 mL of hexane to achieve a total volume of 1.7 mL. The vial was capped and stored in the freezer until analyzed by GC-FID. The remaining 800 µL of sample was dried down, covered with Parafilm, and placed in the freezer – these were discarded after analysed samples were complete.

The prepared samples were run off-site on an Agilent 7890 GC-FID at the Ocean Sciences Centre (Logy Bay, Newfoundland, Canada). A FAME method previously verified within the Harding Lab was utilized to run all lipid samples including the heart, RBC, and liver tissues from the FE1 and FE2 studies. Manual integration was performed on the following nineteen fatty acids followed by subsequent quantification: myristic acid, pentadecanoic acid, palmitic acid, palmitoleic acid, stearic acid, oleic acid, vaccenic acid, linoleic acid, g-linolenic acid, a-linolenic acid, eicosenoic acid, eicosadienoic acid, dihomo-g-linolenic acid, arachidonic acid, eicosapentaenoic acid, docosatetraenoic acid, docosapentaenoic acid, lignoceric acid, docosahexaenoic acid. Although pentadecanoic acid (15:0) is an odd chain fatty acid that is not synthesized naturally, it was quantified as it is evidenced as a potential marker in adipose and

serum samples for the consumption of milk and dairy fat (Brevik, 2005; Jenkins et al., 2015; Wang et al., 2011), and the test diets contained high quantities of dairy fat.

#### **2.5.4.2. Cholesterol Lipoprotein Quantification by Spectrophotometric Assay**

Plasma from the heart punctures in both FE1 and FE2 studies were used to analyze total serum cholesterol 30-minutes post gavage. To quantify, a cholesterol-SL assay kit (Sekure Chemistry, Sekisui Diagnostics PEI Inc.) was used followed by plate reader spectrophotometry. This method was used as the concentration of the samples were expected to fall within the identified reportable range of 1.2 to 600 mg/dL (0.03 to 15.5 mmol/L).

To verify the assay, cholesterol standards were prepared by completing a serial dilution of 200 mg/dL stock solution (Pointe Scientific) with deionized water to achieve the following concentrations: 0, 25, 50, 100, 125, 150, 175, 200, 300, 400 mg/dL. To test that the concentration range of the standard was appropriate, using a 96-well plate, 2  $\mu$ L of each standard was pipetted into a well followed by 200  $\mu$ L of cholesterol reagent (recommended sample to reagent ratio of 1:100). Plasma samples from three different animals were also tested (one from each dietary treatment group). Once completed, the plate was covered in foil and placed in the incubator at 37°C with agitation for 10 minutes. A SynergyMx plate reader (BioTek) was used to read the microplate at the recommended wavelength of 505 nm. The wavelength values for each standard were plotted against the known concentration and produced a linear standard curve with  $R^2 = 0.9949$  (Appendix IX). Due to the absorbance of the samples falling outside of the standard curve, a second test plate was run and analyzed with the samples diluted to a concentration of 1:1 and 2:3 (plasma to deionized water). Moving forward, all samples were run at a plasma to deionized water dilution of 2:3, in duplicate, and the above method was continued until all

samples were completed. The coefficient of variation (CV%) was calculated for each duplicate: if the CV% was greater than 10, the sample was rerun. When the data set was complete, all plates were discarded, and any remaining reagent was placed in the fridge for storage.

#### **2.5.4.3. triacylglycerol Quantification by Spectrophotometric Assay**

Plasma from the heart punctures in both FE1 and FE2 studies were used to analyze total TAG content 30 minutes post gavage. To quantify, a **triacylglycerol-SL** assay kit (Sekure Chemistry, Sekisui Diagnostics PEI Inc.) was used followed by plate reader spectrophotometry. This method was used as the concentration of the samples were expected to fall within the identified reportable range of 3.0 to 1000 mg/dL (0.03 to 11.3 mmol/L).

To verify the assay, glycerol standards were prepared by completing a serial dilution of 260 mg/dL stock solution (Pointe Scientific) with deionized water to achieve the following concentrations: 16.25, 32.5, 65, 97.5, 130, 195, 260, 390, and 520 mg/dL. To test that the concentration range of the standard was appropriate, using a 96-well plate, 3  $\mu$ L of each standard was pipetted into a well followed by 225  $\mu$ L of TAG reagent (recommended sample to reagent ratio of 1:75). Plasma samples from three different animals were also tested (one from each dietary treatment group). Once completed, the plate was covered in foil and placed in the incubator at 37°C with agitation for 10 minutes. A SynergyMx plate reader (BioTek) was used to read the microplate at the recommended wavelength of 505 nm. The wavelength values for each standard were plotted against the known concentration and produced a linear standard curve with  $R^2 = 0.9984$  (Appendix X). Due to the absorbance of the samples falling on the standard curve, no dilution factor was required, and the above method was continued until all samples were completed. The CV% was calculated for each duplicate: if the CV% was greater than 10, the

sample was rerun. When the data set was complete, all plates were discarded, and any remaining reagent was placed in the fridge for storage.

#### **2.5.4.4. High Density Lipoprotein Quantification by Spectrophotometric**

##### **Assay**

Plasma from the heart punctures in both FE1 and FE2 studies were used to analyze total serum HDL 30 minutes post gavage. To quantify, an HDL Ultra Cholesterol assay kit (Sekure Chemistry, Sekisui Diagnostics PEI Inc.) was used followed by plate reader spectrophotometry. This method was used as the concentration of the samples were expected to fall within the identified reportable range of 2.5 to 200 mg/dL (0.065 to 5.2 mmol/L).

The manual procedure for this assay kit was provided by Sekisui Diagnostics. The recommended conditions suggest a reagent 1 (R1) volume of 300  $\mu$ L, a reagent 2 (R2) volume of 100  $\mu$ L, and a sample volume of 3  $\mu$ L. To accommodate for our 350  $\mu$ L well plate, the volumes were reduced by 33% to achieve a total volume of 268.7  $\mu$ L (R1 = 200  $\mu$ L, R2 = 66.7  $\mu$ L, sample = 2  $\mu$ L).

The temperature of the assay was controlled at 37°C for the entirety of the analysis. To run the assay, the procedure was completed in two steps: after pipetting the sample/standard into each vial, R1 was added followed by an incubation period at 37°C with agitation for 10 minutes. The plate was then placed on the plate reader (SynergyMx, BioTek) and analyzed at a wavelength of 600 nm before adding R2. After the addition of R2, a second incubation period was completed under the same parameters, followed by the final plate reading at a wavelength of 600 nm. The wavelength values for each standard were plotted against the known concentration and produced a linear standard curve with  $R^2 = 0.9866$  (Appendix XI). Due to the analyzer not

compensating for the dilution effect on the addition of R2, this was manually calculated as follows:

$$\Delta A = \text{second absorbance reading} - (\text{first absorbance reading} \times \text{dilution factor})$$

$$\text{Where dilution factor} = (\text{R1 vol.} + \text{sample vol.}) / (\text{R1 vol.} + \text{R2 vol.} + \text{sample vol.})$$

To verify the assay, the required Ultra N-geneous HDL Cholesterol Calibrator (Sekure Chemistry, Sekisui Diagnostics PEI Inc.) was utilized. To prepare the calibrator, 1 mL deionized water was added to the vial and inverted to fully dissolve the lyophilized human serum. After 20 minutes, the standard solutions were prepared by completing a dilution of the 60 mg/dL stock solution with deionized water to achieve the following concentrations: 15, 30, 40, and 50 mg/dL. Higher concentrations of 75, 90, and 120 mg/dL were achieved by adding additional volumes of the 60 mg/dL stock solution to the wells (2.5, 3 and 4  $\mu\text{L}$  respectfully). To test that the concentration range of the standard curve was appropriate for the samples, a test plate was run with each concentration, pipetted in duplicate, along with plasma samples from three different animals (one from each dietary treatment group). After confirming that the standard curve was linear with an  $R^2 > 0.95$ , the procedure was continued until all plasma samples were completed in duplicate – the standard curve is displayed in Appendix XI. The CV% was calculated for each duplicate: if the CV% was greater than 10, the sample was rerun. When the data set was complete, all plates were discarded, and any remaining reagent was placed in the fridge for storage.

### **2.5.5. Cardiac Histology**

All hearts from FE2 were immediately placed in labelled vials containing 10% formalin and mailed to Dr. Mohammed Moghadasian at the University of Manitoba for processing. Upon arrival, three female and three male hearts from each dietary treatment group were blindly tested for atherosclerotic plaque formation.

Each heart was tested by cutting a cross section from the aortic arch down to the apex of the heart. H&E staining was performed prior to imaging the sample by photomicrograph; Tri-chrome stain was only required to emphasize lesion formation, if present. These samples were tested against a control and a treatment sample that contained lesion formation. Both animals were low density lipoprotein (LDL) receptor knockout male mice with high susceptibility to developing lesions with cholesterol consumption; the control diet contained a cholesterol supplement, and the treatment diet contained a cholesterol supplement and wild rice supplement. After acquiring all FE2 images, they were visually compared to the control and treatment images that contained lesion formation.

## **2.6. Statistics**

The primary outcome of this study was the effect of fructose content in the diet on various metabolic outcomes and metabolic disease biomarkers in female and male mice. Therefore, the primary statistical analysis was a general linear model multivariate analysis of variance (ANOVA) with sex and dietary treatment as fixed variables. Tukey's post-hoc test ( $p < 0.05$ ) was used to test for sex, diet, and sex-by-diet effects. This analysis showed that only sex affected most dependent variables I assessed, therefore in some cases, I completed a secondary analysis of my data combining both sexes to assess the effect of diet alone on the dependent variables

using two-way ANOVA. Additionally, Student T-Test ( $p < 0.05$ ) was used to test for within diet effects. For body weight, a general linear model multivariate ANOVA with repeated measures was utilized to assess the effect of both time and diet on the dependent variables. Data presented in tables and figures are mean  $\pm$  standard deviation unless otherwise noted. SPSS software was used for all analyses.

### 3. Results

#### 3.1. Fructose Energy Study 1

##### 3.1.1. Effect of Diet on Body Weight Gain

Due to animals arriving at 12-weeks of age, no grow-out period was required. After the 3-day acclimation period, baseline body weight was measured (Week 0) and subsequently recorded on a bi-weekly basis for the duration of the 6-week dietary treatment period. Referring to Figure 3.1 below, dietary treatment had little effect on weight gain throughout the entirety of the study. When grouped by sex, males began the study at a larger weight and gained slightly more weight on average per week (slope = 0.120 g/week) than females (slope = 0.089 g/week), but the small slope value for each group indicates that the animals remained weight stable throughout the intervention. Although there were no statistical differences between dietary treatment groups, the 10% fructose diet trended slightly higher than the 0% fructose diet in both males and females. Interestingly, the weight of the Chow- $\delta$  group began to decline in males immediately after being reverted to chow (Week 2); this decline also occurred in females but was not observed until Week 3 – one week after the animals were placed back on chow. This decline in body weight continued to decrease in the subsequent weeks, both plateauing around Week 5, and ended the study at a comparable weight to the other treatment groups.

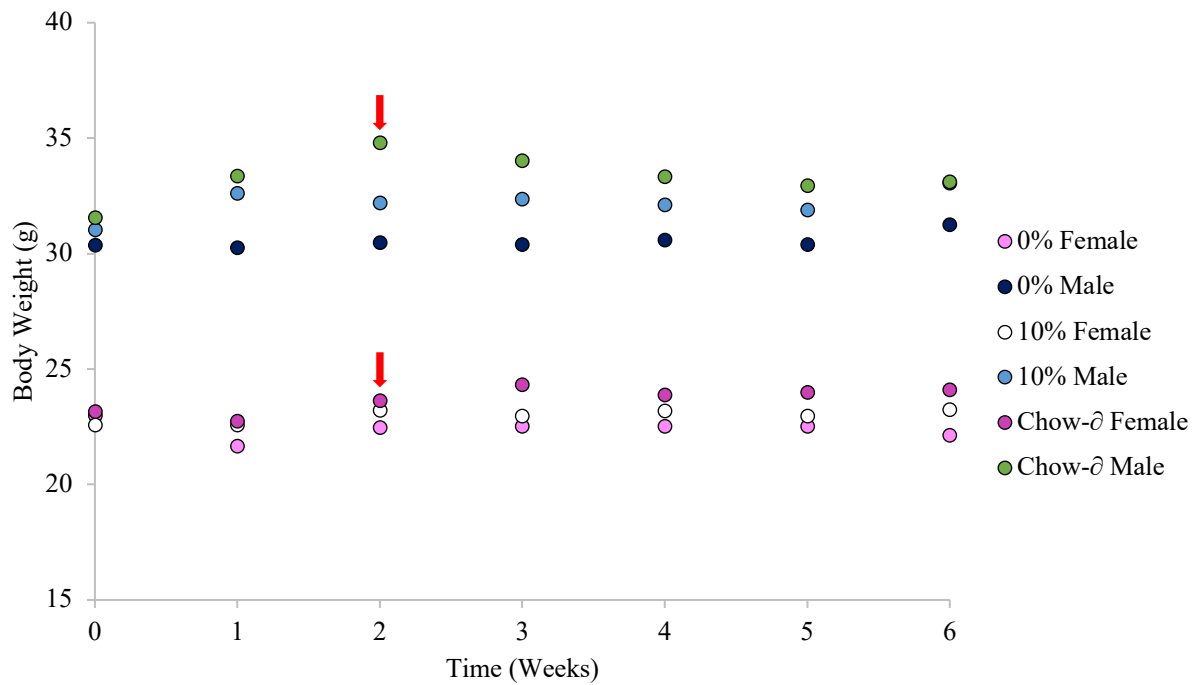


**Figure 3.1 Effect of sex by diet on body weight gain – FE1**

For analysis of body weight gain: n=3 for all groups. General linear model with repeated measures followed by Tukey’s Post-hoc test ( $p < 0.05$ ) was used to test for dietary treatment effects and sex by diet effects. Red arrows indicate the week the 20% diet was reverted to chow becoming Chow-∅ in male and female mice.

0%, 0% fructose; 10%, 10% fructose; Chow-∅, 20% fructose reverted to chow

### 3.1.2. Effect of Diet on Liver Weight

The wet liver weight for each animal was recorded at removal time during the necropsy. No statistical difference was observed across treatment groups (Figure 3.2). A sex effect was expected as the body weight of the males was larger than the females, as noted previously in Figure 3.1, which should correspond to larger organs; however, no sex effect or sex by diet effect was established (Appendix XII Figure A.2). To further investigate the relationship between body weight and liver weight, the wet mass of the liver for each animal was divided by the corresponding body weight to allow for a percent comparison between sexes.

After adjusting the liver weight of each animal by the corresponding body weight, the Chow- $\delta$  treatment had the smallest livers per gram body weight (Figure 3.3); although it tended to be smaller than both other treatments, significance was only observed between the Chow- $\delta$  and 0% fructose group ( $p=0.037$ ). When looking at sex as a factor, females tended to have larger livers per gram body weight than males, but this finding was not statistically significant (Appendix XII Figure A.3). Significance was also not present when investigating sex by diet interactions.

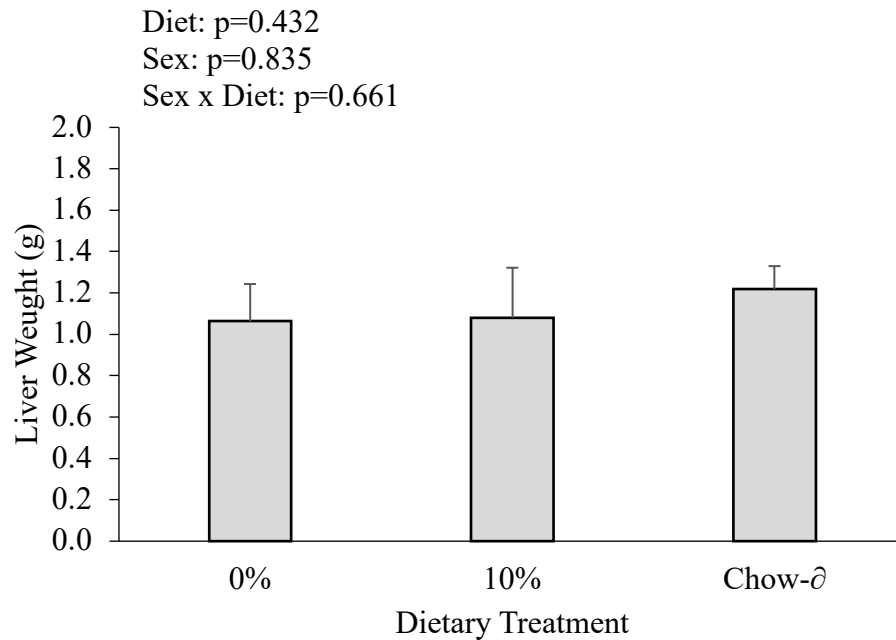


**Figure 3.2 Effect of diet on liver weight of FE1 mice**

Bars represent mean  $\pm$  standard deviations in grams. For analysis of liver weight: n=5 for 0%; n=6 for 10% and Chow-∂. Two-way ANOVA followed by Tukey's Post-hoc test ( $p < 0.05$ ) was used to test for dietary treatment effect. No differences were determined across treatment groups ( $p=0.432$ ).

0%, 0% fructose; 10%, 10% fructose; Chow-∂, 20% fructose reverted to chow

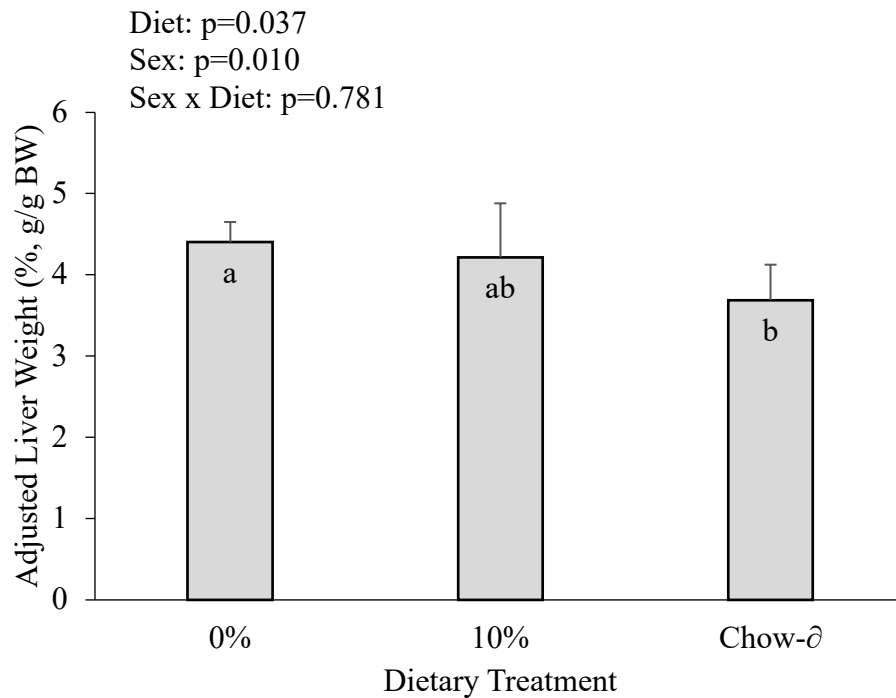


**Figure 3.3 Effect of diet on adjusted liver weight of FE1 mice**

Bars represent mean  $\pm$  standard deviations in percent body weight (% g/g body weight). For analysis of adjusted liver weight: n=5 for 0%; n=6 for 10% and Chow-∂. Two-way ANOVA followed by Tukey's Post-hoc test ( $p < 0.05$ ) was used to test for dietary treatment effect.

Differing letters denote a statistically significant difference in adjusted liver weight between dietary treatment groups ( $p=0.037$ ). However, due to low sample size per group at this level of analysis, this interaction may not be statistically relevant.

0%, 0% fructose; 10%, 10% fructose; 20%, Chow-∂, 20% fructose reverted to chow

### **3.1.3. Validation of Glucometer by Glucose Oxidase Method**

As previously stated, glucose concentrations were measured by glucometer and glucose oxidase plate assay. Glucometer readings were collected at all three time points, but glucose concentration by oxidase assay was only completed for the HP samples. To validate the glucometer readings for the other time points, blood glucose values acquired from HP samples ran by both methods ( $n = 47$ ) were plotted to form a linear regression (Figure 3.4). The correlation coefficient,  $R = 0.956$ , indicates a very strong correlation between the two methods, signifying that the use of a glucometer device is an effective method for obtaining blood glucose concentrations. It is important to note that the glucometer analyses whole blood, whereas oxidase assay method analyzes plasma; this factor could contribute to the small discrepancy between the two methods.

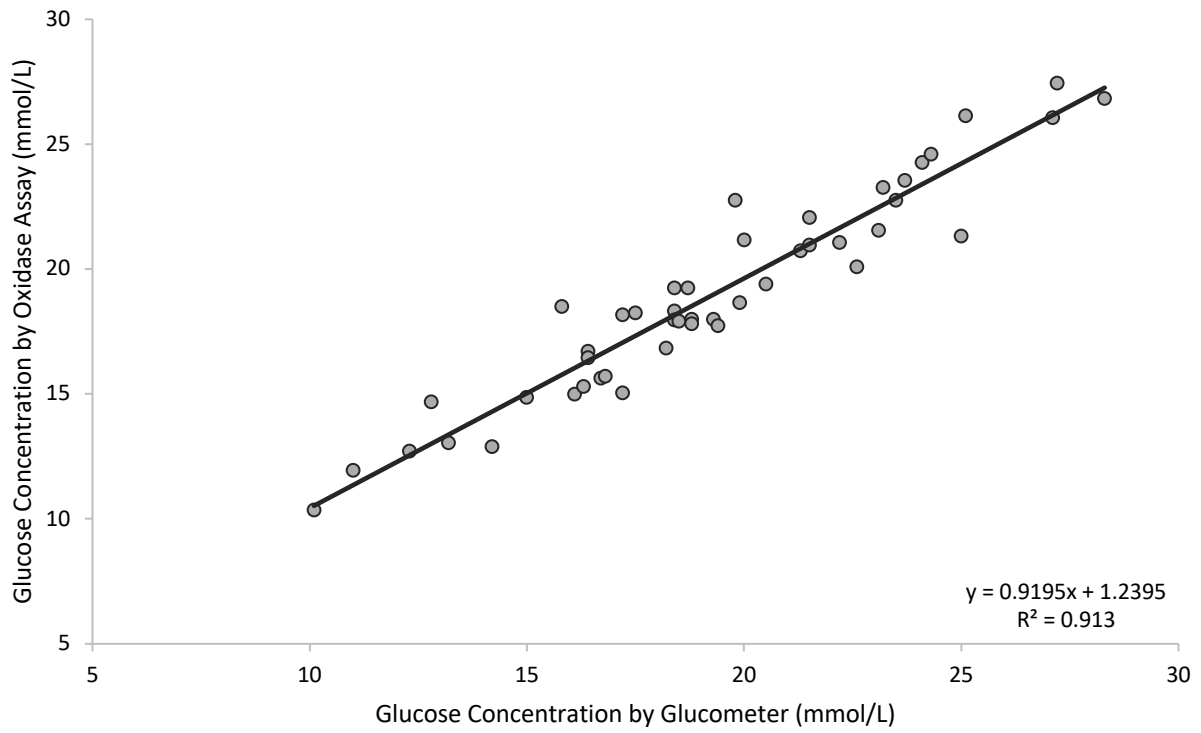


**Figure 3.4 Validation of glucometer method by glucose oxidase method**

### **3.1.1. Effect of Diet on Blood Glucose Concentrations**

Blood glucose concentrations (T=30 minutes) were similar across all dietary treatment groups with only slight variation; 0% fructose group had the highest blood glucose, followed by 10% fructose, and then slightly lower again in the Chow- $\delta$  group (Figure 3.5). Blood glucose concentrations were also very similar between sexes, representing both a lack of sex and sex by diet interaction (Appendix XII Figure A.3).

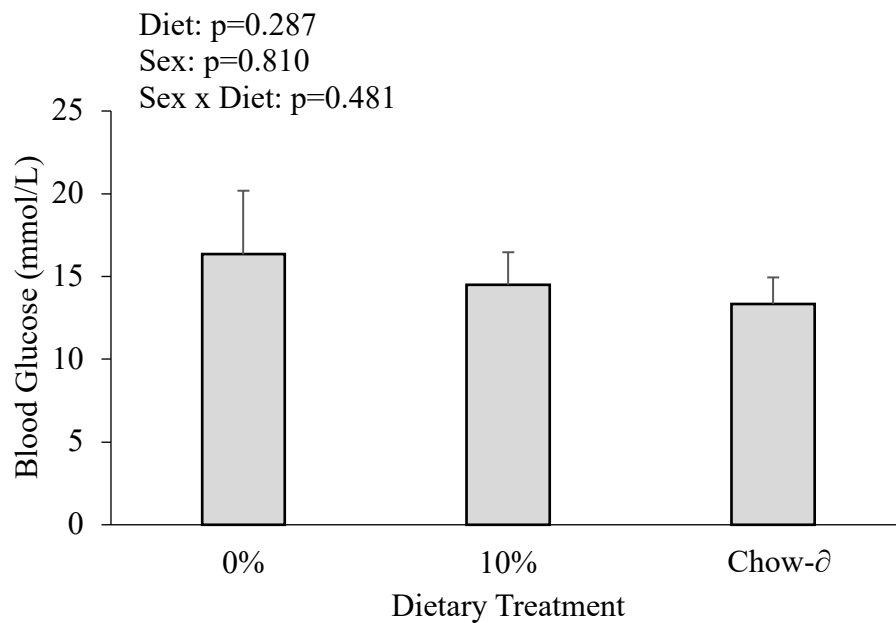


**Figure 3.5 Effect of diet on blood glucose by glucose oxidase method in FE1 mice**

Bars represent mean  $\pm$  standard deviations in mmol/L. For analysis of blood glucose, n=4 for 0%; n=5 for 10% and Chow-∅. Two-way ANOVA followed by Tukey's Post-hoc test ( $p < 0.05$ ) was used to test for dietary treatment effect. No differences were determined across treatment groups ( $p=0.810$ ).

0%, 0% fructose; 10%, 10% fructose; Chow-∅, 20% fructose reverted to chow

### 3.1.2. Effect of Diet on Lipid Quantification and Profile

#### 3.1.2.1. Fatty Acid Profile

The FA profile, categorized by SFAs, MUFAs, n-6 PUFAs, and n-3 PUFAs, was examined in the liver, RBCs, and heart tissue. The lipid profile of these samples are as follows.

The lipid profile differed by dietary treatment group in the liver, with dietary treatment effects in SFA ( $p=0.033$ ), MUFAs ( $p<0.001$ ), and n-6 PUFAs ( $p<0.001$ ) (Figure 3.6).

Investigating further into these differences, the Chow- $\delta$  group was statistically lower in SFAs when compared to the 0% group, but the 10% group was not statistically different from either Chow- $\delta$  or 0%. Concentrations of n-6 PUFAs were also significantly different across all three diets; concentrations were very high in the Chow- $\delta$  group, followed by the 0% group, and the 10% closely behind. Concentrations of n-3 PUFAs tended to be lower in the 0% group, but there were no statistical differences found. When investigating sex differences, statistical significance was only found in n-6 PUFAs, as males shifted higher than females for this FA profile (Appendix XII Figure A.4). No sex by diet interactions were present.

In the RBCs, the FA profile was similar across dietary treatment groups, differing only in MUFAs. All treatments statistically differed in MUFA concentrations; the Chow- $\delta$  group had the lowest, followed by the 0% group, and the 10% group had the highest concentration (Figure 3.7). Although there were no sex differences present for RBCs (Appendix XII Figure A.5), there were sex by diet effects present for all FA classifications: SFAs ( $p=0.035$ ), MUFAs ( $p=0.009$ ), n-6 PUFAs ( $p=0.027$ ), and n-3 PUFAs ( $p=0.004$ ).

In the heart tissue, the lipid profile shifted towards higher n-6 PUFAs concentrations in the Chow- $\delta$  group and shifted towards higher n-3 PUFAs concentrations in the 0% and 10% groups, but no statistical significance was observed across dietary treatment groups (Figure 3.8).

When investigating sex effects, males shifted towards higher n-6 PUFAs while females shifted towards higher n-3 PUFAs, but these shifts were not substantial enough to acquire statistical significance (Appendix XII Figure A.6). Additionally, no sex by diet interactions were found for the heart tissue.

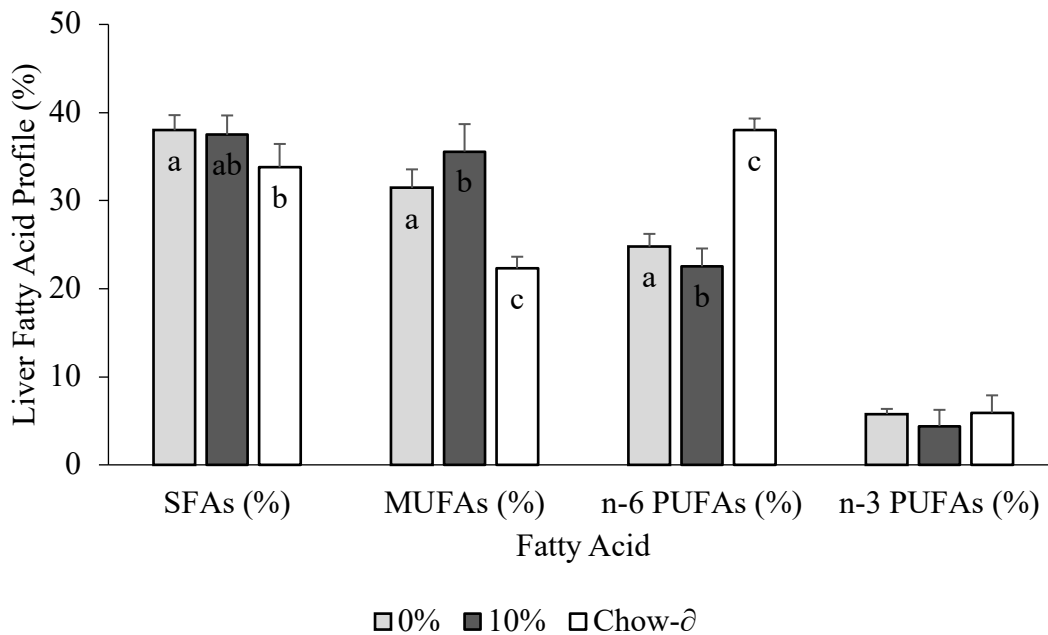


**Figure 3.6 Effect of diet on liver lipid profile of FE1 mice**

Bars represent mean  $\pm$  standard deviations in percent. For analysis of liver lipid profile: n=5 for 0%; n=6 for 10% and Chow-∂. Two-way ANOVA followed by Tukey's Post-hoc test ( $p < 0.05$ ) was used to test for dietary treatment effect. Differing letters for each class of FA (e.g. SFA) denotes statistical significance between dietary treatment group. However, due to low sample size per group at this level of analysis, this interaction may not be statistically relevant.

Diet: SFAs,  $p=0.033$ ; MUFAs,  $p<0.001$ ; n-6 PUFAs,  $p<0.001$ , n-3 PUFAs,  $p=0.303$

Sex: SFAs,  $p=0.970$ ; MUFAs,  $p=0.149$ ; n-6 PUFAs,  $p=0.007$ , n-3 PUFAs,  $p=0.781$

Sex x Diet: SFAs,  $p=0.884$ ; MUFAs,  $p=0.938$ ; n-6 PUFAs,  $p=0.268$ , n-3 PUFAs,  $p=0.706$

0%, 0% fructose; 10%, 10% fructose; Chow-∂, 20% fructose reverted to chow; SFAs, saturated fatty acids; MUFAs; monounsaturated fatty acids; n-6 PUFAs, omega-6 polyunsaturated fatty acids; n-3 PUFAs, omega-3 polyunsaturated fatty acids

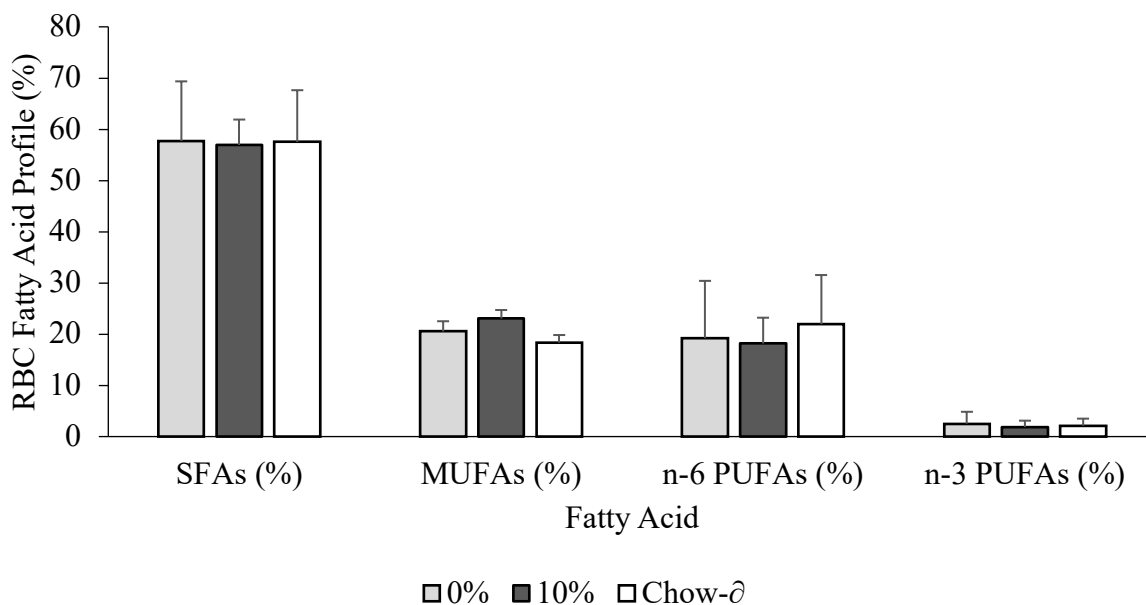


**Figure 3.7 Effect of diet on RBC lipid profile of FE1 mice**

Bars represent mean  $\pm$  standard deviations in percent. For analysis of RBC lipid profile: n=5 for 0% and 10%; n=6 for Chow-d. Two-way ANOVA followed by Tukey's Post-hoc test ( $p < 0.05$ ) was used to test for dietary treatment effect. No differences were determined across treatment groups.

Diet: SFAs,  $p=0.346$ ; MUFAs,  $p=0.765$ ; n-6 PUFAs,  $p=0.427$ , n-3 PUFAs,  $p=0.281$

Sex: **SFAs,  $p=0.001$** ; MUFAs,  $p=0.778$ ; n-6 PUFAs,  $p=0.389$ , n-3 PUFAs,  $p=0.792$

Sex x Diet: **SFAs,  $p=0.035$** ; **MUFAs,  $p=0.009$** ; **n-6 PUFAs,  $p=0.027$** , **n-3 PUFAs,  $p=0.004$**

0%, 0% fructose; 10%, 10% fructose; 20%, Chow-d, 20% fructose reverted to chow; SFAs, saturated fatty acids; MUFAs; monounsaturated fatty acids; n-6 PUFAs, omega-6 polyunsaturated fatty acids; n-3 PUFAs, omega-3 polyunsaturated fatty acids

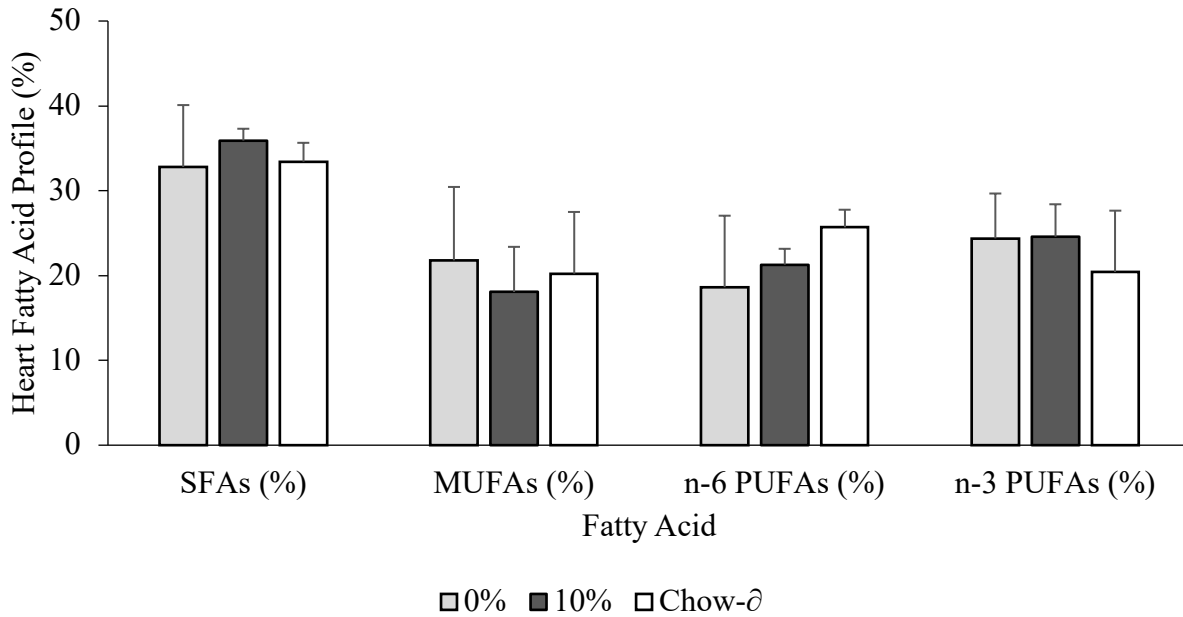


**Figure 3.8 Effect of diet on heart tissue lipid profile of FE1 mice**

Bars represent mean  $\pm$  standard deviations in percent. For analysis of heart tissue lipid profile: n=5 for 0% and 10%; n=6 for Chow-∅. Two-way ANOVA followed by Tukey's Post-hoc test ( $p < 0.05$ ) was used to test for dietary treatment effect. No differences were determined across treatment groups.

Diet: SFAs,  $p=0.822$ ; MUFAs,  $p=0.873$ ; n-6 PUFAs,  $p=0.165$ , n-3 PUFAs,  $p=0.438$

Sex: SFAs,  $p=0.644$ ; MUFAs,  $p=0.886$ ; n-6 PUFAs,  $p=0.138$ , n-3 PUFAs,  $p=0.535$

Sex x Diet: SFAs,  $p=0.423$ ; MUFAs,  $p=0.348$ ; n-6 PUFAs,  $p=0.482$ , n-3 PUFAs,  $p=0.873$

0%, 0% fructose; 10%, 10% fructose; 20%, Chow-∅, 20% fructose reverted to chow; SFAs, saturated fatty acids; MUFAs; monounsaturated fatty acids; n-6 PUFAs, omega-6 polyunsaturated fatty acids; n-3 PUFAs, omega-3 polyunsaturated fatty acids

### 3.1.2.2. Cholesterol Lipoprotein Quantification

Total plasma cholesterol concentrations (T=30 minutes) were similar across all dietary treatment groups and no statistical significance was observed (Figure 3.9). Although fructose content did not affect total cholesterol, sex was a factor ( $p=0.002$ ). Cholesterol concentrations were nearly two-fold higher in males than females for the 0% and 10% fructose groups and were confirmed to be statistically different by Student T-Test for these two treatment groups; there were no sex by diet effects in the Chow- $\delta$  group (Appendix XII Figure A.7). A sex by diet interaction was trending, but not achieved as the significance value was  $p=0.059$ .

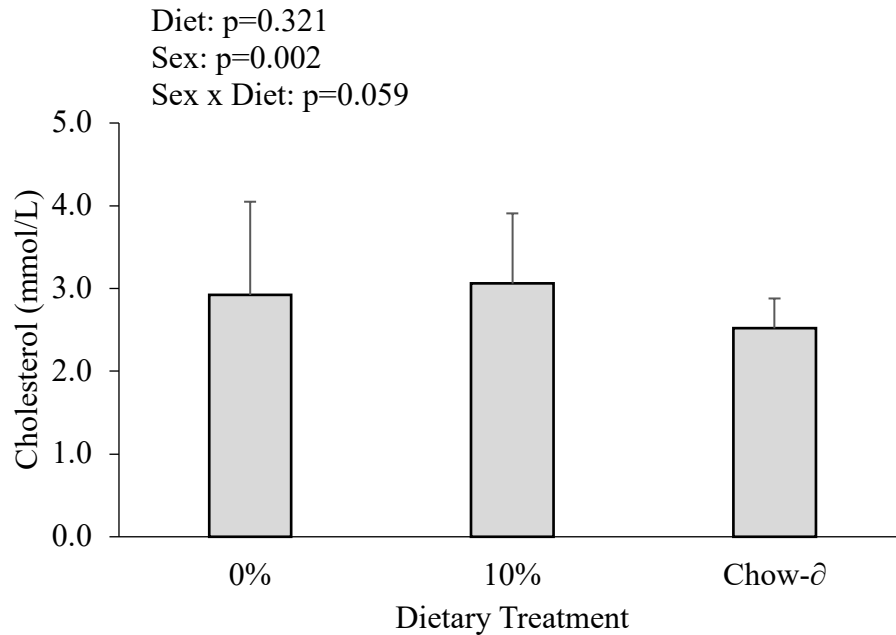


**Figure 3.9 Effect of diet on mean total plasma cholesterol of FE1 mice**

Bars represent mean  $\pm$  standard deviations in mmol/L. For analysis of total plasma cholesterol: n=4 for 0% and Chow-∂; n=5 for 10%. Two-way ANOVA followed by Tukey's Post-hoc test ( $p < 0.05$ ) was used to test for dietary treatment effect. No differences were determined across treatment groups ( $p=0.321$ ).

0%, 0% fructose; 10%, 10% fructose; Chow-∂, 20% fructose reverted to chow

### **3.1.2.3. Triacylglycerol Quantification**

Plasma TAG concentrations (T=30 minutes) slightly decreased across groups with 0% at the highest concentration and Chow- $\delta$  at the lowest; however, no statistical significance was observed (Figure 3.10). After separating by sex, TAG concentrations remained stable across all treatment groups (Appendix XII Figure A.8). No statistical differences were observed when looking at sex alone, or sex by diet as a factor.

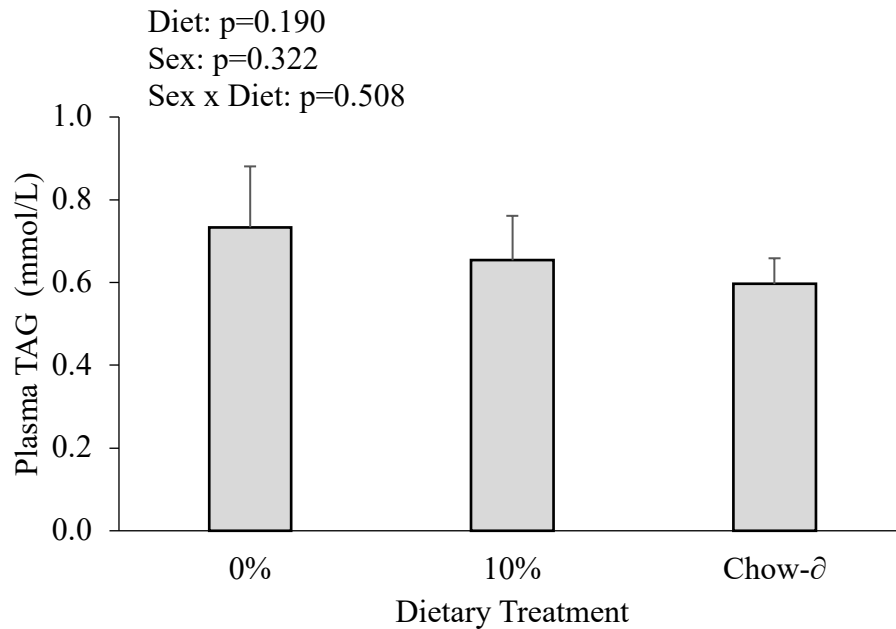


**Figure 3.10 Effect of diet on mean plasma TAG concentrations of FE1 mice**

Bars represent mean  $\pm$  standard deviations in mmol/L. For analysis of plasma TAG concentrations: n=4 for 0%; n=5 for 10%; n=6 for Chow-∅. Two-way ANOVA followed by Tukey's Post-hoc test ( $p < 0.05$ ) was used to test for dietary treatment effect. No differences were determined across treatment groups ( $p=0.190$ ).

0%, 0% fructose; 10%, 10% fructose; Chow-∅, 20% fructose reverted to chow

#### **3.1.2.4. HDL Cholesterol Quantification**

Concentrations of c-HDL in plasma (T=30 minutes) was higher in the 10% fructose treatment group but similar in the 0% fructose and Chow- $\delta$  treatment groups; fructose content therefore did lead to a statistical difference in HDL concentrations (Figure 3.11). Sex was also a factor; although males displayed significantly higher concentrations of c-HDL than females when grouped by sex alone ( $p=0.016$ ), specifically in the Chow- $\delta$  group, this significance was not present when investigating sex by diet interactions (Appendix XII Figure A.9). After further analysis, within treatment group effects were confirmed to be statistically different by Student T-Test.

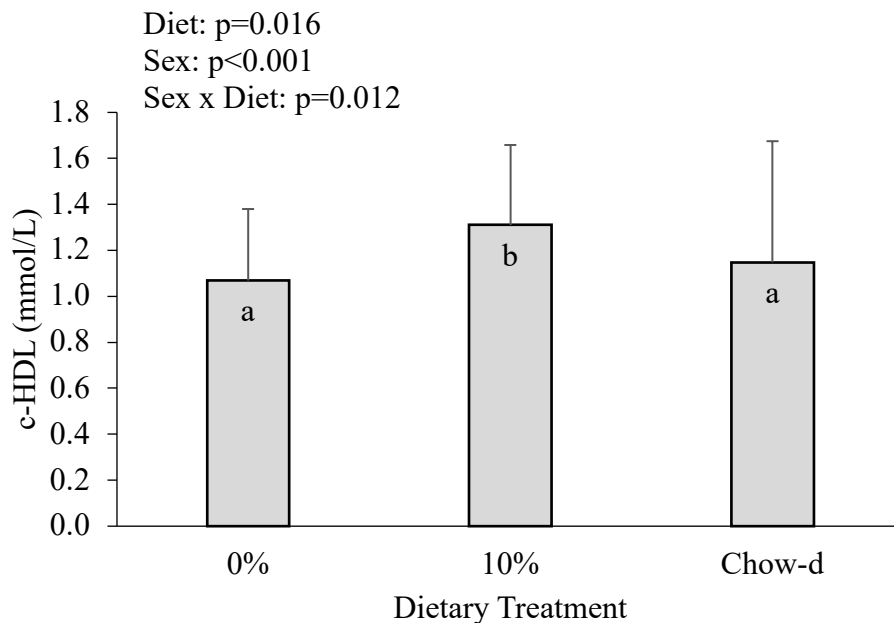


**Figure 3.11 Effect of diet on mean plasma c-HDL cholesterol concentrations of FE1 mice**

Bars represent mean  $\pm$  standard deviations. For analysis of plasma c-HDL concentrations: n=4 for 0%; n=5 for 10% and Chow-d. Two-way ANOVA followed by Tukey's Post-hoc test ( $p < 0.05$ ) was used to determine differences by dietary treatment, sex, and sex by diet interactions.

Differing letters denote a statistically significant difference in mean c-HDL cholesterol

concentrations between dietary treatment groups. Female c-HDL values were lower than males

( $p < 0.001$ ) and a sex by diet interaction was noted ( $p = 0.012$ ). However, due to low sample size

per group at this level of analysis, this interaction may not be statistically relevant.

0%, 0% fructose; 10%, 10% fructose; Chow-d, 20% fructose reverted to chow

### 3.1.2.5. Non-HDL Cholesterol Quantification

Non-HDL concentrations were quantified by finding the difference between total cholesterol and c-HDL cholesterol concentrations. Non-HDL concentrations were similar across the 0% and 10% fructose groups, but lower in the Chow- $\delta$  group; however, no statistical significance was present (Figure 3.12). Although fructose content did not affect non-HDL concentrations, sex was a factor. Non-HDL concentrations were higher in males than females for the 0% and 10% treatment groups, and the Chow- $\delta$  diet had the opposite effect where females had 2-fold higher concentrations than the males (Appendix XII Figure A.10). There was also a sex by diet interaction with  $p=0.04$ .

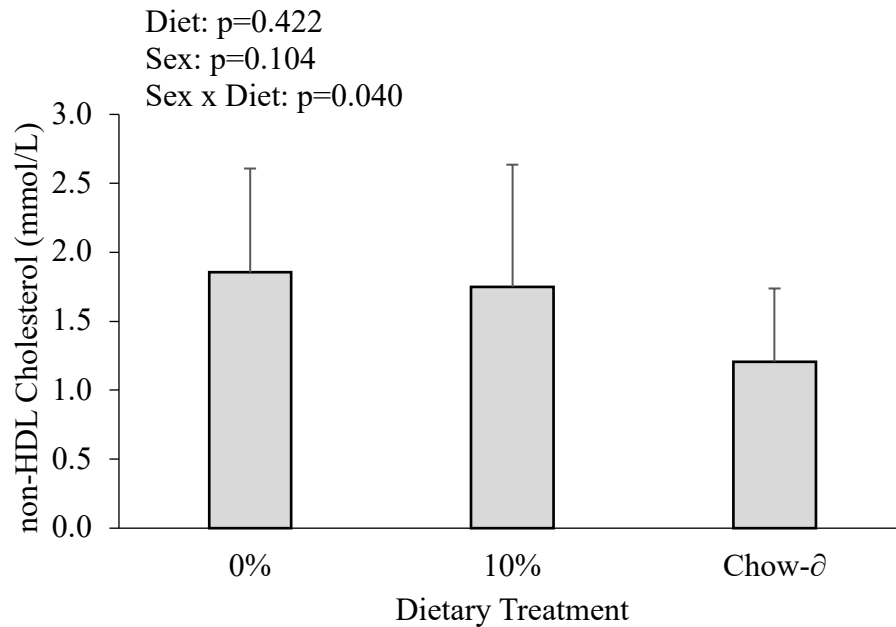


**Figure 3.12 Effect of diet on mean plasma non-HDL cholesterol concentrations of FE1 mice**

Bars represent mean  $\pm$  standard deviations in mmol/L. For analysis of plasma non-HDL concentrations: n=4 for 0% and Chow- $\delta$ ; n=5 for 10%. Two-way ANOVA followed by Tukey's Post-hoc test ( $p < 0.05$ ) was used to test for dietary treatment effect. No differences were determined across treatment groups ( $p=0.422$ ).

0%, 0% fructose; 10%, 10% fructose; 20%, 20% fructose

## **3.2. Fructose Energy Study 2**

### **3.2.1. Effect of Diet on Dietary Intake**

Dietary intake was tracked for three consecutive days as is presented in Figure 3.13. Tracking was only done in a small sample size (n=12) of the animals to ensure enough food was provided to allow for *ad libitum* feeding. Although the animals consuming 20% fructose averaged the lowest food intake, all animals tested consumed similar quantities and there were no statistical differences in food intake between treatment groups. Sex was also not a factor as males and females tracked comparable food intakes for each treatment.

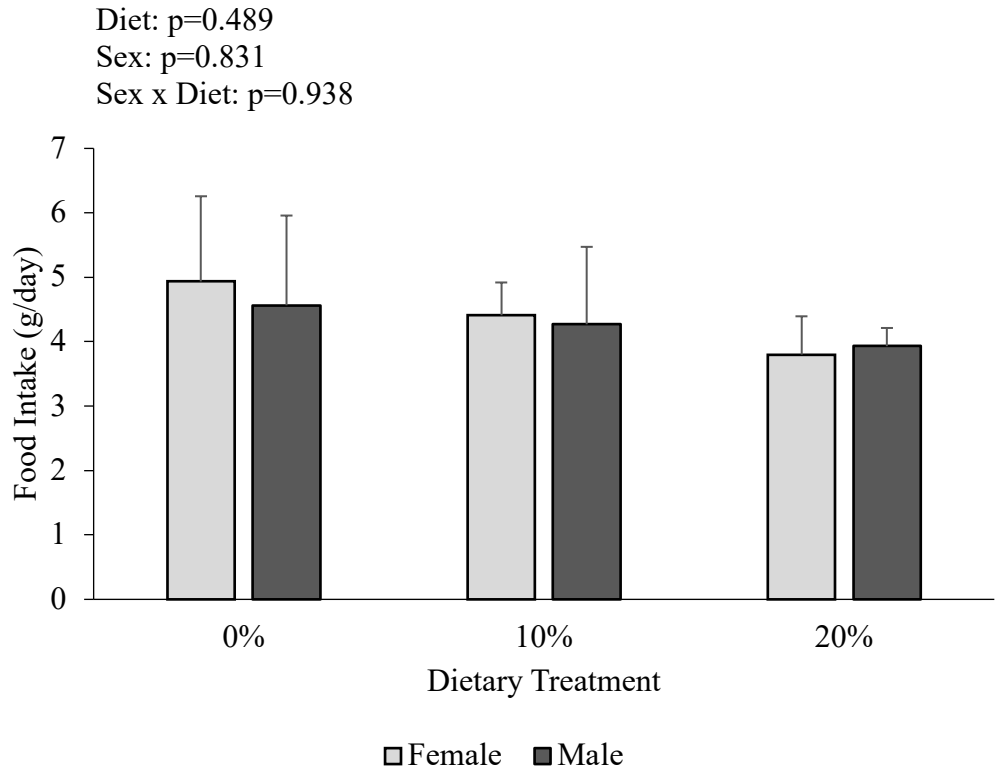


**Figure 3.13 Effect of sex by diet on dietary intake in FE2 mice**

Bars represent mean  $\pm$  standard deviations in g/day. For analysis of dietary intake, n=4 for 0, 10%, and 20%. A two-way ANOVA followed by Tukey's Post-hoc test ( $p < 0.05$ ) was used to test for dietary treatment effect. No differences were determined across dietary treatment groups ( $p=0.489$ ). Additionally, there were no differences determined between sex within the same dietary treatment or within the same sex across dietary treatment.

0%, 0% fructose; 10%, 10% fructose; 20%, 20% fructose

### 3.2.2. Effect of Diet on Body Weight Gain

Body weight was measured and recorded on a bi-weekly basis throughout the 9-week grow-out period (represented by negative weeks) followed by a 15-week dietary treatment. Referring to Figure 3.14 below, all dietary groups gained weight similarly over the entirety of the study, when grouped by sex; however, there was a clear sex difference throughout both periods of the study. Males began the study at a larger weight and continued to gain more weight on average per week (slope = 0.732 g/week) than females (slope = 0.419 g/week) during the grow-out period; this difference was exacerbated upon initiating the treatment diets. Upon initiating the dietary treatments, represented by week 0, there was a large spike in male body weight across all treatment groups that was not present in females between weeks 0 and 1. Although this immediate weight increase was unique to males, the average weight gain per week during the treatment period approximately doubled in both sexes from their initial slope calculated in the grow-out period (males = 1.261 g/week, females = 0.873 g/week). Although there were no statistical differences between dietary treatment groups in average weight gain, the 10% fructose diet trended slightly higher in both males and females, followed by 0% fructose, and then 20% fructose.

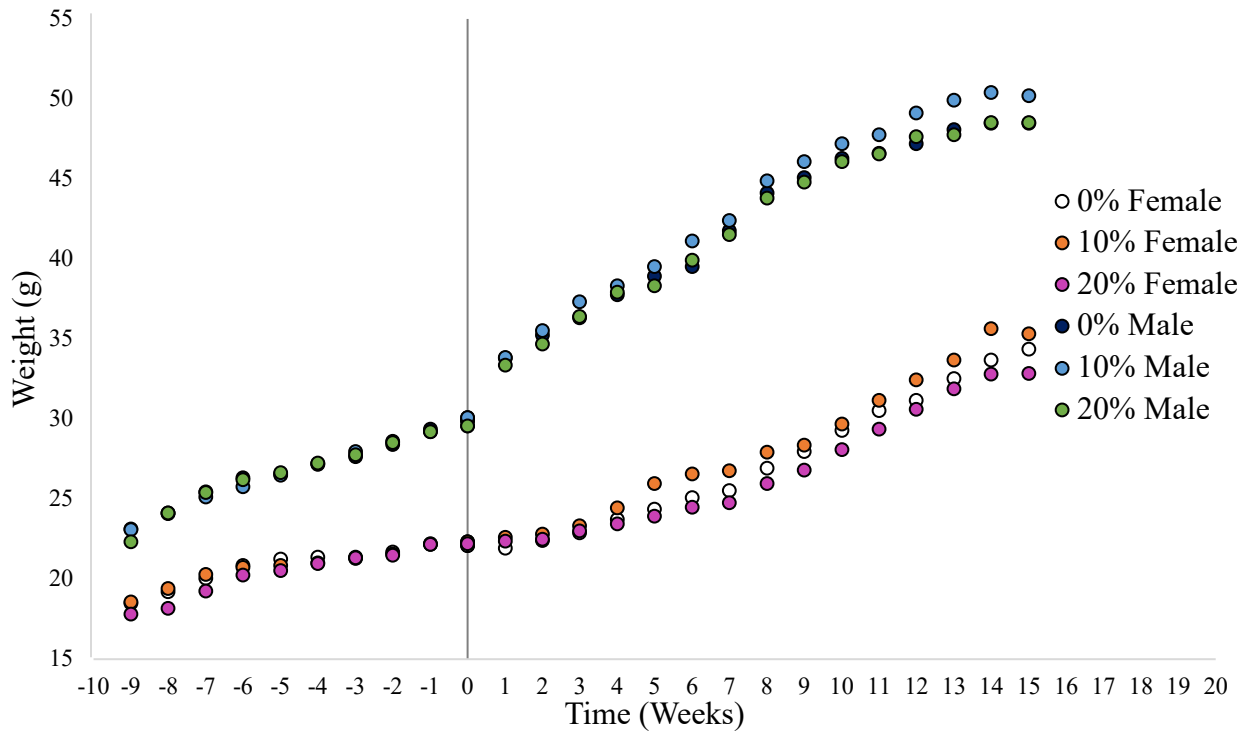


**Figure 3.14 Effect of sex by diet on body weight gain in FE2 mice**

Lines represent mean body weight in grams. For analysis of body weight gain: n=8 for 0% females, and 10% males; n=9 for 10% and 20% females, 0% and 20% males. General linear model with repeated measures followed by Tukey's Post-hoc test ( $p < 0.05$ ) was used to test for dietary treatment effects and sex by diet effects.

0%, 0% fructose; 10%, 10% fructose; 20%, 20% fructose

### **3.2.3. Effect of Added Sugars on Glucose and Fructose Metabolism**

#### **3.2.3.1. Glucometer**

Glucometer readings were recorded at three time points – two prior to necropsy and one during necropsy – to acquire immediate readings that would later be validated by a glucose oxidase plate assay. Baseline blood glucose concentrations were similar across all groups (Figure 3.15A) and tended to be slightly higher in males than females (Appendix XII Figure A.11 - A), but this difference was not statistically significant. Similarly, blood glucose concentrations across treatment groups were comparable at the T=15-minute timepoint (Figure 3.15B) but tended to be slightly higher in females (Appendix XII Figure A.11 - B); however, there were no significant differences. Consistent with the other timepoints, there was only slight variation at T=30-minutes across treatment groups (Figure 3.15C). Interestingly, when looking just at sex, females did have higher blood glucose concentrations than their male counterparts at T=30 minutes ( $p = 0.039$ ). When data were split by sex alone, there was no significance, but there is a sex by diet interaction present at the 30-minute timepoint (Appendix XII Figure A.11 - C).

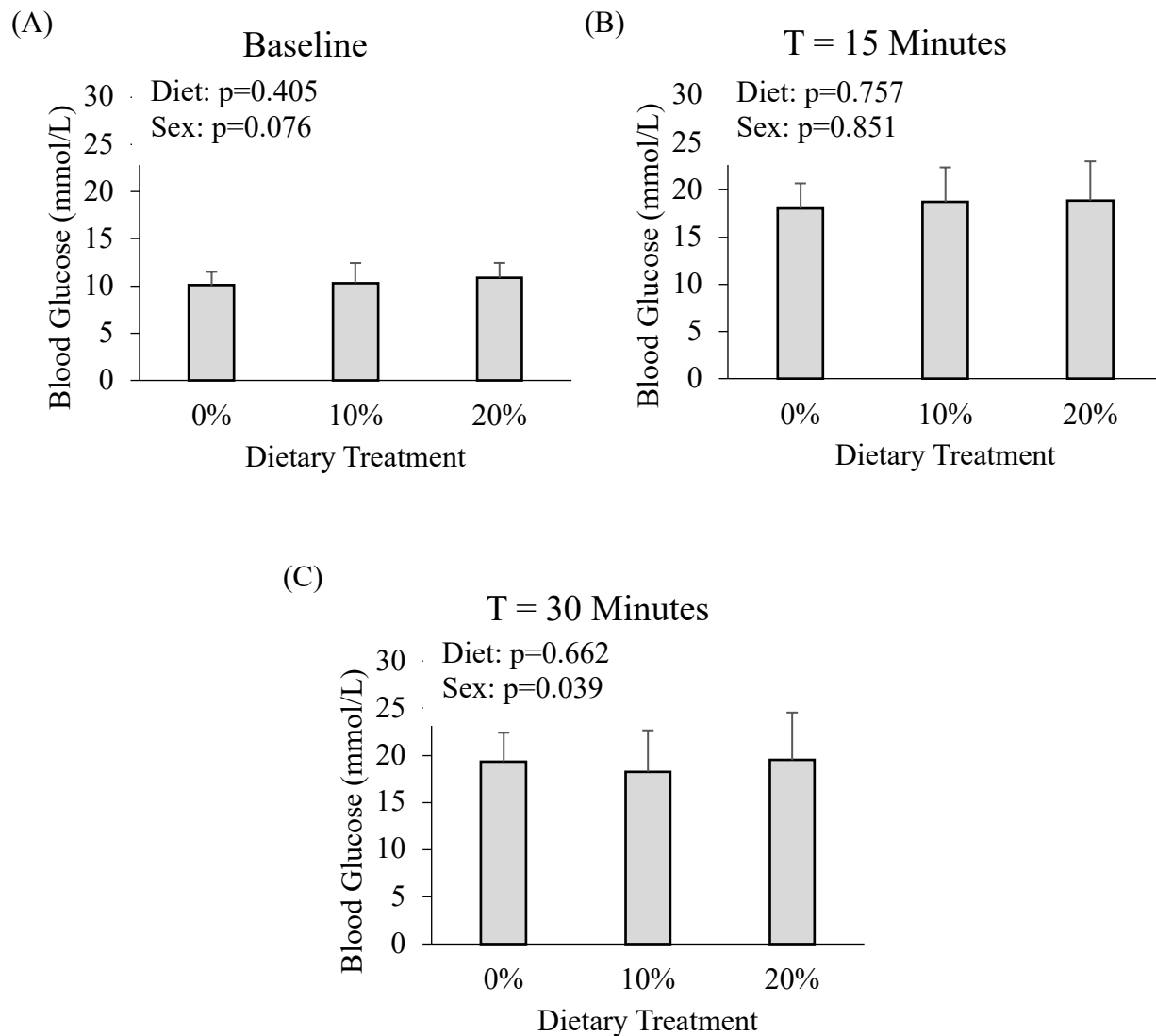


**Figure 3.15 Effect of diet on blood glucose concentration at various time points in FE2 mice**

(A) Baseline, T = 0 minutes (B) T = 15 minutes (C) HP, T = 30 minutes

Bars represent mean  $\pm$  standard deviations in mmol/L. For analysis of blood glucose

concentration:  $n=18$  for 0% and 10%;  $n=17$  for 20%. Two-way ANOVA followed by Tukey's

Post-hoc test ( $p < 0.05$ ) was used to test for dietary treatment effect. No dietary differences were

determined across treatment groups at any timepoint (baseline,  $p=0.405$ ; 15 minutes,  $p=0.757$ ; 30

minutes,  $p=0.662$ ). 0%, 0% fructose; 10%, 10% fructose; 20%, 20% fructose

### **3.2.3.2. Glucose Oxidase**

Blood glucose concentrations (T=30 minutes) were run by glucose oxidase plate assay method to validate the glucometer data collected during necropsy. Blood glucose concentrations were similar across all dietary treatment groups and no statistical significance was observed (Figure 3.16). Although fructose content did not affect blood glucose, sex was a factor ( $p = 0.036$ ). Unlike the glucometer data at this timepoint, females tended to have higher blood glucose than males across all dietary treatments, but this difference was not significant as there was a lack of sex by diet interaction (Appendix XII Figure A.12).

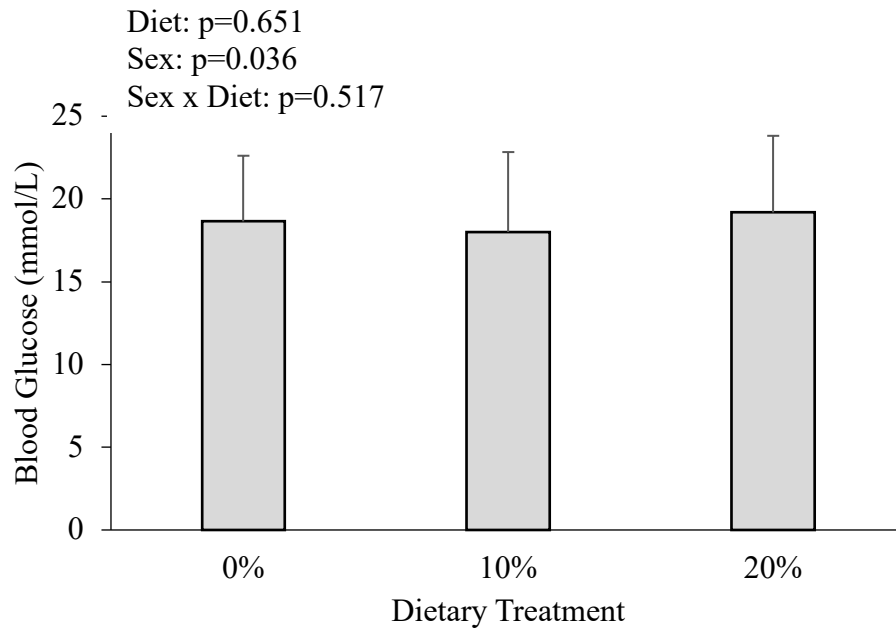


**Figure 3.16 Effect of diet on blood glucose by glucose oxidase method in FE2 mice**

Bars represent mean  $\pm$  standard deviations in mmol/L. For analysis of blood glucose, n=17 for 0%, 10%, and 20%. Two-way ANOVA followed by Tukey's Post-hoc test ( $p < 0.05$ ) was used to test for dietary treatment effect. No differences were determined across treatment groups ( $p = 0.651$ ).

0%, 0% fructose; 10%, 10% fructose; 20%, 20% fructose

### 3.2.3.3. Isotopic Enrichment by GC-MS

To study systemic fructose metabolism, fasted mice were gavaged with a 1:1 mixture of glucose to U-<sup>13</sup>C-fructose. The labelled carbons were then traced by GC-MS to investigate if the conversion rate of fructose to glucose was dependent on previous fructose exposure through the diet. The tracer:tracee ratios (TTR) for ions associated with glucose and fructose metabolism were calculated to determine enrichment. An increase in the TTR indicates a higher amount of orally provided <sup>13</sup>C-fructose tracer appearing in fructose and glucose in blood. This increase in TTR, particularly in glucose, indicates metabolism of fructose occurring in the enterocyte and liver. There were three ion pairs monitored for glucose (133 m/z:131 m/z, 191 m/z:189 m/z, 293 m/z:298 m/z) and two ion pairs monitored for fructose (104:101 m/z, 206:203 m/z) to establish the if dietary treatment impacted the conversion of fructose to glucose. Feeding 20% fructose content in the diet was associated with a lower TTR for both fructose ion pairs (Figure 3.18); the effect of diet on lower TTR was trending for 104:101 m/z but was found to be significant for 206:203 m/z (p=0.010). When investigating sex by diet effects, the lower TTR previously noted appears to be a result of females having a lower TTR than males in the 20% fructose group (Appendix XII Figure A.13); similar to diet effects, although the females had a lower TTR than their male counterparts consuming the 20% fructose diet, this difference was trending for 104:101 m/z but significant for 206:203 m/z (p=0.038).

When investigating glucose metabolism, dietary fructose was associated with an increase in TTR for all three ion pairs; the TTR for the 20% treatment group was higher than the 10% fructose group, indicating that this conversion occurs in a dose dependent manner (Figure 3.19). When looking at within diet effects, female mice consuming 10% fructose had a higher TTRs than males for all ion pairs, and this difference was statistically significant for ions 133 m/z:131

m/z and 191 m/z:189 m/z. Female mice consuming 20% fructose also had a higher TTRs than males for all ion pairs, all this was found to be statistically different for all groups (Appendix XII Figure A.14). A sex by diet difference was not statistically present for isotopic enrichment.

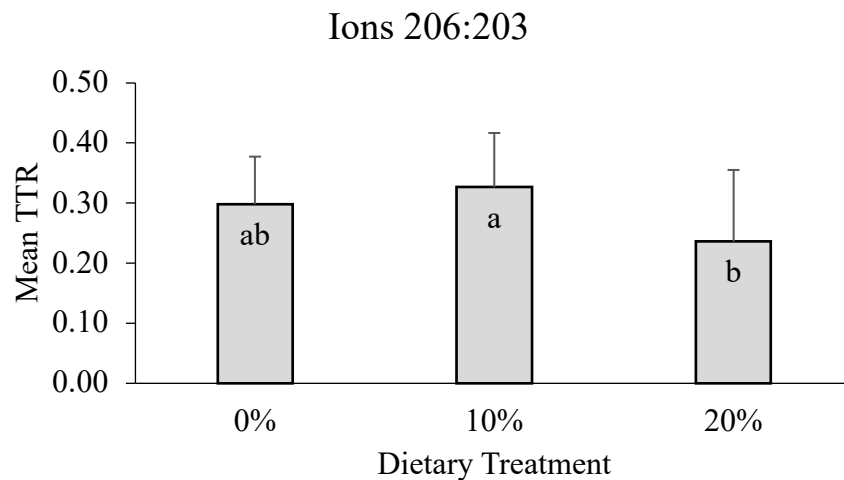
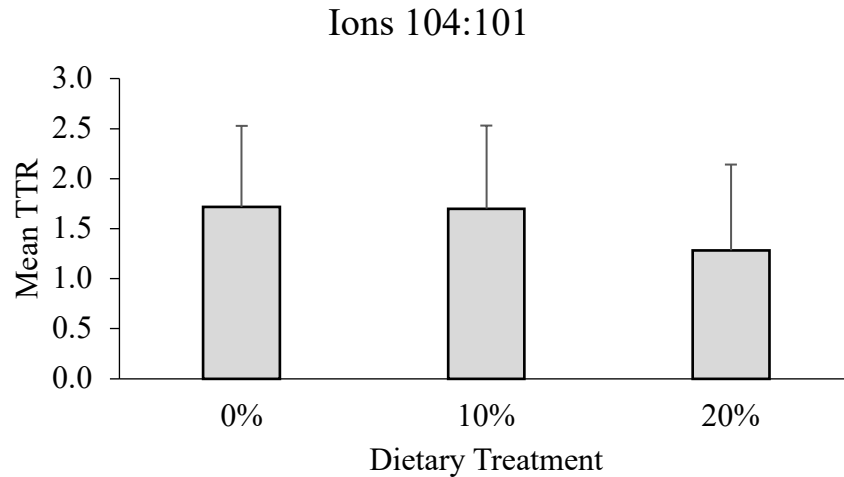


**Figure 3.17 Effect of diet on mean fructose TTR for various ions at T = 30 minutes in FE2 mice**

Bars represent mean  $\pm$  standard deviations in percent. For analysis of mean TTR: n=14 for 0%; n=17 for 10%; n=15 for 20%. Two-way ANOVA followed by Tukey's Post-hoc test ( $p < 0.05$ ) was used to test for dietary treatment effect. Additionally, Student T-Test ( $p < 0.05$ ) was used to test for within diet effects. Differing letters denote a statistically significant difference in mean TTR between dietary treatment groups.

0%, 0% fructose; 10%, 10% fructose; 20%, 20% fructose

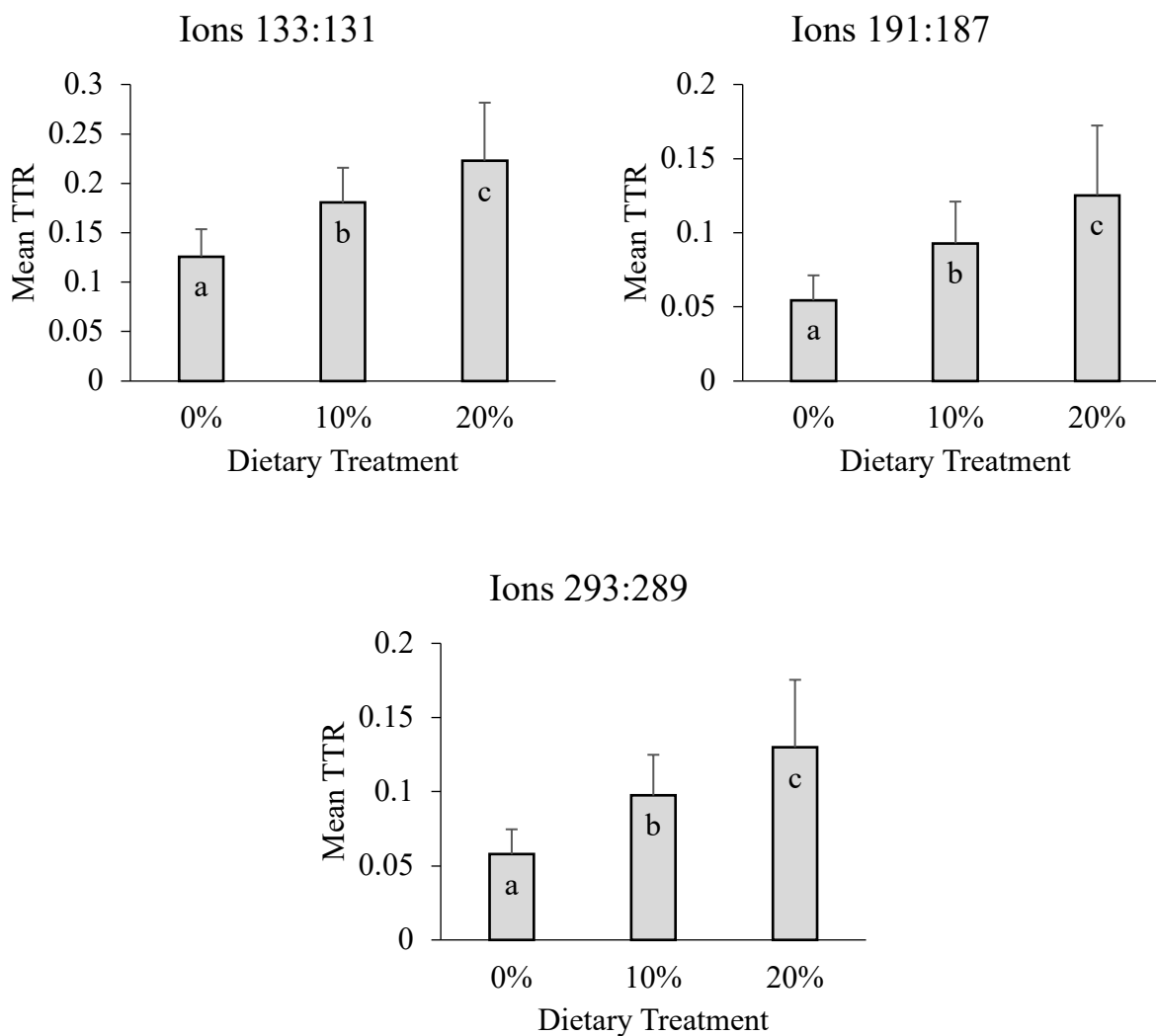


**Figure 3.18 Effect of diet on mean glucose TTR for various ions at T = 30 minutes in FE2 mice**

Bars represent mean  $\pm$  standard deviations in percent. For analysis of mean TTR: n=17 for 0%; n=16 for 10%; n=15 for 20%. Two-way ANOVA followed by Tukey's Post-hoc test ( $p < 0.05$ ) was used to test for dietary treatment effect. Additionally, Student T-Test ( $p < 0.05$ ) was used to test for within diet effects. Differing letters denote a statistically significant difference in mean TTR between dietary treatment groups.

0%, 0% fructose; 10%, 10% fructose; 20%, 20% fructose

### **3.2.4. Effect of Diet on Lipid Profile**

#### **3.2.4.1. Effect of Diet on Liver Weight**

The wet liver weight for each animal was recorded at removal time during the necropsy. No statistical difference was observed across treatment groups (Figure 3.19), but there was a significant sex-based difference observed ( $p < 0.001$ ): the significance of this finding was confirmed by Student T-Test (Appendix XII Figure A.15). A sex effect was expected as the body weight of the males was much larger than the females, as observed previously in Figure 3.14, which should correspond to larger organs. To account for the difference in body weight, the liver weight value for each animal was divided by the corresponding body weight for each mouse to allow for a percent comparison between sexes.

After adjusting the liver weight of each animal by the corresponding body weight, as before, no statistical significance was observed across treatment groups (Figure 3.20). Although fructose content did not affect adjusted liver weight, sex was still a factor ( $p < 0.001$ ). Even after correcting liver weight by body weight, male livers were approximately three-fold larger than their female counterparts across all dietary treatment groups. Although this within treatment effect was evident and confirmed by Student T-Test, there was no sex by diet interaction present (Appendix XII Figure A.16).

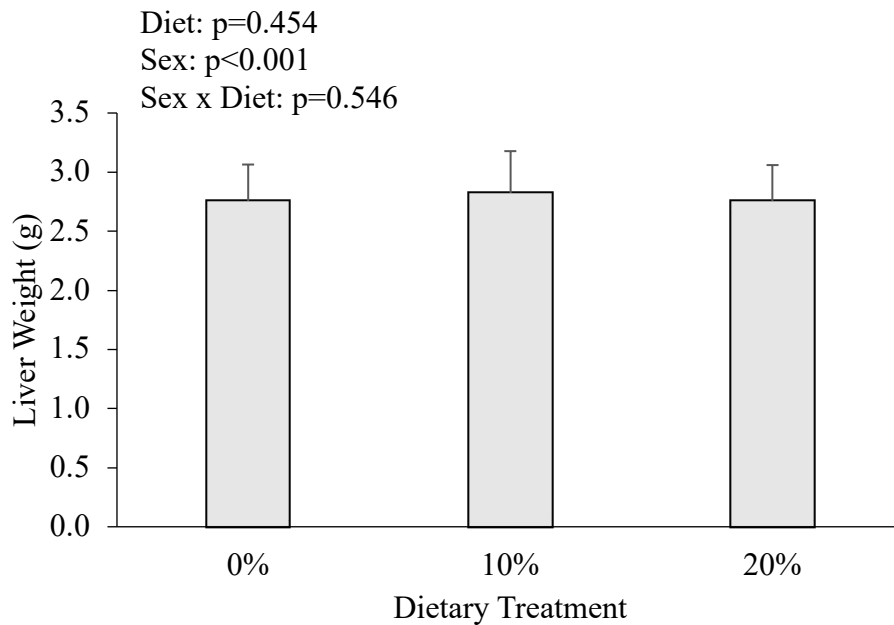


**Figure 3.19 Effect of diet on liver weight of FE2 mice**

Bars represent mean  $\pm$  standard deviations in grams. For analysis of liver weight, n=17 for 0% and 10%, n=18 for 20%. Two-way ANOVA followed by Tukey's Post-hoc test ( $p < 0.05$ ) was used to test for dietary treatment effect. No differences were determined across treatment groups ( $p=0.454$ ).

0%, 0% fructose; 10%, 10% fructose; 20%, 20% fructose

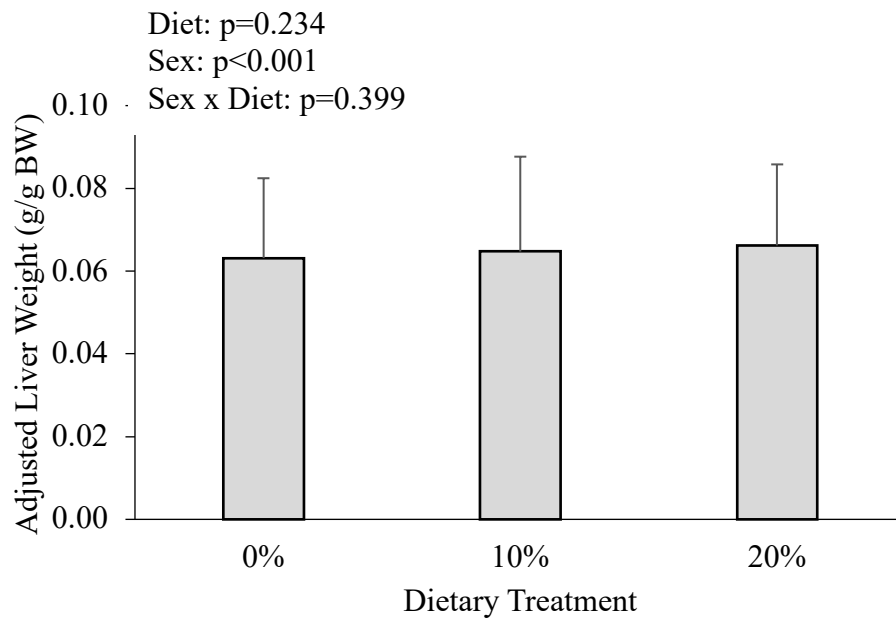


**Figure 3.20 Effect of diet on adjusted liver weight of FE2 mice**

Bars represent mean  $\pm$  standard deviations in percent body weight (g/g body weight). For analysis of adjusted liver weight: n=17 for 0% and 10%; n=18 for 20%. Two-way ANOVA followed by Tukey's Post-hoc test ( $p < 0.05$ ) was used to test for dietary treatment effect. No differences were determined across treatment groups ( $p < 0.001$ ).

0%, 0% fructose; 10%, 10% fructose; 20%, 20% fructose

#### **3.2.4.2. Fatty Acid Profile**

The FA profile, categorized by SFAs, MUFAs, n-6 PUFAs, and n-3 PUFAs, was examined in the RBCs, and the liver. The lipid profile of these samples are as follows.

In the RBCs, the lipid profile remained consistent across all dietary treatment groups and no statistical significance was observed (Figure 3.21). When investigated by sex, males trended towards higher MUFAs while females trended towards higher SFAs, n-3 and n-6 PUFAs, but these shifts were not substantial enough to acquire statistical significance (Appendix XII Figure A.17).

In the liver, the lipid profile remained consistent across all dietary treatment groups and no statistical significance was observed (Figure 3.22). Although fructose content did not affect the lipid profile in this organ, sex was a factor. When investigated by sex alone, males displayed a shift towards higher MUFAs concentrations while females shifted towards higher SFAs, n-3 and n-6 PUFAs concentrations; all four categories of the lipid profile were therefore statistically significant when investigated in male versus female mice (SFAs,  $p=0.390$ ; MUFAs,  $p=0.414$ ; n-6 PUFAs,  $p=0.567$ , n-3 PUFAs,  $p=0.718$ ), however, no sex by diet interactions were present (Appendix XII Figure A.18).

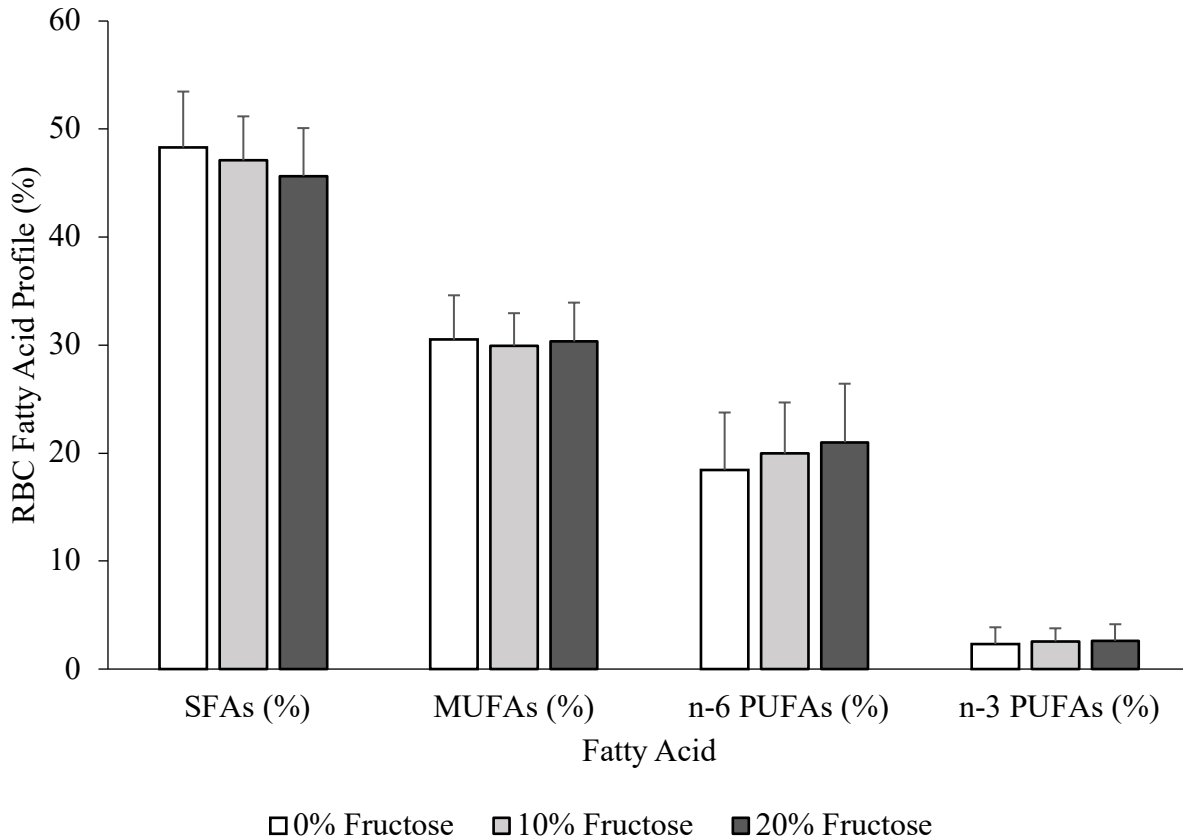


**Figure 3.21 Effect of diet on RBC lipid profile of FE2 mice**

Bars represent mean  $\pm$  standard deviations in percent. For analysis of RBC lipid profile, n=18 for 0% and 10%, n=17 for 20%. Two-way ANOVA followed by Tukey's Post-hoc test ( $p < 0.05$ ) was used to test for dietary treatment effect. No differences were determined across treatment groups.

Diet: SFAs,  $p=0.240$ ; MUFAs,  $p=0.883$ ; n-6 PUFAs,  $p=0.349$ , n-3 PUFAs,  $p=0.818$

Sex: SFAs,  $p=0.212$ ; MUFAs,  $p=0.415$ ; n-6 PUFAs,  $p=0.481$ , n-3 PUFAs,  $p=0.880$

Sex x Diet: SFAs,  $p=0.977$ ; MUFAs,  $p=0.485$ ; n-6 PUFAs,  $p=0.640$ , n-3 PUFAs,  $p=0.741$

0%, 0% fructose; 10%, 10% fructose; 20%, 20% fructose; SFAs, saturated fatty acids; MUFAs; monounsaturated fatty acids; n-6 PUFAs, omega-6 polyunsaturated fatty acids; n-3 PUFAs, omega-3 polyunsaturated fatty acids

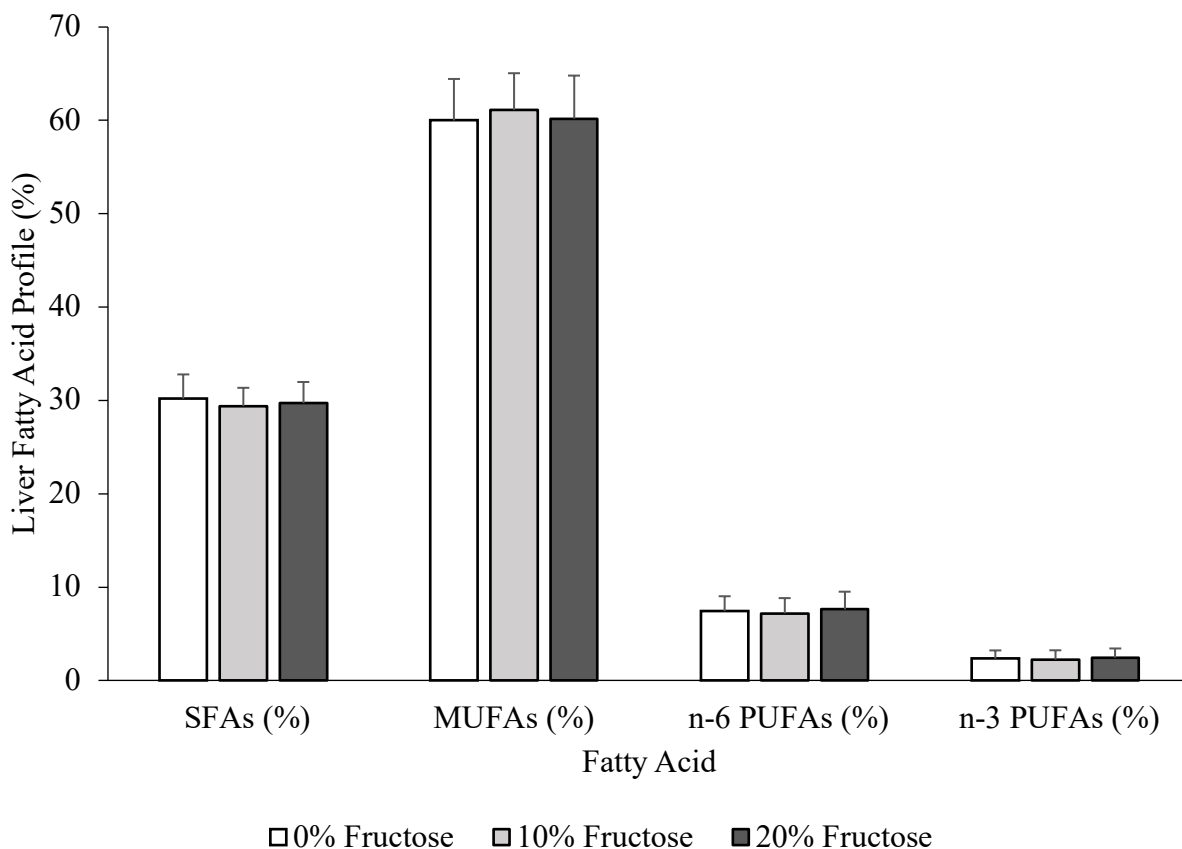


**Figure 3.22 Effect of diet on liver lipid profile of FE2 mice**

Bars represent mean  $\pm$  standard deviations in percent. For analysis of liver lipid profile: n=17 for 0%; n=18 for 10% and 20%. Two-way ANOVA followed by Tukey's Post-hoc test ( $p < 0.05$ ) was used to test for dietary treatment effect. No differences were determined across treatment groups.

Diet: SFAs,  $p=0.390$ ; MUFAs,  $p=0.414$ ; n-6 PUFAs,  $p=0.567$ , n-3 PUFAs,  $p=0.718$

Sex: SFAs,  $p<0.001$ ; MUFAs,  $p<0.001$ ; n-6 PUFAs,  $p<0.001$ , n-3 PUFAs,  $p<0.001$

Sex x Diet: SFAs,  $p=0.951$ ; MUFAs,  $p=0.839$ ; n-6 PUFAs,  $p=0.515$ , n-3 PUFAs,  $p=0.463$

0%, 0% fructose; 10%, 10% fructose; 20%, 20% fructose; SFAs, saturated fatty acids; MUFAs; monounsaturated fatty acids; n-6 PUFAs, omega-6 polyunsaturated fatty acids; n-3 PUFAs, omega-3 polyunsaturated fatty acids

#### **3.2.4.3. Fatty Acid Quantification**

To further investigate the FA profile, 19 FAs were individually quantified by GC-MS and then categorized to quantify total FAs, SFAs, MUFAs, n-6 PUFAs, and n-3 PUFAs in the RBCs, and the liver. The FA quantity of these samples are as follows.

In the liver tissue, quantification across all 19 FAs remained consistent across all dietary treatment groups for females and no statistical significance was observed (Table 3.1). In males, the only significance found was in DPA (22:5w3); the 0% fructose diet resulted in higher quantities of this omega-3 FA when compared to the 10% and 20% treatment groups.

In the RBCs (T=30 minutes), quantification across all 19 FAs remained consistent across all dietary treatment groups for both females and males, and no statistical significance was observed (Table 3.2).

**Table 3.1 Quantification of fatty acids in liver tissue in FE2 mice**

Fatty Acid		Females (µmol/g)				Males (µmol/g)			
Common Name	Notation	0% (n=8)	10% (n=9)	20% (n=9)	p-value	0% (n=9)	10% (n=9)	20% (n=9)	p-value
Myristic Acid	14:0	6.59 ±2.18	6.65 ±1.93	5.59 ±1.12	0.39	8.99 ±3.29	8.68 ±1.90	7.99 ±1.88	0.68
Pentadecanoic Acid	15:0	1.65 ±0.25	1.68 ±0.35	1.43 ±0.26	0.16	1.89 ±0.61	1.81 ±0.39	1.63 ±0.31	0.48
Palmitic Acid	16:0	127.2 ±22.2	137.7 ±33.5	112.3 ±15.2	0.12	190.8 ±41.5	190.0 ±31.7	185.3 ±23.4	0.93
Palmitoleic Acid	16:1w7	37.14 ±10.08	39.68 ±12.86	29.32 ±5.73	0.10	67.51 ±19.08	64.98 ±12.33	60.57 ±13.54	0.63
Stearic Acid	18:0	22.61 ±2.87	23.80 ±2.26	22.71 ±2.54	0.57	19.13 ±1.62	19.17 ±1.80	18.32 ±1.17	0.44
Oleic Acid	18:1w9	216.3 ±52.7	246.8 ±77.7	204.1 ±46.0	0.33	337.4 ±90.0	352.6 ±52.4	341.7 ±68.8	0.90
Vaccenic Acid	18:1w7	36.16 ±15.47	39.83 ±16.95	30.71 ±8.41	0.40	75.80 ±20.36	80.88 ±11.82	78.66 ±13.78	0.79
Linoleic Acid	18:2w6	21.80 ±2.00	22.61 ±3.52	19.24 ±2.21	0.04	26.61 ±7.43	25.30 ±6.05	23.76 ±3.99	0.61
g-Linolenic Acid	18:3w6	0.41 ±0.21	0.42 ±0.27	0.43 ±0.14	0.97	0.46 ±0.21	0.53 ±0.09	0.38 ±0.17	0.20
a-Linolenic Acid	18:3w3	0.61 ±0.15	0.61 ±0.18	0.48 ±0.13	0.13	0.64 ±0.31	0.54 ±0.16	0.47 ±0.15	0.30
Eicosenoic Acid	20:1w9	0.59 ±0.35	0.76 ±0.51	0.92 ±1.15	0.67	3.76 ±1.69	3.83 ±1.12	3.56 ±0.69	0.89
Eicosadienoic Acid	20:2w6	2.41 ±0.64	2.35 ±0.34	2.66 ±0.59	0.45	3.24 ±0.65	3.36 ±0.67	3.18 ±0.50	0.82
Dihomo-g-Linolenic Acid	20:3w6	2.72 ±0.42	2.92 ±0.38	2.87 ±0.32	0.54	3.55 ±0.44	3.56 ±0.49	3.44 ±0.32	0.81
Arachidonic Acid	20:4w6	15.19 ±2.87	15.43 ±2.88	16.16 ±2.58	0.75	14.51 ±1.78	15.64 ±1.64	15.17 ±2.27	0.46
Eicosapentaenoic Acid	20:5w3	1.35 ±0.30	1.34 ±0.22	1.38 ±0.28	0.96	1.24 ±0.36	1.22 ±0.13	1.11 ±0.22	0.52
Docosatetraenoic Acid	22:4w6	0.31 ±0.06	0.34 ±0.12	0.28 ±0.18	0.71	0.35 ±0.28	0.34 ±0.23	0.34 ±0.21	0.99
Docosapentaenoic Acid	22:5w3	0.55 ±0.20	0.53 ±0.24	0.49 ±0.19	0.85	<b>0.71</b> <b>±0.21<sup>a</sup></b>	<b>0.55</b> <b>±0.14<sup>b</sup></b>	<b>0.56</b> <b>±0.05<sup>b</sup></b>	<b>0.05</b>
Lignoceric Acid	24:0	0.06 ±0.02	0.06 ±0.03	0.07 ±0.02	0.57	0.08 ±0.02	0.09 ±0.02	0.09 ±0.02	0.59
Docosahexaenoic Acid	22:6w3	12.01 ±2.91	11.46 ±5.00	12.19 ±3.06	0.92	10.61 ±2.13	11.58 ±1.89	10.23 ±3.21	0.50
Total Fatty Acids	Total	505.6 ±95.2	555.05 ±140.5	463.37 ±75.2	0.22	767.3 ±179.3	784.64 ±115.8	758.0 ±120.3	0.92
SFA	Total	158.1 ±23.0	169.9 ±36.5	142.1 ±16.9	0.11	220.9 ±45.7	219.7 ±35.1	214.8 ±26.7	0.93
MUFA	Total	290.2 ±77.3	327.1 ±107.0	265.1 ±58.5	0.30	484.5 ±125.7	502.3 ±76.8	484.5 ±95.1	0.91
n-6 PUFA	Total	42.84 ±4.21	44.06 ±4.31	41.66 ±4.73	0.52	48.72 ±8.68	48.73 ±6.66	46.28 ±3.91	0.68
n-3 PUFA	Total	14.52 ±3.37	13.95 ±5.33	14.53 ±3.42	0.95	13.20 ±2.56	13.89 ±1.99	12.37 ±3.08	0.47

Data represents means  $\pm$  standard deviations in  $\mu\text{mol/g}$ . Fatty acid concentrations were calculated using the response factor generated by the internal standard (heptadecanoic acid). For analysis of FA quantification, a two-way ANOVA followed by Tukey's Post-hoc test ( $p < 0.05$ ) was used to test for sex by diet effects. Superscript letters within a row represent significant difference in FA concentration between diet within sex,  $p < 0.05$ .

MUFAs; monounsaturated fatty acids; n-6 PUFAs, omega-6 polyunsaturated fatty acids; n-3 PUFAs, omega-3 polyunsaturated fatty acids

0%, 0% fructose; 10%, 10% fructose; 20%, 20% fructose

**Table 3.2 Fatty acid percent composition of RBC membranes of FE2 mice**

Fatty Acid		Females (µmol/g)				Males (µmol/g)			
Common Name	Notation	0% (n=9)	10% (n=8)	20% (n=9)	p-value	0% (n=9)	10% (n=9)	20% (n=9)	p-value
Myristic Acid	14:0	0.072 ±0.044	0.061 ±0.027	0.052 ±0.052	0.487	0.039 ±0.011	0.038 ±0.020	0.044 ±0.013	0.690
Pentadecanoic Acid	15:0	0.038 ±0.017	0.032 ±0.095	0.022 ±0.013	0.055	0.039 ±0.015	0.042 ±0.009	0.034 ±0.017	0.517
Palmitic Acid	16:0	4.719 ±0.636	3.832 ±1.271	3.708 ±0.880	0.070	5.393 ±1.246	5.443 ±0.634	5.294 ±1.259	0.957
Palmitoleic Acid	16:1w7	0.266 ±0.226	0.157 ±0.048	0.134 ±0.050	0.123	0.351 ±0.179	0.335 ±0.146	0.259 ±0.172	0.466
Stearic Acid	18:0	2.622 ±0.416	2.700 ±0.676	2.760 ±0.314	0.834	2.586 ±0.361	2.273 ±0.168	2.438 ±0.405	0.150
Oleic Acid	18:1w9	3.654 ±0.770	3.326 ±1.171	3.507 ±0.423	0.720	3.986 ±0.747	3.837 ±0.489	3.961 ±0.821	0.874
Vaccenic Acid	18:1w7	0.555 ±0.079	0.544 ±0.145	0.573 ±0.061	0.837	0.953 ±0.231	0.931 ±0.158	0.976 ±0.260	0.908
Linoleic Acid	18:2w6	1.001 ±0.217	0.911 ±0.303	0.905 ±0.239	0.677	1.108 ±0.337	0.949 ±0.187	1.183 ±0.353	0.263
g-Linolenic Acid	18:3w6	0.081 ±0.054	0.075 ±0.027	0.070 ±0.022	0.811	0.066 ±0.019	0.056 ±0.013	0.058 ±0.013	0.352
a-Linolenic Acid	18:3w3	0.020 ±0.022	0.010 ±0.011	0.011 ±0.011	0.346	0.014 ±0.011	0.008 ±0.007	0.008 ±0.005	0.169
Eicosenoic Acid	20:1w9	0.061 ±0.036	0.059 ±0.021	0.073 ±0.031	0.564	0.079 ±0.034	0.075 ±0.022	0.072 ±0.039	0.907
Eicosadienoic Acid	20:2w6	0.156 ±0.091	0.108 ±0.074	0.135 ±0.070	0.458	0.158 ±0.087	0.151 ±0.084	0.346 ±0.371	0.137
Dihomo-g-Linolenic Acid	20:3w6	0.252 ±0.095	0.268 ±0.066	0.268 ±0.084	0.903	0.347 ±0.167	0.358 ±0.133	0.401 ±0.126	0.707
Arachidonic Acid	20:4w6	1.443 ±0.717	1.383 ±0.386	1.486 ±0.665	0.942	1.577 ±1.000	1.910 ±0.944	1.961 ±0.987	0.669
Eicosapentaenoic Acid	20:5w3	0.036 ±0.028	0.032 ±0.018	0.041 ±0.038	0.825	0.023 ±0.020	0.024 ±0.025	0.027 ±0.029	0.946
Docosatetraenoic Acid	22:4w6	0.043 ±0.040	0.067 ±0.061	0.027 ±0.038	0.223	0.106 ±0.056	0.091 ±0.057	0.082 ±0.064	0.694
Docosapentaenoic Acid	22:5w3	0.060 ±0.045	0.037 ±0.028	0.040 ±0.037	0.397	0.037 ±0.034	0.047 ±0.036	0.047 ±0.043	0.806
Lignoceric Acid	24:0	0.025 ±0.018	0.024 ±0.017	0.012 ±0.013	0.192	0.014 ±0.008	0.013 ±0.012	0.029 ±0.049	0.428
Docosahexaenoic Acid	22:6w3	0.30 ±0.23	0.26 ±0.10	0.30 ±0.19	0.877	0.317 ±0.265	0.396 ±0.245	0.409 ±0.310	0.743
Total Fatty Acids	Total	15.41 ±2.20	13.88 ±3.98	14.13 ±2.39	0.14	17.19 ±3.88	16.97 ±1.96	17.63 ±3.60	0.908
SFA	Total	7.476 ±0.881	6.646 ±1.879	6.554 ±1.095	0.292	8.070 ±1.49	7.809 ±0.77	7.839 ±1.614	0.904
MUFA	Total	4.546 ±1.023	4.085 ±1.351	4.287 ±0.501	0.655	5.370 ±1.110	5.166 ±0.755	5.269 ±1.262	0.921
n-6 PUFA	Total	2.977 ±1.065	2.811 ±0.805	2.892 ±1.024	0.941	3.361 ±1.528	3.516 ±1.316	4.031 ±1.347	0.576
n-3 PUFA	Total	0.417 ±0.300	0.341 ±0.140	0.395 ±0.272	0.819	0.391 ±0.324	0.475 ±0.307	0.492 0.382	0.798

Data represents means  $\pm$  standard deviations in  $\mu\text{mol/g}$ . Fatty acid concentrations were calculated using the response factor generated by the internal standard (heptadecanoic acid). For analysis of FA quantification, A two-way ANOVA followed by Tukey's Post-hoc test ( $p < 0.05$ ) was used to test for sex by diet effects. No differences were determined between sex within the same dietary treatment or within the same sex across dietary treatment.

MUFAs; monounsaturated fatty acids; n-6 PUFAs, omega-6 polyunsaturated fatty acids; n-3 PUFAs, omega-3 polyunsaturated fatty acids

0%, 0% fructose; 10%, 10% fructose; 20%, 20% fructose

#### **3.2.4.4. Triacylglycerol Quantification**

Plasma TAG concentrations (T=30 minutes) were similar across all dietary treatment groups and no statistical significance was observed (Figure 3.23). Although TAG concentrations trended higher in male mice than female mice for all treatment groups, no statistical differences were observed when looking at sex alone, or sex by diet as a factor (Appendix XII Figure A.19).

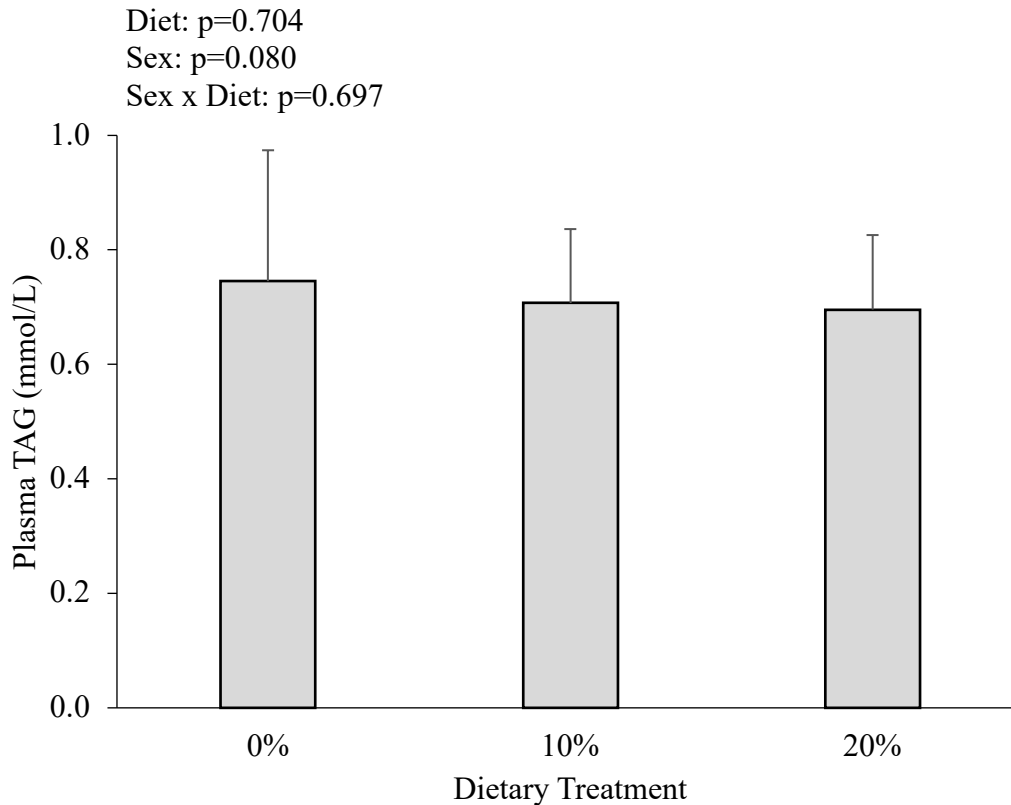


**Figure 3.23 Effect of diet on mean plasma TAG concentrations of FE2 mice**

Bars represent mean  $\pm$  standard deviations in mmol/L. For analysis of plasma TAG concentrations: n=18 for 0% and 10%; n=17 for 20%. Two-way ANOVA followed by Tukey's Post-hoc test ( $p < 0.05$ ) was used to test for dietary treatment effect. No differences were determined across treatment groups ( $p=0.080$ ).

0%, 0% fructose; 10%, 10% fructose; 20%, 20% fructose

#### **3.2.4.5. Cholesterol Lipoprotein Quantification**

Total plasma cholesterol concentrations (T=30 minutes) were similar across all dietary treatment groups and no statistical significance was observed (Figure 3.24). Although fructose content did not affect total cholesterol ( $p=0.664$ ), sex was a factor ( $p<0.001$ ). Cholesterol concentrations were over two-fold higher in males than females across all dietary treatment groups. The cholesterol levels in males were found to be significantly higher than the female mice within the same treatment group, but no sex by diet interaction was present (Appendix XII Figure A.20).

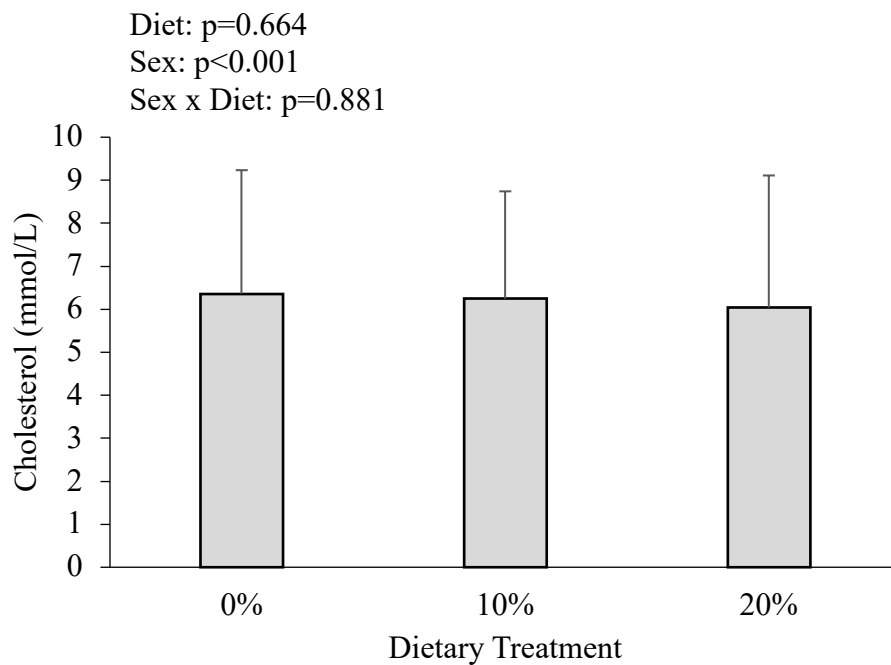


**Figure 3.24 Effect of diet on mean total plasma cholesterol of FE2 mice**

Bars represent mean  $\pm$  standard deviations in mmol/L. For analysis of total plasma cholesterol,  $n=17$  for 0%, 10%, and 20%. Two-way ANOVA followed by Tukey's Post-hoc test ( $p < 0.05$ ) was used to test for dietary treatment effect. No differences were determined across treatment groups ( $p=0.664$ ).

0%, 0% fructose; 10%, 10% fructose; 20%, 20% fructose

#### **3.2.4.6. HDL Quantification**

Concentrations of c-HDL in plasma (T=30 minutes) was similar across all dietary treatment groups and no statistical significance was observed (Figure 3.25). Although fructose content alone did not affect c-HDL concentrations ( $p=0.553$ ), sex was a factor ( $p<0.001$ ). Males had higher concentrations of c-HDL than females when grouped by sex alone, but this significance was not present when investigating sex by diet interactions (Appendix XII Figure A.21).

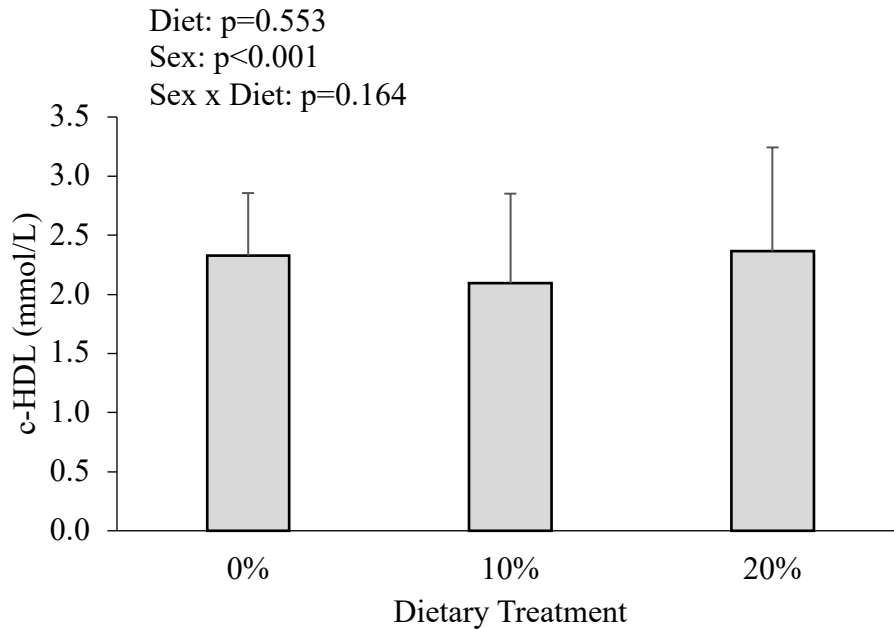


**Figure 3.25 Effect of diet on mean plasma c-HDL cholesterol concentrations of FE2 mice**

Bars represent mean  $\pm$  standard deviations. For analysis of plasma c-HDL concentrations,  $n=17$  for 0%, 10%, and 20%. Two-way ANOVA followed by Tukey's Post-hoc test ( $p < 0.05$ ) was used to test for dietary treatment effect. No differences were determined across treatment groups ( $p=0.553$ ).

0%, 0% fructose; 10%, 10% fructose; 20%, 20% fructose

#### **3.2.4.7. Non-HDL Quantification**

After quantifying HDL-cholesterol concentrations – associated with positive cardiovascular health – non-HDL cholesterol was subsequently quantified by finding the difference between total cholesterol and c-HDL cholesterol concentrations from 3.2.4.6.. Non-HDL concentrations were similar across all dietary treatment groups and no statistical significance was observed (Figure 3.26). Although fructose content did not affect non-HDL concentrations ( $p=0.426$ ), sex was a factor ( $p<0.001$ ). Non-HDL concentrations were nearly three-fold higher in males than females across all dietary treatment groups. The non-HDL cholesterol levels in males were found to be significantly higher than the female mice within the same treatment group, but no sex by diet interaction was present (Appendix XII A.22).

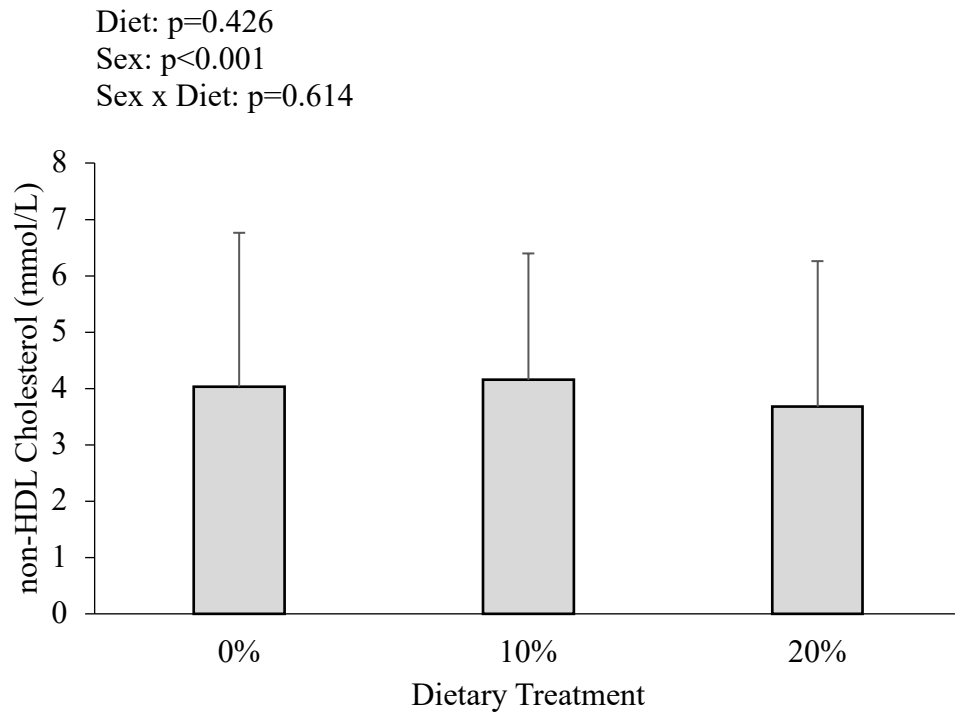


**Figure 3.26 Effect of diet on mean plasma non-HDL cholesterol concentrations of FE2 mice**

Bars represent mean  $\pm$  standard deviations in mmol/L. For analysis of plasma non-HDL concentrations,  $n=17$  for 0%, 10%, and 20%. Two-way ANOVA followed by Tukey's Post-hoc test ( $p < 0.05$ ) was used to test for dietary treatment effect. No differences were determined across treatment groups ( $p=0.426$ ).

0%, 0% fructose; 10%, 10% fructose; 20%, 20% fructose

### **3.2.5. Effect of Diet on Cardiac Pathology**

Cardiac pathology of male and female heart tissues were compared to a control containing lesion formation as displayed in Figure 3.49. No pathology was detected in the aortic roots, coronary arteries, or heart tissues. The coronary arteries and the aorta were also free of atherosclerotic lesions and appeared normal with intact endothelia lining for all animals in this study.

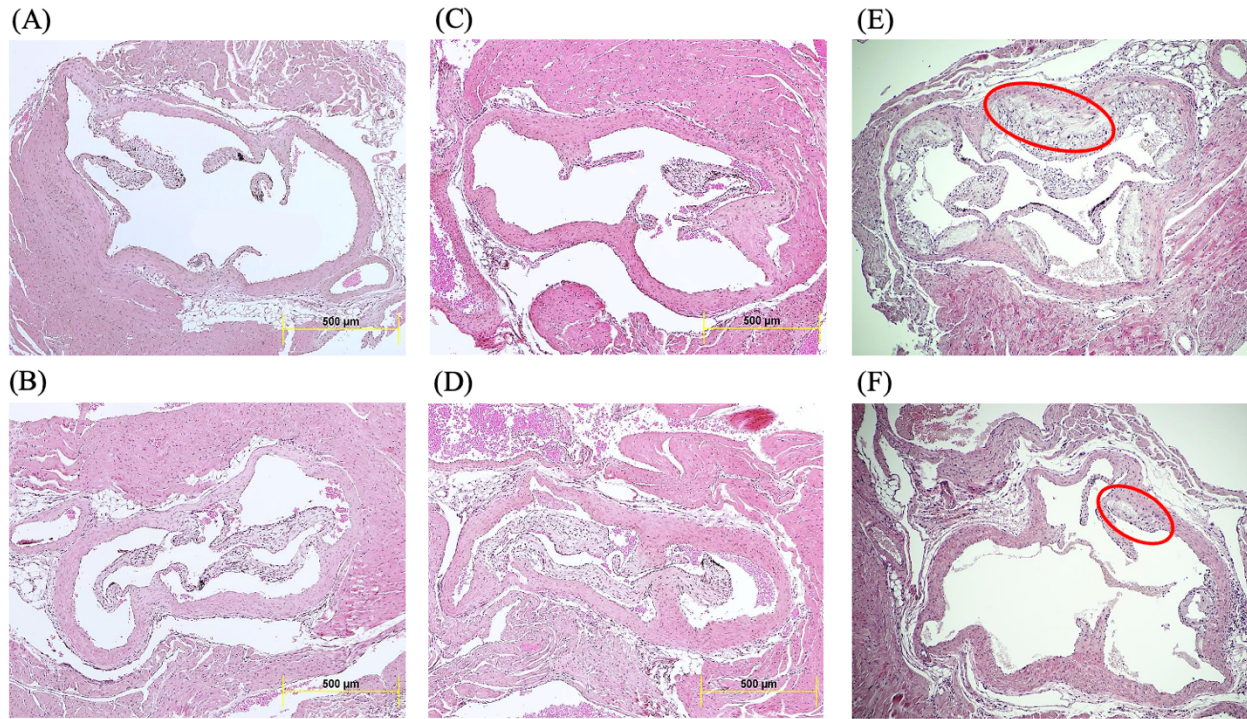


**Figure 3.27 Effect of diet on cardiac pathology of FE2 mice**

(A) Photomicrograph heart cross-section from aortic arch to heart apex using H&E staining of a male from 0% fructose treatment group

(B) Photomicrograph heart cross-section from aortic arch to heart apex using H&E staining of a male from 20% fructose treatment group

(C) Photomicrograph heart cross-section from aortic arch to heart apex using H&E staining of a female from 0% fructose treatment group

(D) Photomicrograph heart cross-section from aortic arch to heart apex using H&E staining of a female from 20% fructose treatment group

(E) Photomicrograph of control heart cross-section from aortic arch to heart apex using H&E staining followed by Tri-chrome staining to emphasize lesion formation

(F) Photomicrograph of control heart cross-section from aortic arch to heart apex using H&E staining followed by Tri-chrome staining to emphasize lesion formation

## 4. Discussion

The primary hypothesis of this study was that dietary fructose paired with a hypercaloric diet will result in the presence or increased risk of developing cardiometabolic risk factors including: obesity, high liver fat content, an unfavourable lipid profile shifting towards SFA and n-6 PUFAs, and high LDL-cholesterol content. Additionally, it was hypothesized that exposure to fructose in the diet would result in an increased ability to convert fructose to glucose and other metabolites.

### 4.1. The Effect Fructose on Sugar Metabolism

One of the most exciting outcomes of this study was the demonstration of  $^{13}\text{C}$ -fructose being converted to glucose in a dose dependent manner depending on dietary intervention. Oral fructose consumption does not circulate as fructose, rather, it is converted to fructose-derived metabolites including glucose, lactate, and glycerate in portal circulation (Tappy et al., 2018, 2019; Jang et al. 2019). Based on the fragmentation patterns reported for glucose and fructose in previous studies (Price, 2004; Wahjudi et al., 2010), three TTR ion pairs involved in glucose metabolism and two TTR ion pairs involved in fructose metabolism were investigated to demonstrate the enrichment of labelled glucose (Appendix XII; Appendix XIII).

Figure 3.29 indicates that mice, specifically female mice (Figure 3.30), consuming 20% fructose in their diet have an increased ability to clear fructose from the plasma; this phenomenon is represented by a lower TTR (206:203 m/z) for this treatment group. A lower TTR value is an indication that the fructose administered by gavage was metabolized and cleared at an increased rate in comparison to the other treatment groups. Additionally, in all glucose TTR ion pairs tested (133 m/z:131 m/z, 191 m/z:187 m/z: 293 m/z:289 m/z), test diets containing

higher fructose content were associated with an increase in glucose TTR ion pairs in plasma at 30-minutes post-gavage (Figure 3.31). Regardless of ion pair, plasma glucose TTR were over 2-fold higher in the 20% fructose group compared to the 0% fructose group in the FE2 study. To link these findings, a mouse with prior fructose exposure not only has an increased ability to metabolize and clear a bolus dose of fructose, but these metabolites are subsequently forming glucose. This increased enrichment of glucose suggests that, aligning with our hypothesis, previous fructose exposure leads to a physical adaptation that enhances fructose absorption and clearance by converting fructose to glucose, enabling entry to the glycolytic pathway. A previous finding by Jang et al. (2019) reiterates that clearance of fructose is augmented by prior fructose exposure through investigating the associated gene expression related to fructose consumption. The group found that previous consumption of fructose induces a rapid and strong upregulation of genes involved in its uptake and catabolism – including Glut5, G6pc, Fbp-1, and aldolase B – which are required for the conversion of fructose to glucose. They also found that this adaptation is reversible, and that discontinuing fructose consumption results in a decrease in gene expression back to baseline in as little as 7-days in rats. The Chow- $\delta$  group in FE1 is representative of consuming high quantities of fructose followed by a drastic decrease in fructose consumption, however, isotope tracing was not completed in the FE1 study.

#### **4.2. The Effect of Fructose on Blood Glucose Concentrations**

With the understanding that a large portion of oral fructose is converted to glucose, and that prior fructose exposure appears to augment this conversion, blood glucose concentrations were a critical measurement in this study. Blood glucose was measured solely by glucose oxidase method at the time of heart puncture (T=30-minutes) in FE1 but was additionally

measured by glucometer method at three timepoints in FE2; additional time points provided further insight to glucose concentrations prior to and post gavage. Surprisingly, blood glucose concentrations were not affected by prior fructose exposure at any time point in FE1 or FE2. Interestingly, when analyzing sex by diet differences, females tended to have higher blood glucose concentrations than males within the fructose treatment groups for both studies. Blood glucose concentrations were over 5 mmol/L higher in females consuming 20% fructose compared to their male counterparts at 30-minutes post-gavage in FE2. The tendency for females to have higher post-prandial blood glucose concentrations suggests that either: females have a greater adaptive ability to convert fructose to glucose at an increased rate, or females have a decreased ability to clear blood glucose into the glycolytic pathway.

A decreased ability to clear post-prandial glucose is associated with insulin resistance: a common consequence of metabolic distress associated with T2DM. Stone et al. (2021) describe metabolic flexibility as the ability to adapt to utilization of metabolic fuels such as carbohydrates, lipids, and proteins as they become available. The group suggests that female mice are protected from metabolic inflexibility – a condition that occurs in the presence of insulin resistance, obesity, and diabetes – whereas male mice are susceptible and therefore this inflexibility often leads to poor glucose clearance. Due to females, not males, having higher blood glucose concentrations in our research, the study by Stone et al. (2021) suggests that the higher blood glucose levels in females are more likely to be associated with an increased conversion of fructose to glucose rather than an inability for females to clear glucose.

Furthermore, a study by Galipeau et al. (2002) on rats consuming up to 60% fructose suggest that female rats have counter mechanisms, likely linked to hormones, that protect against the adverse effects of fructose. Even with extreme fructose consumption, sexually mature female rats in this

study displayed protective effects against fructose-induced hypertension, hyperinsulinemia, and insulin resistance when compared to male rats or sexually immature female rats. These findings reiterate significant findings that estrogen has beneficial effects on lipoproteins, insulin, and glucose metabolism by increasing glycogen accumulation, glucose uptake, and lipogenesis (Godsland, 1996; Tramunt et al., 2020).

#### **4.3. The Effect of Fructose on Body Weight and Liver Weight Gain**

Although consumption of a Western-type diet has been strongly associated with obesity, the exact trigger(s) have not been clearly elucidated. The test diets used in both studies were created to imitate a Westernized Diet, varying only in fructose content. The short duration of FE1 was likely the reason that very little changes in body weight occurred throughout the 6-weeks of treatment. In FE2, there were drastic changes in weight gain from the onset of the test diets until the completion of the study in comparison to the grow-out chow phase; interestingly, fructose was not the trigger as all treatment groups gained weight at a comparable rate per week. Although there was no effect of fructose, all animals showed signs of obesity including rotundness, lethargy, and excessive visceral fat, suggesting that the energy density of the diet was the driver of the weight gain versus any single macronutrient. Additionally, there was a clear sex difference; the test diet had a greater impact on males than females. Although diet consumption was not an outcome for this study, the additional weight gain in males could be due to higher food consumption leading to a higher calorie surplus than their female counterparts. A more probable consequence based on the literature is that carbohydrate and subsequent lipid metabolism occur differentially in males than females (Godsland, 1996; Tramunt et al., 2020) – these sex differences in lipid metabolism became evident upon further investigation.

In both studies, the liver was weighed upon removal. As expected, the large body mass of the male mice resulted in larger livers before adjusting for body weight. Even after adjusting for body weight, male livers were still nearly 2-fold larger than the corresponding female livers in both FE1 and FE2, irrespective of dietary treatment. When looking into the literature, a study by Saito et al. (2015) put the discrepancy of liver size into perspective; while the female livers matched closely to the control group, the male livers in our study were even larger than STAM<sup>TM</sup> mice consuming a high-fat diet – a model used to demonstrate NASH progressing to fibrosis. Like body weight gain, the mass of the liver is clearly dependent on sex, and not dietary treatment. At the time of necropsy, the liver tissue of the males was notably light in color compared to their female counterparts, a common signifier of high-fat content. To further examine the sex differences in liver weight, the total lipid content and lipid profile must be investigated.

#### **4.4. The Effect of Fructose on Total Lipid Quantification and Profile**

Unlike the RBC's which remained consistent across study, dietary treatment and sex there were significant differences in the lipid profile of the liver tissues. When investigating the lipid profile in FE2, males shifted towards a higher MUFAs profile – associated with a healthier lipid profile – while females shifted towards a higher SFAs profile – associated with an unhealthier lipid profile. It is important to note however, that although females shifted towards a SFAs profile, male livers still contained much higher concentrations of SFAs on average (0% =  $220.9 \pm 45.7$ , 10% =  $219 \pm 35.1$ , 20% =  $214.8 \pm 26.7$   $\mu\text{mol/g}$ ) than that of the females (0% =  $156.7 \pm 23.0$ , 10% =  $169.9 \pm 36.5$ , 20% =  $142.1 \pm 16.9$   $\mu\text{mol/g}$ ) as the male livers were larger and contained more lipid content overall. When investigating total FA content, males also had

significantly more liver fat (0% =  $767.3 \pm 179.3$ , 10% =  $784.64 \pm 115.8$ , 20% =  $758.0 \pm 120.3$   $\mu\text{mol/g}$ ) than females (0% =  $505.6 \pm 95.2$ , 10% =  $555.05 \pm 140.5$ , 20% =  $463.37 \pm 75.2$   $\mu\text{mol/g}$ ), which is likely linked to the larger liver weight and pale color noted at necropsy. Additionally, there was a sex by diet effect for docosapentaenoic acid (DPA) content in male livers; DPA was significantly higher in the 0% fructose group when compared to the 10% and 20% fructose groups. The fructose containing diets being linked to a decrease in liver DPA content warrants additional investigation as this omega-3 FA is associated with brain and heart health. Although plasma TAG concentrations were slightly higher in males, these changes were not significant, so plasma TAG was not distinctly impacted by diet or sex in either study.

#### **4.5. The Effect of Fructose on Plasma Cholesterol Quantification and Profile**

Cholesterol content was not impacted by diet but did demonstrate considerable sex-effects. Total plasma cholesterol was over 2-fold higher in males than females. Although HDL cholesterol is higher in males and is associated with health, the extremely high non-HDL cholesterol concentrations in males – over 3-fold higher in males than females – negate any potential positive impacts of the higher HDL concentrations. High total cholesterol and non-HDL cholesterol – LDL and VLDL – is a phenotypic trait present in individuals with obesity, NAFLD, T2DM, and other diseased states associated with dyslipidemia.

#### **4.6. The Effect of Fructose on Cardiac Pathology and Atherosclerosis**

The heart tissues in FE2 were used to investigating the impact of fructose on the formation of lesions and plaque formation that could result in atherosclerosis. Fructose consumption did not have any visible impact on cardiac pathology regardless of treatment group

or sex. This was an expected outcome as the C57BL/J6 mouse model does not normally develop atherosclerosis without the addition of high-quantities of cholesterol in the diet (Grundtman et al., 2012; Moghadasian, 2002)

#### **4.7. Conclusion and Future Directions**

Although the results of this study are conflicting in some ways, they summarize the complexities of cardiometabolic diseases and demonstrate that fructose alone appears to have very little effect on cardiometabolic outcomes. In this study, we showed that weight gain, liver weight, hepatic lipid profile, and hepatic cholesterol content and profile are all dependent on sex, irrespective of dietary fructose content. Females demonstrated that even in a hypercaloric state, hormonal differences such as increased estrogen levels likely provide an innate metabolic protection, while males were prone to deleterious lipid profiles and weight gain.

The sex and sex by diet effects in the isotope tracer portion of this study are fascinating and a novelty in this study. By investigating TTRs, we found that animals consuming oral fructose have an adaptive ability to clear fructose, and a key metabolite formed during this clearance is fructose. Not only does habitual fructose exposure warrant this protection, but females have an additional protective ability compared to their male counterparts to clear fructose and form glucose. To further this research, an internal standard is required to allow the quantification of fructose and glucose rather than investigating TTR alone. With the knowledge that prior fructose exposure demonstrates an increase in clearance rate, quantifying enzymes involved in the metabolism of fructose and the subsequent production of other intermediates should be measured; specifically, quantifying enzymes involved in lipogenesis would be critical to understanding if fructose leads to the upregulation of DNL and other lipogenic precursors.

Lastly, due to the original understanding that the liver was the major location of metabolism for fructose, the potential impact on other organs has yet to be elucidated. Recent studies including this one, demonstrate that the small intestine is a major location for metabolism, but other organs with GLUT5 expression such as the kidney also need to be studied. At the time of necropsy, two left kidneys were calcified and necrotic upon removal; although the kidney tissues were not processed within the scope of this study, they will be processed by a lab mate to further investigate the role of the kidney in fructose metabolism.

In conclusion, fructose does not appear to be a sole factor in the development or progression of diseased states. Males do have a predisposition to developing unfavourable characteristics associated with cardiometabolic risk factors, but these occur irrespective of dietary treatment. Prior exposure to fructose does demonstrate a protective ability to clear fructose and form glucose, and this ability is further heightened in females. Further isotope research is required to both quantify this clearance as well as to investigate the fate of fructose once it is diverted into the glycolytic pathway to form glucose.

## 5. References

- Adeva-Andany, M. M., Pérez-Felpete, N., Fernández-Fernández, C., Donapetry-García, C., & Pazos-García, C. (2016). Liver glucose metabolism in humans. *Bioscience Reports*, *36*(6), 1–15.
- Alexander, J., Chang, G. Q., Dourmashkin, J. T., & Leibowitz, S. F. (2006). Distinct phenotypes of obesity-prone AKR/J, DBA2J and C57BL/6J mice compared to control strains. *International Journal of Obesity*, *30*(1), 50–59.
- Anandita Agarwala, Erin D. Michos, Zainab Samad, Ballantyne, C. M., & Salim S. Viran. (2020). The use of sex-specific factors in the assessment of women’s cardiovascular risk. *Circulation*, *141*(7), 592–599.
- Appelman, Y., van Rijn, B. B., ten Haaf, M. E., Boersma, E., & Peters, S. A. E. (2014). Sex differences in cardiovascular risk factors and disease prevention. *Atherosclerosis*, *241*(1), 211–218.
- Ballestri, S., Nascimbeni, F., Baldelli, E., Marrazzo, A., Romagnoli, D., & Lonardo, A. (2017). NAFLD as a sexual dimorphic disease: role of gender and reproductive status in the development and progression of nonalcoholic fatty liver disease and inherent cardiovascular risk. *Advances in Therapy*, *34*(6), 1291–1326.
- Basciano, H., Federico, L., & Adeli, K. (2005). Fructose, insulin resistance, and metabolic dyslipidemia. *Nutrition and Metabolism*, *2*, 1–14.
- Bray, G. A., Nielsen, S. J., & Popkin, B. M. (2004). Consumption of high-fructose corn syrup in beverages may play a role in the epidemic of obesity. *American Journal of Clinical Nutrition*, *79*(4), 537–543.
- Brevik, A., Veierød, M. B., Drevon, C. A., & Andersen, L. F. (2005). Evaluation of the odd fatty

- acids 15:0 and 17:0 in serum and adipose tissue as markers of intake of milk and dairy fat. *European Journal of Clinical Nutrition*, 59(12), 1417–1422.
- Brisbois, T. D., Marsden, S. L., Harvey Anderson, G., & Sievenpiper, J. L. (2014). Estimated intakes and sources of total and added sugars in the Canadian diet. *Nutrients*, 6(5), 1899–1912.
- Buettner, R., Schölmerich, J., & Bollheimer, L. C. (2007). High-fat diets: modeling the metabolic disorders of human obesity in rodents. *Obesity*, 15(4), 798–808.
- Campos, V. C., & Tappy, L. (2016). Physiological handling of dietary fructose-containing sugars: implications for health. *International Journal of Obesity*, 40(S1), S6–S11.
- Chalasani, N., Younossi, Z., Lavine, J. E., Diehl, A. M., Brunt, E. M., Cusi, K., & Sanyal, A. J. (2012). The diagnosis and management of non-alcoholic fatty liver disease: practice guideline by the American Association for the Study of Liver Diseases, American College of Gastroenterology, and the American Gastroenterological Association. *Hepatology*, 55(6), 2005–2023.
- Chen, L. Q., Cheung, L. S., Feng, L., Tanner, W., & Frommer, W. B. (2015). Transport of sugars. *Annual Review of Biochemistry*, 84, 865–894.
- Chiavaroli, L., Wang, Y. F., Ahmed, M., Praneet Ng, A., DiAngelo, C., Marsden, S. L., & Sievenpiper, J. L. (2022). Intakes of nutrients and food categories in Canadian children and adolescents across levels of sugars intake: Cross-sectional analyses of the Canadian Community Health Survey 2015 Public Use Microdata File. *Applied Physiology, Nutrition, and Metabolism*, 1–32. Retrieved from <https://pubmed.ncbi.nlm.nih.gov/35007181/>
- Colonna, W. J., Samaraweera, U., Clarke, M. A., & Cleary, M. (2006). Sugar.
- David Wang, D., Sievenpiper, J. L., De Souza, R. J., Cozma, A. I., Chiavaroli, L., Ha, V., &

- Jenkins, D. J. A. (2014). Effect of fructose on postprandial triglycerides: A systematic review and meta-analysis of controlled feeding trials. *Atherosclerosis*, 232(1), 125–133.
- Egli, L., Lecoultre, V., Theytaz, F., Campos, V., Hodson, L., Schneiter, P., & Tappy, L. (2013). Exercise prevents fructose-induced hypertriglyceridemia in healthy young subjects, (November 2012), 4–10.
- Elliott, S. S., Keim, N. L., Stern, J. S., Teff, K., & Havel, P. J. (2002). Fructose, weight gain, and the insulin resistance syndrome. *American Journal of Clinical Nutrition*, 76(5), 911–922.
- Ferraris, R. P., Choe, J., & Patel, C. R. (2018). Intestinal absorption of fructose. *Annual Review of Nutrition*, 38, 41-67.
- Galipeau, D., Verma, S., & McNeill, J. H. (2002). Female rats are protected against fructose-induced changes in metabolism and blood pressure. *American Journal of Physiology - Heart and Circulatory Physiology*, 283(6 52-6), 2478–2484.
- Geneva: World Health Organization. (2015). WHO Guideline: Sugars intake for adults and children.
- Godsland, I. F. (1996). The influence of female sex steroids on glucose metabolism and insulin action. *Journal of Internal Medicine*, 738, 1–60.
- Grundtman, C., & Moghadasian, M. H. (2012). Animal models of atherosclerosis. *Inflammation and Atherosclerosis*, 9783709103(5), 133–169.
- Gugliucci, A. (2017). Formation of fructose-mediated advanced glycation end products and their roles in metabolic and inflammatory diseases. *Advances in Nutrition*, 8(1), 54–62.
- Helstad, S. (2019). Corn Sweeteners. In *Corn: Chemistry and Technology* (Third Edit, 551–591).
- Jang, C., Hui, S., Lu, W., Cowan, A. J., Morscher, R. J., Lee, G., & Rabinowitz, J. D. (2018). The small intestine converts dietary fructose into glucose and organic acids. *Cell*

- Metabolism*, 27(2), 351-361.e3.
- Jang, C., Hui, S., Lu, W., Tesz, G. J., Birnbaum, M. J., Rabinowitz, J. D., & Rabinowitz, J. D. (2018). The small intestine converts dietary fructose into glucose and organic acids. *Cell Metabolism*, 27(2), 351–361.
- Jenkins, B., West, J. A., & Koulman, A. (2015). A review of odd-chain fatty acid metabolism and the role of pentadecanoic acid (C15:0) and heptadecanoic acid (C17:0) in health and disease. *Molecules*, 20(2), 2425–2444.
- Jensen, T., Abdelmalek, M. F., Sullivan, S., Nadeau, K. J., Green, M., Roncal, C., & Riley, T. H. (2018). Fructose and sugar: A major mediator of non-alcoholic fatty liver disease. *Journal of Hepatology*, 68(5), 1063–1075.
- Kirs, E., Pall, R., Martverk, K., & Laos, K. (2011). Physicochemical and melissopalynological characterization of Estonian summer honeys. *Procedia Food Science*, 1(December 2011), 616–624.
- Klair, J. S., Yang, J. D., Abdelmalek, M. F., Guy, C. D., Gill, R. M., Yates, K., & Suzuki, A. (2016). A longer duration of estrogen deficiency increases fibrosis risk among postmenopausal women with nonalcoholic fatty liver disease. *Hepatology*, 64(1), 85–91.
- Lambert, J. E., Ramos-Roman, M. A., Browning, J. D., & Parks, E. J. (2014). Increased de novo lipogenesis is a distinct characteristic of individuals with nonalcoholic fatty liver disease. *Gastroenterology*, 146(3), 726–735.
- Liu, S., Munasinghe, L. L., Ohinmaa, A., & Veugelers, P. J. (2020). Added, free and total sugar content and consumption of foods and beverages in Canada. *Health Reports*, 31(10), 14-24.
- Löfgren, L., Ståhlman, M., Forsberg, G. B., Saarinen, S., Nilsson, R., & Hansson, G. I. (2012). The BUME method: A novel automated chloroform-free 96-well total lipid extraction

- method for blood plasma. *Journal of Lipid Research*, 53(8), 1690–1700.
- Marinou, K., Adiels, M., Hodson, L., Frayn, K. N., Karpe, F., & Fielding, B. A. (2011). Young women partition fatty acids towards ketone body production rather than VLDL-TAG synthesis, compared with young men. *British Journal of Nutrition*, 105(6), 857–865.
- Marques-Lopes, I., Ansorena, D., Astiasaran, I., Forga, L., & Martínez, J. A. (2001). Postprandial de novo lipogenesis and metabolic changes induced by a high-carbohydrate, low-fat meal in lean and overweight men. *American Journal of Clinical Nutrition*, 73(2), 253–261.
- Marriott, B. P., Cole, N., & Lee, E. (2009). National estimates of dietary fructose intake increased from 1977 to 2004 in the United States. *The Journal of Nutrition*, 139(6), 1228S-1235S.
- Mehnert, H. (1976). Sugar substitutes in the diabetic diet. *Internationale Zeitschrift Fur Vitamin- Und Ernährungsforschung. Beiheft*, 15, 295-324.
- Moghadasian, M. H. (2002). Experimental atherosclerosis: A historical overview. *Life Sciences*, 70(8), 855-65.
- Pereira, R. M., Botezelli, D., Cristina, K., Mekary, R. A., Cintra, D. E., Pauli, R., & Moura, L. P. De. (2017). Fructose consumption in the development of obesity and the effects of different protocols of physical exercise on the hepatic metabolism. *Nutrients*, 1–21.
- Price, N. P. J. (2004). Acyclic sugar derivatives for GC/MS analysis of <sup>13</sup>C-enrichment during carbohydrate metabolism. *Analytical Chemistry*, 76(22), 6566–6574.
- Saito, K., Uebanso, T., Maekawa, K., Ishikawa, M., Taguchi, R., Nammo, T., & Saito, Y. (2015). Characterization of hepatic lipid profiles in a mouse model with nonalcoholic steatohepatitis and subsequent fibrosis. *Scientific Reports*, 5(August), 1–9.

- Samir, S., Cohen, D. E., & Kahn, R. C. (2016). Role of dietary fructose and hepatic de novo lipogenesis in fatty liver disease. *Digestive Diseases and Sciences*, *61*(5), 1282–1293.
- Sharabi, K., Tavares, C. D. J., Rines, A. K., & Puigserver, P. (2015). Molecular pathophysiology of hepatic glucose production. *Molecular Aspects Medicine*, *176*(46), 21–33.
- Smith, S., Yearsley, M., & Levin, D. (2017). Patient sex, reproductive status, and synthetic hormone use associated with histologic severity of nonalcoholic steatohepatitis. *Clinical Gastroenterology and Hepatology*, *15*(1), 127-131.e2.
- Stone, A. C., Noland, R. C., Mynatt, R. L., Velasquez, S. E., Bayless, D. S., Ravussin, E., & Warfel, J. D. (2021). Female mice are protected from metabolic decline associated with lack of skeletal muscle IGF1. *Biology*, *10*(6).
- Suárez, G., Rajaram, R., Oronsky, A. L., & Gawinowicz, M. A. (1989). Nonenzymatic glycation of bovine serum albumin by fructose (fructation). *Journal of Biological Chemistry*, *264*(7), 3674–3679.
- Sun, S. Z., & Empie, M. W. (2012). Fructose metabolism in humans – what isotopic tracer studies tell us, 1–15.
- Surwit, R. S., Feinglos, M. N., Rodin, J., Sutherland, A., Petro, A. E., Opara, E. C., & Rebuffe-Scrive, M. (1995). Differential effects of fat and sucrose on the development of obesity and diabetes in C57BL/6J and A J mice. *Metabolism*, *44*(5), 645–651.
- Tappy, L. (2018). Fructose metabolism and noncommunicable diseases: Recent findings and new research perspectives. *Current Opinion in Clinical Nutrition and Metabolic Care*, *21*(3), 214–222.
- Tappy, L. (2019). Health outcomes of a high fructose intake: the importance of physical activity. *The Journal of Physiology*, *14*(September 2018), 3561–3571.

- Tappy, L., & Le, K. A. (2010). Metabolic effects of fructose and the worldwide increase in obesity. *Physiological Reviews*, *90*(1), 23-46.
- Tappy, L., & Rosset, R. (2019). Health outcomes of a high fructose intake: the importance of physical activity. *Journal of Physiology*, *597*(14), 3561–3571.
- Tramunt, B., Smati, S., Grandgeorge, N., Lenfant, F., Arnal, J. F., Montagner, A., & Gourdy, P. (2020). Sex differences in metabolic regulation and diabetes susceptibility. *Diabetologia*, *63*(3), 453–461.
- Wahjudi, P. N., Patterson, M. E., Lim, S., Yee, J. K., Mao, C. S., & Paul Lee, W.-N. (2010). Measurement of glucose and fructose in clinical samples using gas chromatography/mass spectrometry. *Clinical Biochemistry*, *43*(1–2), 198–207.
- Wang, X., Cao, Y., Fu, Y., Guo, G., & Zhang, X. (2011). Liver fatty acid composition in mice with or without nonalcoholic fatty liver disease. *Lipids in Health and Disease*, *10*(1), 234.
- White, J. S. (2008). Straight talk about high-fructose corn syrup: what it is and what it ain't. *The American Journal of Clinical Nutrition*, *88*, 1716–1721.
- Yang, J. D., Abdelmalek<sup>2</sup>, M. F., Pang, H., Guy, C. D., Smith<sup>2</sup>, A. D., Diehl, A. M., & Suzuki<sup>1</sup>, A. (2014). Gender and menopause impact severity of fibrosis among patients with nonalcoholic steatohepatitis. *Clinical Gastroenterology and Hepatology*, *59*(4), 1406–1414.
- Zhang, Y. H., An, T., Zhang, R. C., Zhou, Q., Huang, Y., & Zhang, J. (2013). Very high fructose intake increases serum LDL-cholesterol and total cholesterol: A meta-analysis of controlled feeding trials. *Journal of Nutrition*, *143*(9), 1391–1398.

## 6. Appendices

### Appendix I: Composition of standard chow diet (NC1770956)

<b>Macronutrients</b>		
Crude Protein	%	18.6
Fat (ether extract) <sup>a</sup>	%	6.2
Carbohydrate (available) <sup>b</sup>	%	44.2
Crude Fiber	%	3.5
Neutral Detergent Fiber <sup>c</sup>	%	14.7
Ash	%	5.3
Energy Density <sup>d</sup>	kcal/g (kJ/g)	3.1 (13.0)
Calories from Protein	%	24
Calories from Fat	%	18
Calories from Carbohydrate	%	58
<b>Minerals</b>		
Calcium	%	1.0
Phosphorus	%	0.7
Non-Phytate Phosphorus	%	0.4
Sodium	%	0.2
Potassium	%	0.6
Chloride	%	0.4
Magnesium	%	0.2
Zinc	mg/kg	70
Manganese	mg/kg	100
Copper	mg/kg	15
Iodine	mg/kg	6
Iron	mg/kg	200
Selenium	mg/kg	0.23
<b>Amino Acids</b>		
Aspartic Acid	%	1.4
Glutamic Acid	%	3.4
Alanine	%	1.1
Glycine	%	0.8
Threonine	%	0.7
Proline	%	1.6
Serine	%	1.1
Leucine	%	1.8
Isoleucine	%	0.8
Valine	%	0.9
Phenylalanine	%	1.0
Tyrosine	%	0.6
Methionine	%	0.4
Cystine	%	0.3
Lysine	%	0.9
Histidine	%	0.4
Arginine	%	1.0
Tryptophan	%	0.2

<b>Vitamins</b>		
Vitamin A <sup>e, f</sup>	IU/g	15.0
Vitamin D <sub>3</sub> <sup>e, g</sup>	IU/g	1.5
Vitamin E	IU/kg	110
Vitamin K <sub>3</sub> (menadione)	mg/kg	50
Vitamin B <sub>1</sub> (thiamin)	mg/kg	17
Vitamin B <sub>2</sub> (riboflavin)	mg/kg	15
Niacin (nicotinic acid)	mg/kg	70
Vitamin B <sub>6</sub> (pyridoxine)	mg/kg	18
Pantothenic Acid	mg/kg	33
Vitamin B <sub>12</sub> (cyanocobalamin)	mg/kg	0.08
Biotin	mg/kg	0.40
Folate	mg/kg	4
Choline	mg/kg	1200
<b>Fatty Acids</b>		
C16:0 Palmitic	%	0.7
C18:0 Stearic	%	0.2
C18:1 $\omega$ 9 Oleic	%	1.2
C18:2 $\omega$ 6 Linoleic	%	3.1
C18:3 $\omega$ 3 Linolenic	%	0.3
Total Saturated	%	0.9
Total Monounsaturated	%	1.3
Total Polyunsaturated	%	3.4
<b>Other</b>		
Cholesterol	mg/kg	--

<sup>a</sup> Ether extract is used to measure fat in pelleted diets, while an acid hydrolysis method is required to recover fat in extruded diets. Compared to ether extract, the fat value for acid hydrolysis will be approximately 1% point higher.

<sup>b</sup> Carbohydrate (available) is calculated by subtracting neutral detergent fiber from total carbohydrates.

<sup>c</sup> Neutral detergent fiber is an estimate of insoluble fiber, including cellulose, hemicellulose, and lignin. Crude fiber methodology underestimates total fiber.

<sup>d</sup> Energy density is a calculated estimate of *metabolizable energy* based on the Atwater factors assigning 4 kcal/g to protein, 9 kcal/g to fat, and 4 kcal/g to available carbohydrate.

<sup>e</sup> Indicates added amount but does not account for contribution from other ingredients.

<sup>f</sup> 1 IU vitamin A = 0.3  $\mu$ g retinol

<sup>g</sup> 1 IU vitamin D = 25 ng cholecalciferol

For nutrients not listed, insufficient data is available to quantify.

**Appendix II: Composition of mineral mix #210050**

<b>Dyets#</b>	<b>#210050</b>
<b>Description</b>	<b>AIN-93M</b>
<b>g/kg</b>	<b>35</b>
<b>Ca</b>	5,000
<b>P</b>	1,992
<b>K</b>	3,600
<b>Na</b>	1,019
<b>Cl</b>	1,571
<b>S</b>	300
<b>Mg</b>	507
<b>Fe</b>	35
<b>Cu</b>	6
<b>Mn</b>	10
<b>Zn</b>	30
<b>Cr</b>	1
<b>I</b>	0.2
<b>Se</b>	0.15
<b>Al</b>	N/A
<b>F</b>	1
<b>Co</b>	N/A
<b>B</b>	0.5
<b>Mo</b>	0.15
<b>Br</b>	N/A
<b>Si</b>	5
<b>Ni</b>	0.5
<b>Li</b>	0.1
<b>V</b>	0.1

**Appendix III: Composition of vitamin mix #310081**

<b>Number</b>		<b>#310081</b>
<b>Rate g/Kg</b>	<b>Unit</b>	<b>10</b>
<b>Ingredient</b>		
<b>Thiamin HCl</b>	mg	6
<b>Riboflavin</b>	mg	6
<b>Pyridoxine HCl</b>	mg	7
<b>Niacin</b>	mg	30
<b>Calcium Pantothenate</b>	mg	16
<b>Folic Acid</b>	mg	2
<b>Biotin</b>	mg	0.2
<b>Cyanocobalamin</b>	mcg	25
<b>(B12)</b>		
<b>Menadione Sodium Bisulfite</b>	mg	0
<b>Vitamin A Palmitate</b>	IU.	4000
<b>Vitamin E Acetate</b>	IU.	75
<b>Vitamin D3</b>	IU.	1000
<b>Vitamin D2</b>	IU.	0
<b>Ascorbic Acid</b>	mg	0
<b>Inositol</b>	mg	0
<b>Choline Bitartrate</b>	mg	0
<b>p-Aminobenzoic Acid</b>	mg	0
<b>Niacinamide</b>	mg	0
<b>Vitamin K1</b>	mg	0.75

**Appendix IV: Composition of 0% fructose diet**

DYET #104809			
Modified Western Diet without Added Sucrose and 0% Fructose Derived Calories			
<b>Ingredient</b>	<b>kcal./gm</b>	<b>grams/kg</b>	<b>kcal./kg</b>
Casein	3.58	195	698
DL-Methionine	4	3	12
Fructose	3.8	0	0
Cornstarch	3.6	367.96	1325
Dyetrose	3.8	125	475
Anhydrous Milk Fat	9	210	1890
Cellulose	0	50	0
Mineral Mix #210050	0.47	35	16.45
Vitamin Mix #310081*	3.92	10	39.2
Choline Bitartrate	0	2.5	0
Cholesterol	0	1.5	0
Ethoxyquin	0	0.04	0
		<b>1000</b>	<b>4455.41</b>

\*Maltodextrin as carrier

**Appendix V: Composition of 10% fructose diet**

DYET #104810 Modified Western Diet without Added Sucrose and 10% Fructose Derived Calories			
<b>Ingredient</b>	<b>kcal./gm</b>	<b>grams/kg</b>	<b>kcal./kg</b>
Casein	3.58	195	698
DL-Methionine	4	3	12
Fructose	3.8	120	456
Cornstarch	3.6	277.96	1001
Dyetrose	3.8	95	361
Anhydrous Milk Fat	9	210	1890
Cellulose	0	50	0
Mineral Mix #210050	0.47	35	16.45
Vitamin Mix #310081*	3.92	10	39.2
Choline Bitartrate	0	2.5	0
Cholesterol	0	1.5	0
Ethoxyquin	0	0.04	0
		<b>1000</b>	<b>4473.41</b>

\*Maltodextrin as carrier

**Appendix VI: Composition of 20% fructose diet**

DYET #104811 Modified Western Diet without Added Sucrose and 20% Fructose Derived Calories			
<b>Ingredient</b>	<b>kcal./gm</b>	<b>grams/kg</b>	<b>kcal./kg</b>
Casein	3.58	195	698
DL-Methionine	4	3	12
Fructose	3.8	240	912
Cornstarch	3.6	188.96	680
Dyetrose	3.8	64	243
Anhydrous Milk Fat	9	210	1890
Cellulose	0	50	0
Mineral Mix #210050	0.47	35	16.45
Vitamin Mix #310081*	3.92	10	39.2
Choline Bitartrate	0	2.5	0
Cholesterol	0	1.5	0
Ethoxyquin	0	0.04	0
		<b>1000</b>	<b>4491.21</b>

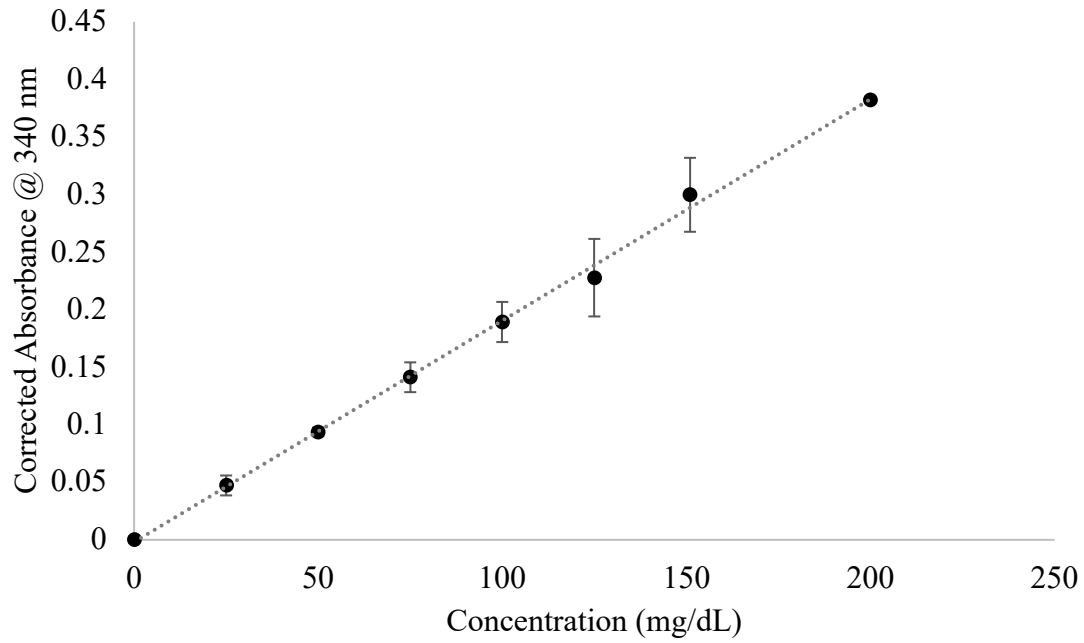
\*Maltodextrin as carrier

**Appendix VII: Average food consumption per day by sex and dietary treatment in FE1 mice**

	Females			Males		
	% Fructose					
	0%	10%	20%	0%	10%	20%
Average Food Consumption by diet (g/day)	3.76	3.74	4.73	4.78	4.95	3.98
Average Food Consumption by sex (g/day)	4.08			4.57		

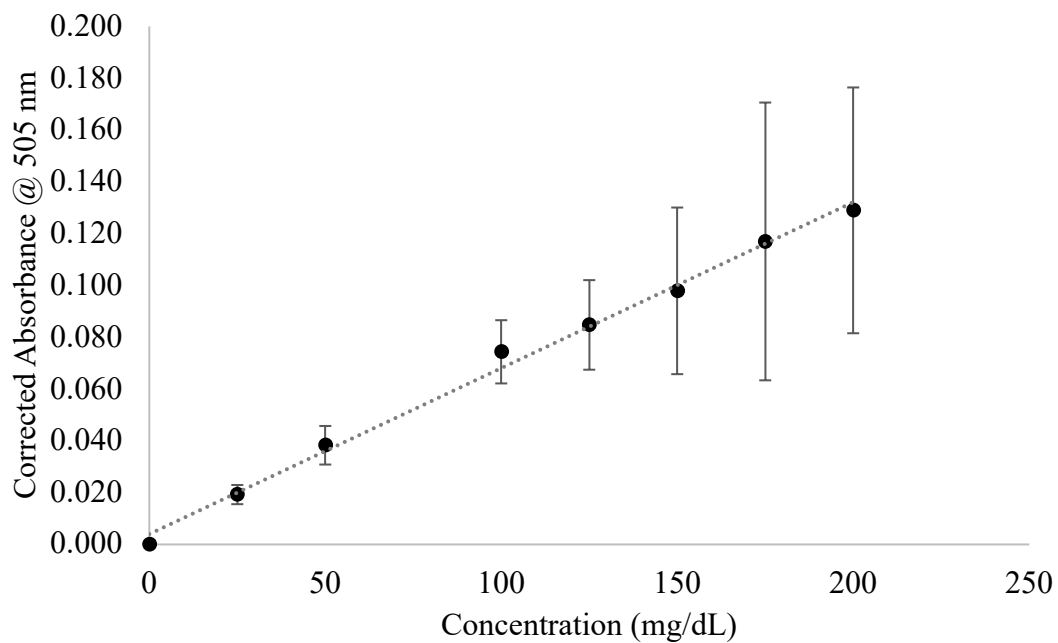
**Appendix VIII: Glucose standard curve formed by plotting known glucose standards against corrected absorbance readings at 340 nm. Line of best fit  $y = 0.0019x - 0.0019$  with**

$$R^2 = 0.9978$$



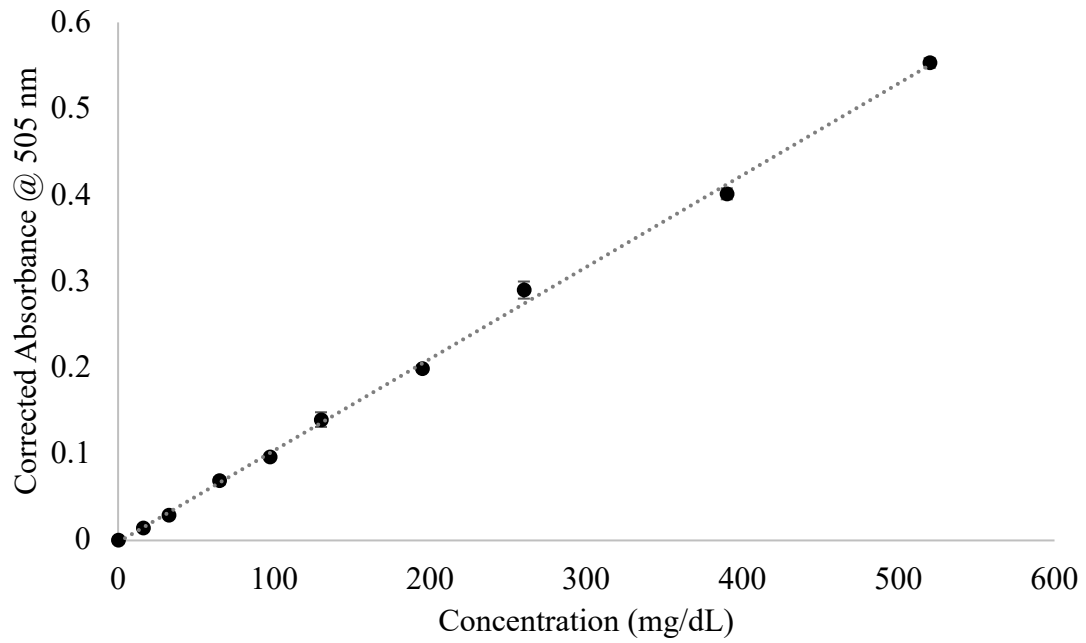
**Appendix IX: Cholesterol standard curve formed by plotting known cholesterol standards against corrected absorbance readings at 505 nm. Line of best fit  $y = 0.0006x + 0.004$  with**

$$R^2 = 0.9949$$



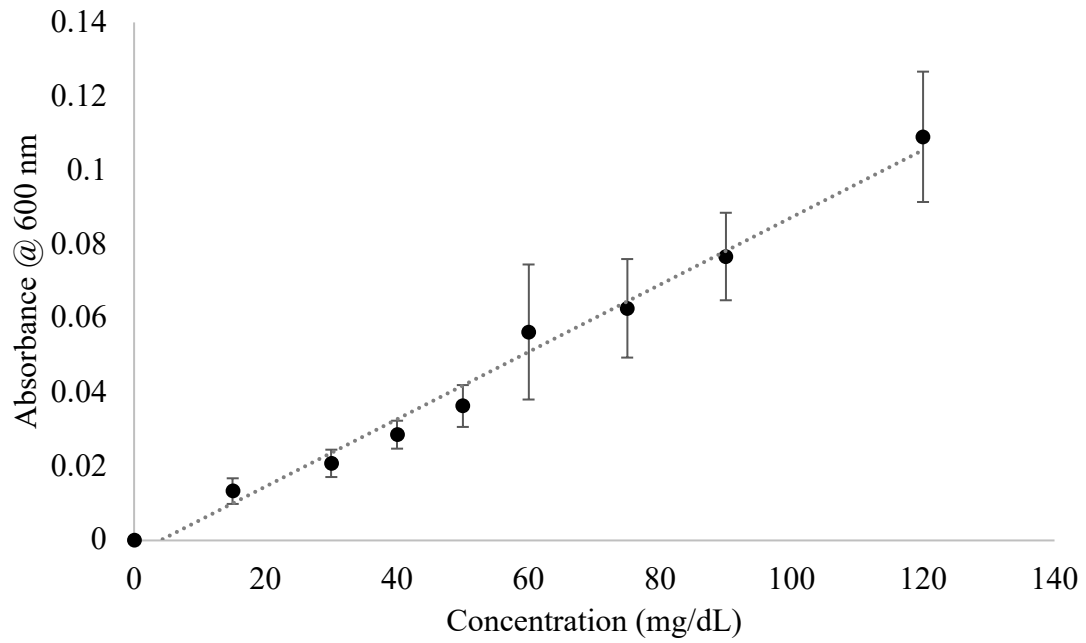
**Appendix X: Triacylglycerol standard curve formed by plotting known triacylglycerol standards against corrected absorbance readings at 505 nm. Line of best fit  $y = 0.0011x -$**

**$0.0021$  with  $R^2 = 0.9984$**



**Appendix XI: HDL standard curve formed by plotting known HDL standards against corrected absorbance readings at 600 nm. Line of best fit  $y = 0.0009x - 0.0036$  with**

$$R^2 = 0.9866$$



## Appendix XII: Additional data demonstrating sex differences

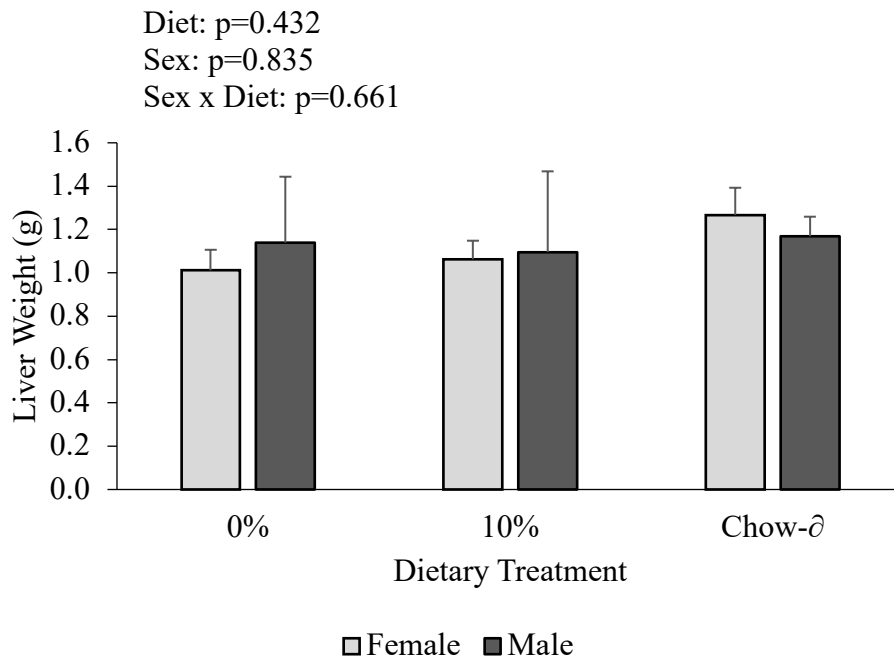


**Figure A.1: Effect of sex by diet on liver weight of FE1 mice**

Bars represent mean  $\pm$  standard deviations in grams. For analysis of liver weight:  $n=2$  for male 0%;  $n=3$  for all other treatment groups. A two-way ANOVA followed by Tukey's Post-hoc test ( $p < 0.05$ ) was used to test for sex by diet effects. No differences were determined between sex within the same dietary treatment or within the same sex across dietary treatment.

0%, 0% fructose; 10%, 10% fructose; Chow-∅, 20% fructose reverted to chow

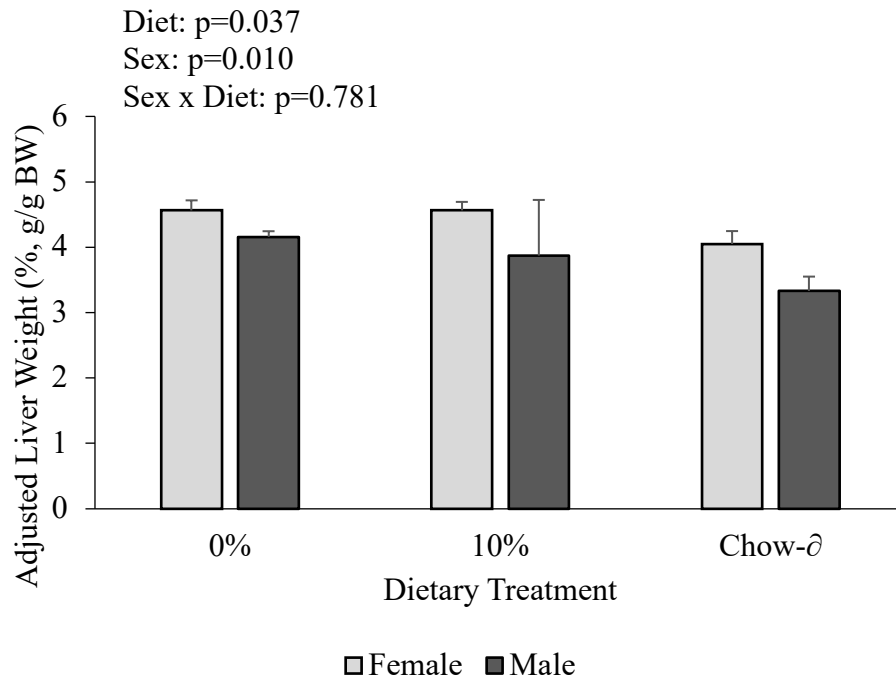


**Figure A.2: Effect of sex by diet on adjusted liver weight of FE1 mice**

Bars represent mean  $\pm$  standard deviations in percent body weight (% g/g body weight). For analysis of liver weight: n=2 for male 0%; n=3 for all other treatment groups. A two-way ANOVA followed by Tukey's Post-hoc test ( $p < 0.05$ ) was used to test for sex by diet effects. No differences were determined between sex within the same dietary treatment or within the same sex across dietary treatment.

0%, 0% fructose; 10%, 10% fructose; Chow-∂, 20% fructose reverted to chow

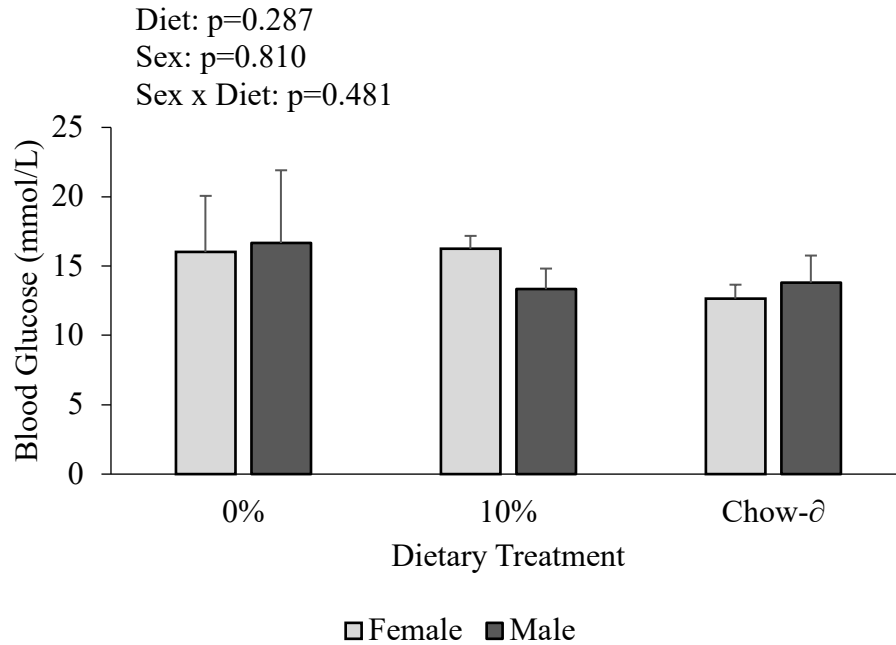


**Figure A.3: Effect of sex by diet on blood glucose by glucose oxidase method in FE1 mice**

Bars represent mean  $\pm$  standard deviations in mmol/L. For analysis of blood glucose: n=2 for female 0%, 10%, Chow-d, male 0%; n=3 for male 10% and Chow-d. A two-way ANOVA followed by Tukey's Post-hoc test ( $p < 0.05$ ) was used to test for sex by effects. No differences were determined between sex within the same dietary treatment or within the same sex across dietary treatment.

0%, 0% fructose; 10%, 10% fructose; Chow-d, 20% fructose reverted to chow

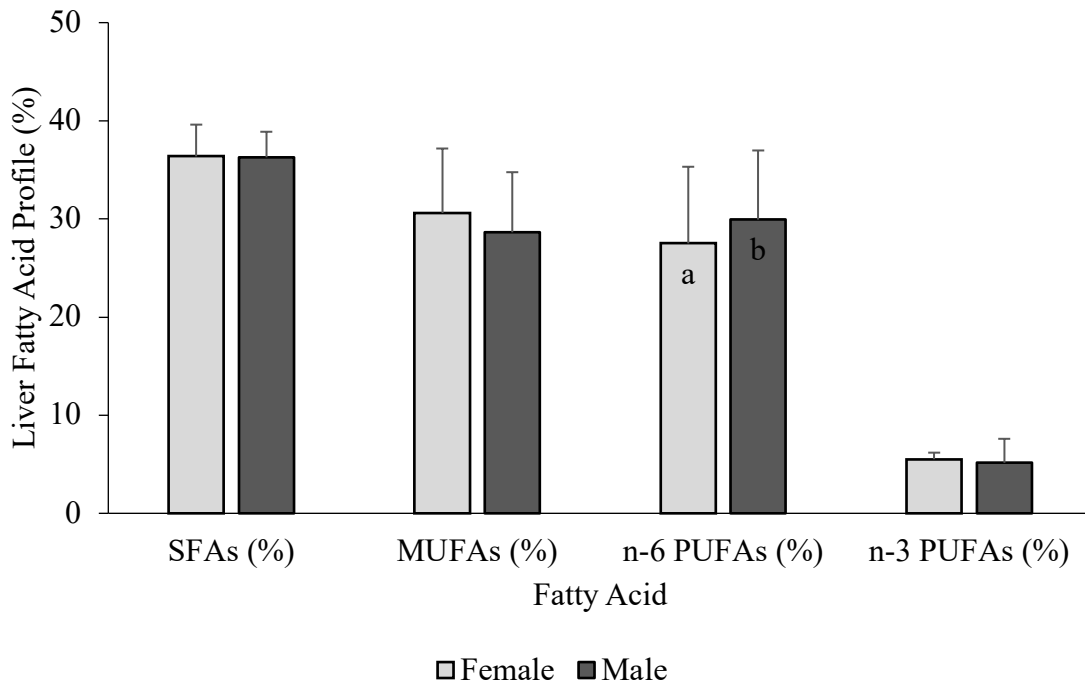


**Figure A.4: Effect of sex on liver lipid profile of FE1 mice**

Bars represent mean  $\pm$  standard deviations in percent. For analysis of liver lipid profile: n=9 for females; n=8 for males. Two-way ANOVA followed by Tukey's Post-hoc test ( $p < 0.05$ ) was used to test for sex by diet effects. Letters within a class of FA (e.g. n-6 PUFAs) denotes statistical significance between females and males.

Diet: SFAs,  $p=0.033$ ; MUFAs,  $p<0.001$ ; n-6 PUFAs,  $p<0.001$ , n-3 PUFAs,  $p=0.303$

Sex: SFAs,  $p=0.970$ ; MUFAs,  $p=0.149$ ; n-6 PUFAs,  $p=0.007$ , n-3 PUFAs,  $p=0.781$

Sex x Diet: SFAs,  $p=0.884$ ; MUFAs,  $p=0.938$ ; n-6 PUFAs,  $p=0.268$ , n-3 PUFAs,  $p=0.706$

MUFAs; monounsaturated fatty acids; n-6 PUFAs, omega-6 polyunsaturated fatty acids; n-3 PUFAs, omega-3 polyunsaturated fatty acids

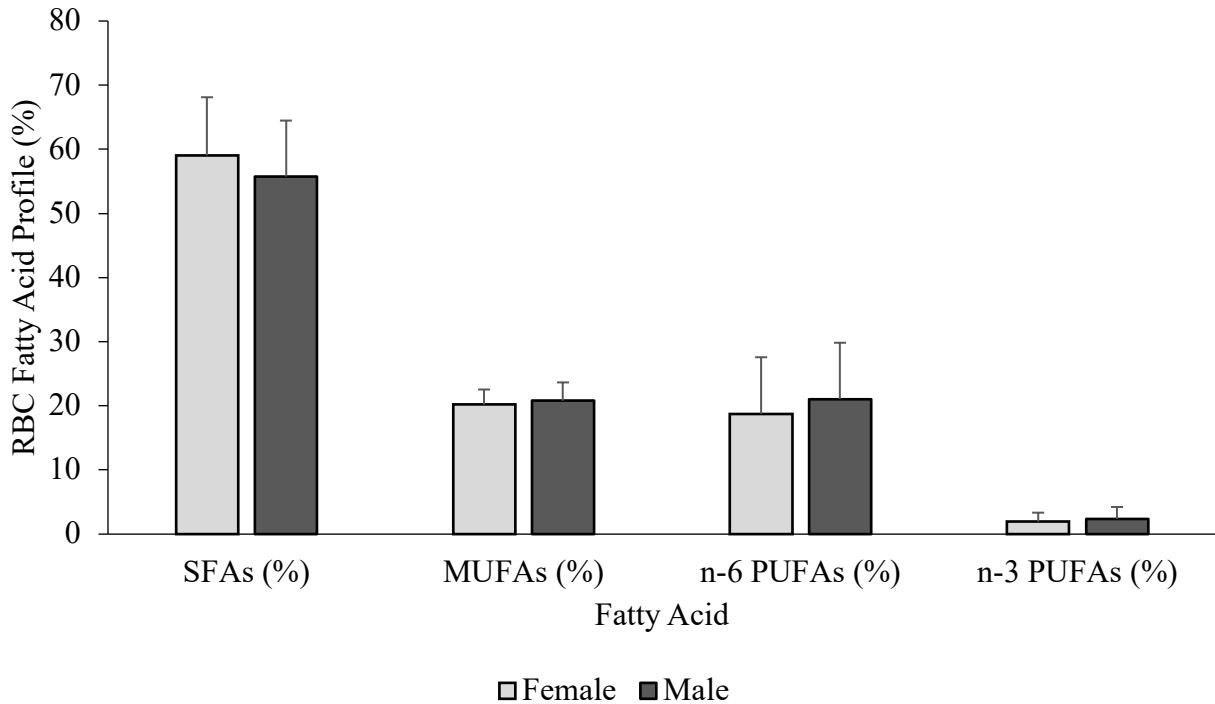


**Figure A.5: Effect of sex on RBC lipid profile of FE1 mice**

Bars represent mean  $\pm$  standard deviations in percent. For analysis of RBC lipid profile: n=8 for females and males. Two-way ANOVA followed by Tukey's Post-hoc test ( $p < 0.05$ ) was used to test for sex by diet effects. No differences were determined between sex.

Diet: SFAs,  $p=0.346$ ; MUFAs,  $p=0.765$ ; n-6 PUFAs,  $p=0.427$ , n-3 PUFAs,  $p=0.281$

Sex: **SFAs,  $p=0.001$** ; MUFAs,  $p=0.778$ ; n-6 PUFAs,  $p=0.389$ , n-3 PUFAs,  $p=0.792$

Sex x Diet: **SFAs,  $p=0.035$** ; **MUFAs,  $p=0.009$** ; **n-6 PUFAs,  $p=0.027$** , **n-3 PUFAs,  $p=0.004$**

MUFAs; monounsaturated fatty acids; n-6 PUFAs, omega-6 polyunsaturated fatty acids; n-3 PUFAs, omega-3 polyunsaturated fatty acids

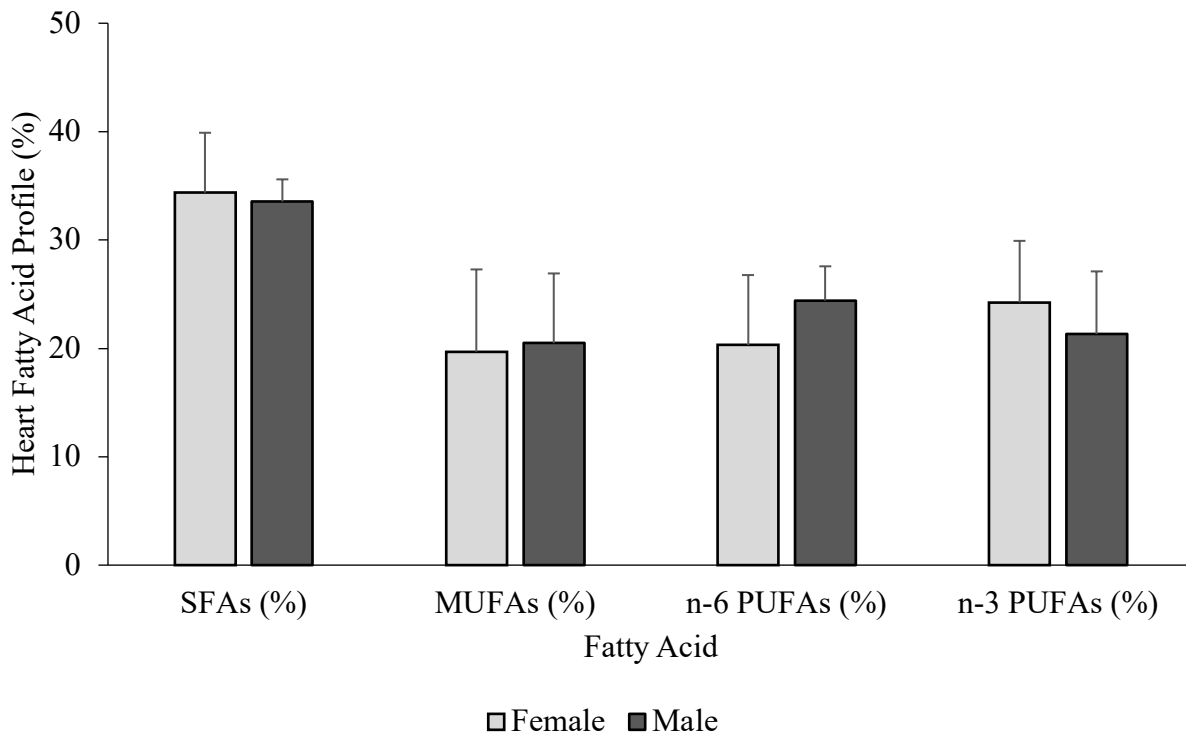


**Figure A.6: Effect of sex on heart tissue lipid profile of FE1 mice**

Bars represent mean  $\pm$  standard deviations in percent. For analysis of heart tissue lipid profile: n=9 for females; n=7 for males. Two-way ANOVA followed by Tukey's Post-hoc test ( $p < 0.05$ ) was used to test for sex by diet effects. No differences were determined within sex.

Diet: SFAs,  $p=0.822$ ; MUFAs,  $p=0.873$ ; n-6 PUFAs,  $p=0.165$ , n-3 PUFAs,  $p=0.438$

Sex: SFAs,  $p=0.644$ ; MUFAs,  $p=0.886$ ; n-6 PUFAs,  $p=0.138$ , n-3 PUFAs,  $p=0.535$

Sex x Diet: SFAs,  $p=0.423$ ; MUFAs,  $p=0.348$ ; n-6 PUFAs,  $p=0.482$ , n-3 PUFAs,  $p=0.873$

MUFAs; monounsaturated fatty acids; n-6 PUFAs, omega-6 polyunsaturated fatty acids; n-3 PUFAs, omega-3 polyunsaturated fatty acids

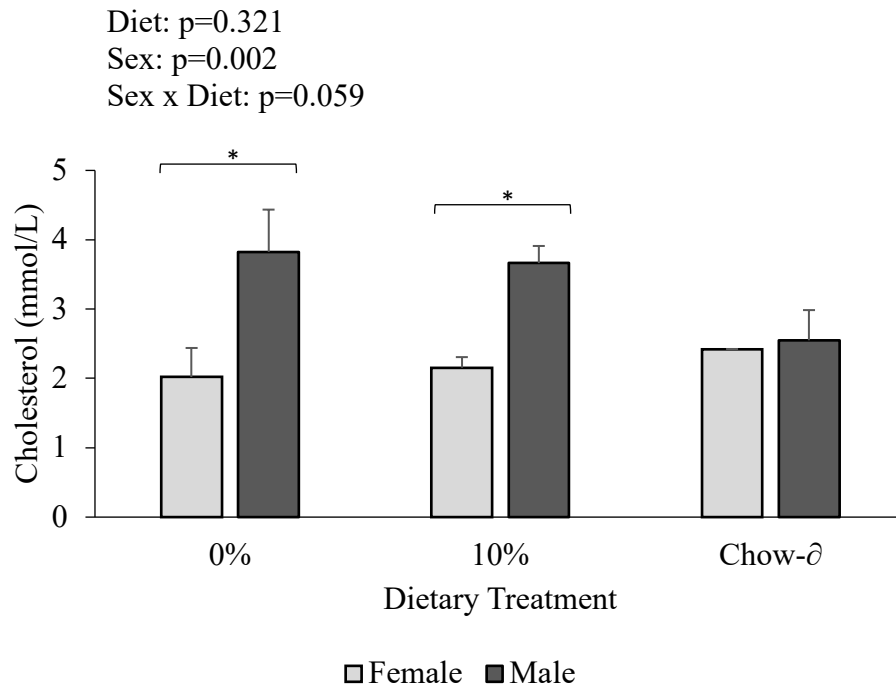


**Figure A.7: Effect of sex by diet on total mean plasma cholesterol of FE1 mice**

Bars represent mean  $\pm$  standard deviations in mmol/L. For analysis of total plasma cholesterol:  $n=1$  for Chow- $\delta$  female,  $n=2$  for 0% female, 10% female, and 0% male;  $n=3$  for 10% male and Chow- $\delta$  male. A two-way ANOVA followed by Tukey's Post-hoc test ( $p < 0.05$ ) was used to test for sex by diet effects. Additionally, Student T-Test ( $p < 0.05$ ) was used to test for within diet effects. Differing symbols within the same sex across dietary treatment groups denotes a statistically significant difference mean cholesterol concentrations. \* denotes statistical differences in mean cholesterol concentrations between sex within the same dietary treatment. 0%, 0% fructose; 10%, 10% fructose; Chow- $\delta$ , 20% fructose reverted to chow

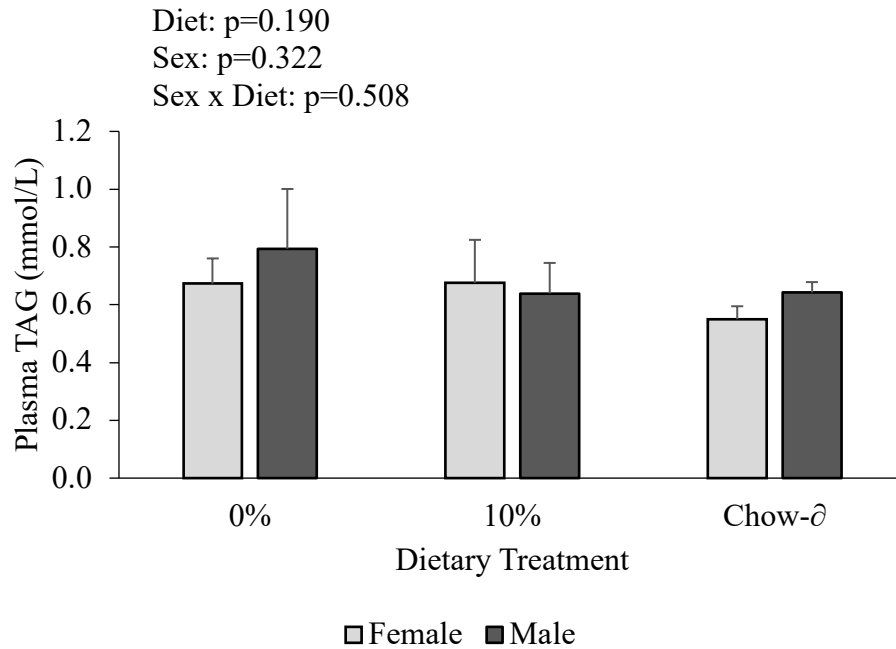


**Figure A.8: Effect of sex by diet on mean plasma TAG concentrations of FE1 mice**

Bars represent mean  $\pm$  standard deviations in mmol/L. For analysis of plasma TAG concentrations: n=2 for 0% female, 10% female, and 0% male; n=3 for Chow-∂ female, 10% male, and Chow-∂ male. A two-way ANOVA followed by Tukey's Post-hoc test ( $p < 0.05$ ) was used to test for sex by diet effects. No differences were determined between sex within the same dietary treatment or within the same sex across dietary treatment.

0%, 0% fructose; 10%, 10% fructose; Chow-∂, 20% fructose reverted to chow

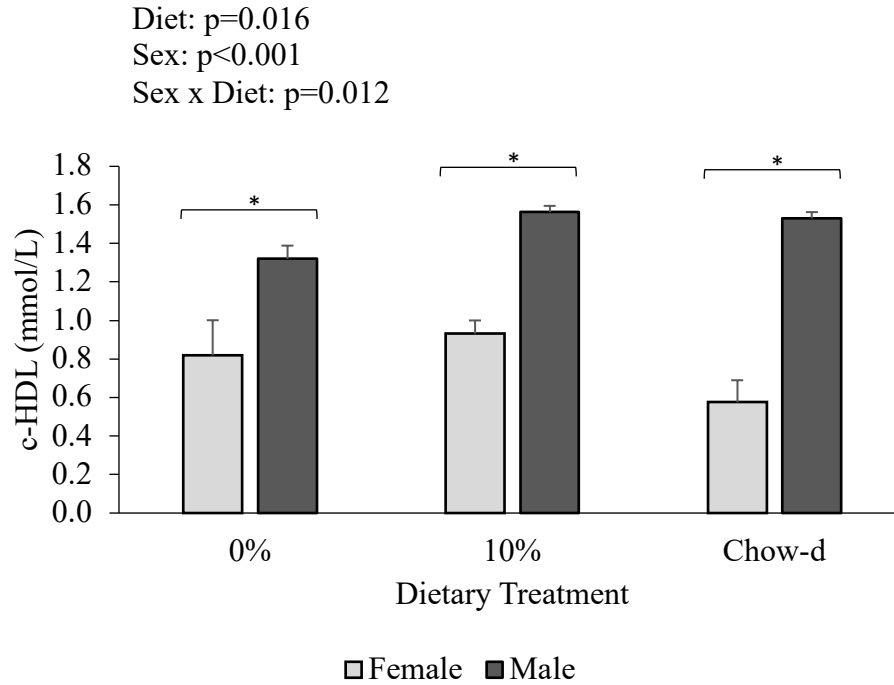


**Figure A.9: Effect of sex by diet on mean plasma c-HDL cholesterol concentrations of FE1 mice**

Bars represent mean  $\pm$  standard deviations. For analysis of plasma c-HDL cholesterol concentrations:  $n=2$  for 0% female, 10% female, Chow- $\delta$  female, and 0% male;  $n=3$  for 10% male and Chow- $\delta$  male. A two-way ANOVA followed by Tukey's Post-hoc test ( $p < 0.05$ ) was used to test for sex by diet effects. Additionally, Student T-Test ( $p < 0.05$ ) was used to test for within diet effects. \* denotes statistical differences in c-HDL cholesterol concentrations between sex within the same dietary treatment.

0%, 0% fructose; 10%, 10% fructose; Chow- $\delta$ , 20% fructose reverted to chow

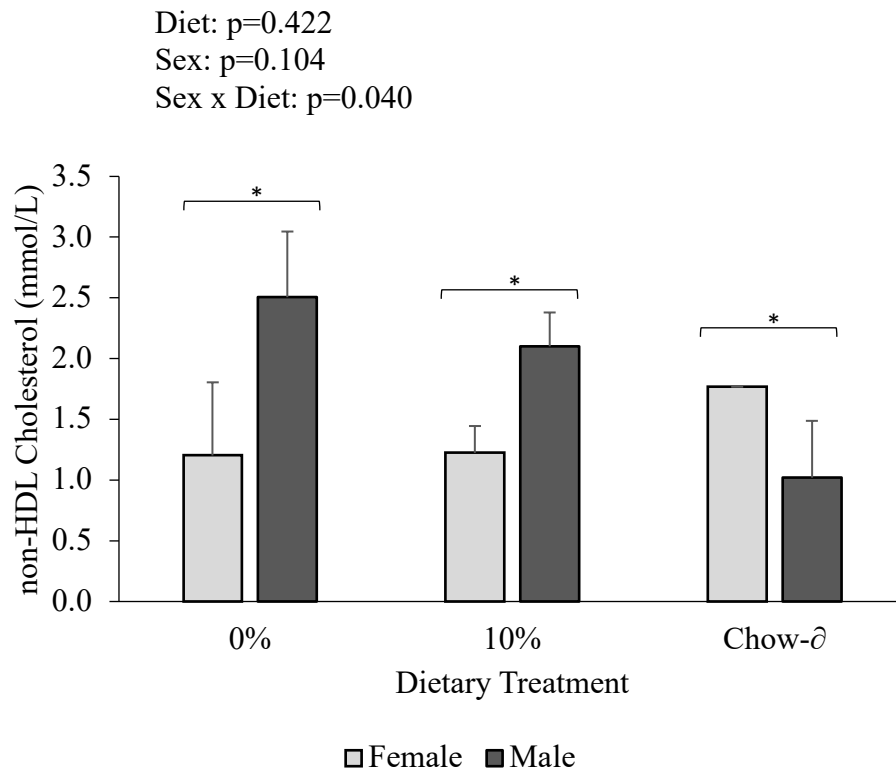


**Figure A.10: Effect of sex by diet on mean plasma non-HDL cholesterol concentrations of FE1 mice**

Bars represent mean  $\pm$  standard deviations in mmol/L. For analysis of plasma non-HDL cholesterol concentrations  $n=2$  for 0% female, 10% female, Chow-∂ female, and 0% male;  $n=3$  for 10% male and Chow-∂ male. A two-way ANOVA followed by Tukey's Post-hoc test ( $p < 0.05$ ) was used to test for sex by diet effects. Additionally, Student T-Test ( $p < 0.05$ ) was used to test for within diet effects. \* denotes statistical differences non-HDL cholesterol concentrations between sex within the same dietary treatment.

0%, 0% fructose; 10%, 10% fructose; 20%, 20% fructose

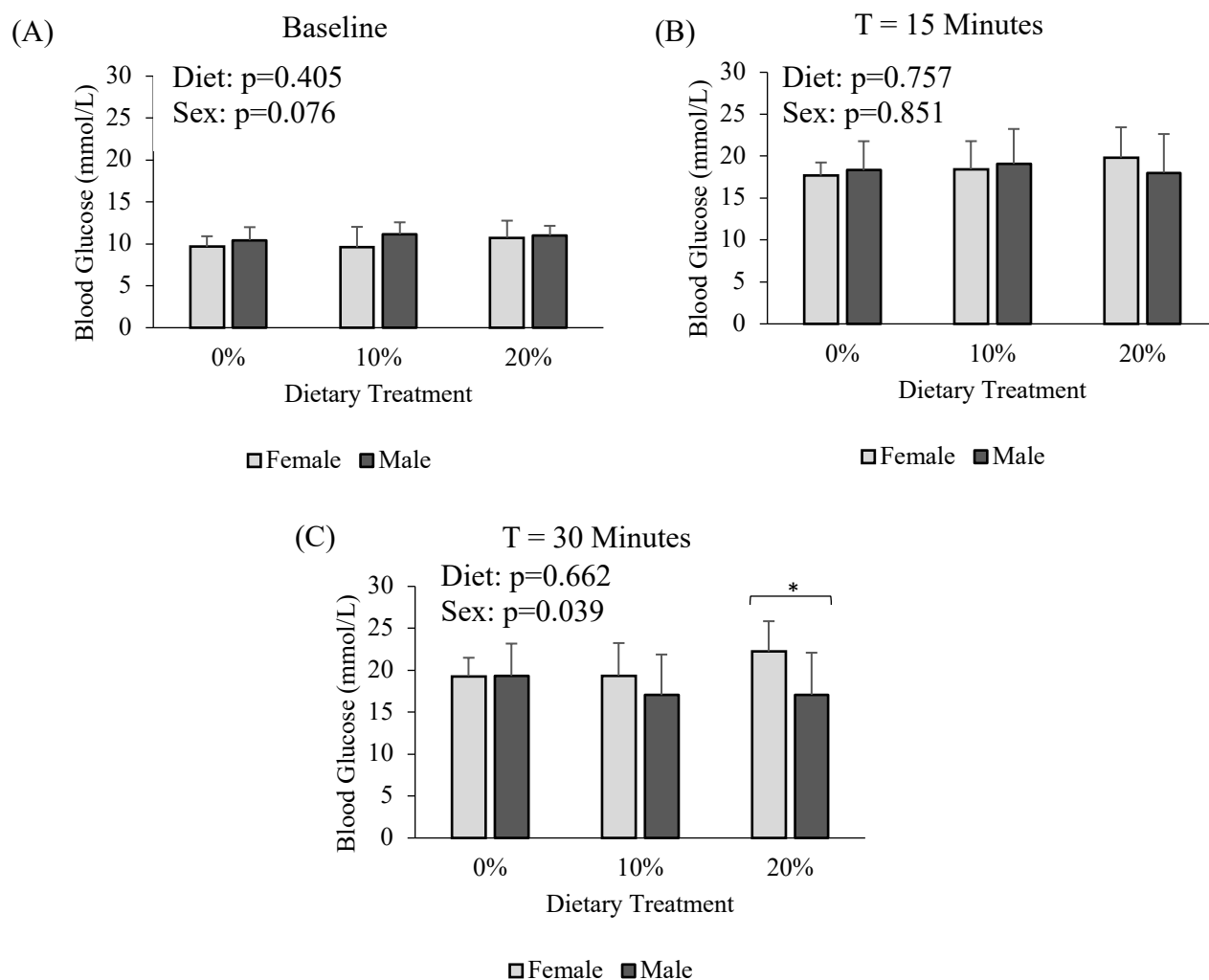


**Figure A.11: Effect of sex by diet on blood glucose concentrations by glucometer method at various time points in FE2 mice**

(A) Baseline, T = 0 minutes (B) T = 15 minutes (C) HP, T = 30 minutes

Bars represent mean  $\pm$  standard deviations in mmol/L. For analysis of blood glucose concentration:  $n=8$  for 0% female, 20% female, 10% male;  $n=9$  for 10% female, 0% male, 20% male. A two-way ANOVA followed by Tukey's Post-hoc test ( $p<0.05$ ) was used to test for sex by diet effects. Additionally, Student T-Test ( $p<0.05$ ) was used to test for within diet effects. \* denotes statistical differences in blood glucose concentrations between sex within the same dietary treatment.

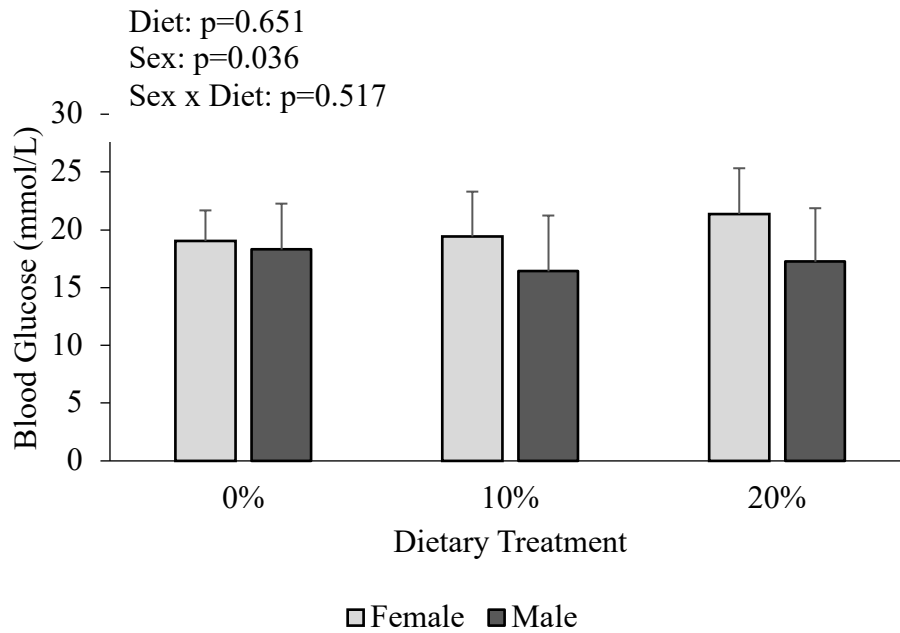


**Figure A.12: Effect of sex by diet on blood glucose by glucose oxidase method in FE2 mice**

Bars represent mean  $\pm$  standard deviations in mmol/L. For analysis of blood glucose, n=25 for females and n=26 for males. A two-way ANOVA followed by Tukey's Post-hoc test ( $p < 0.05$ ) was used to test for sex effects. Between sex effects were present ( $p = 0.036$ ) but this significance was not present when sex by diet interactions were investigated.

0%, 0% fructose; 10%, 10% fructose; 20%, 20% fructose

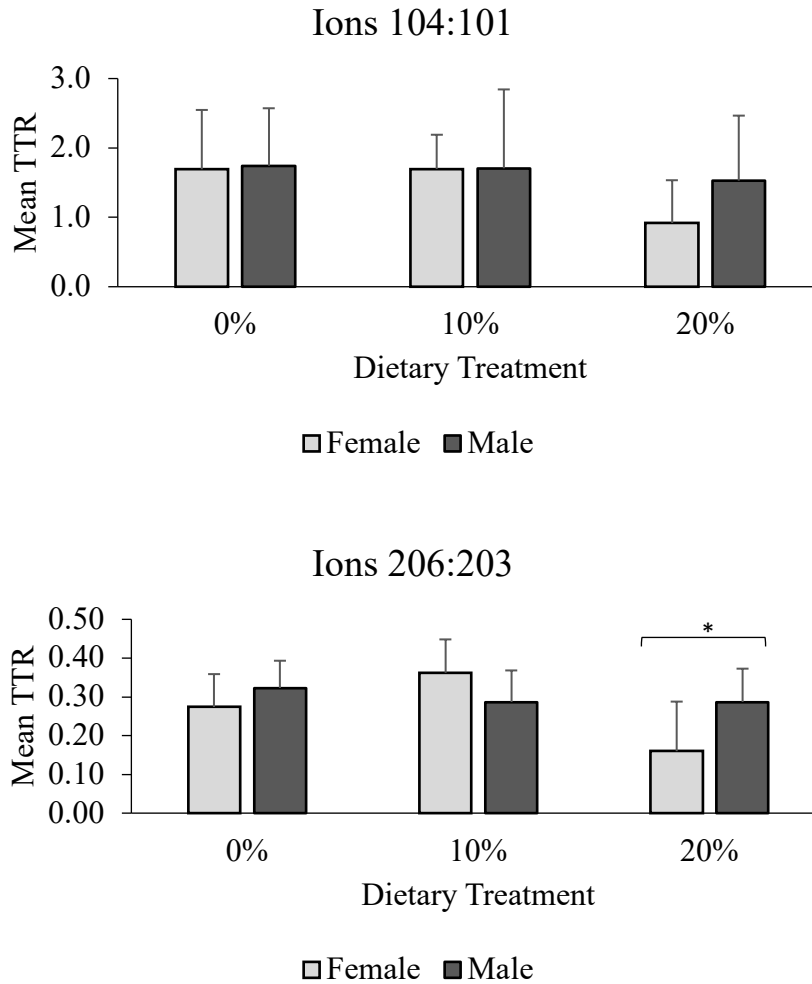


**Figure A.13: Effect of sex by diet on mean fructose TTR for various ions at T = 30 minutes in FE2 mice**

Bars represent mean  $\pm$  standard deviations in percent. For analysis of mean TTR: n=6 for 20% females; n=7 for 0% females and males; n=8 for 10% males; n=9 for 10% females and 20% males. A two-way ANOVA followed by Tukey’s Post-hoc test ( $p < 0.05$ ) was used to test for dietary treatment effect. Additionally, Student T-Test ( $p < 0.05$ ) was used to test for within diet effects. \* denotes statistical differences in mean TTR between sex within the same dietary treatment.

0%, 0% fructose; 10%, 10% fructose; 20%, 20% fructose

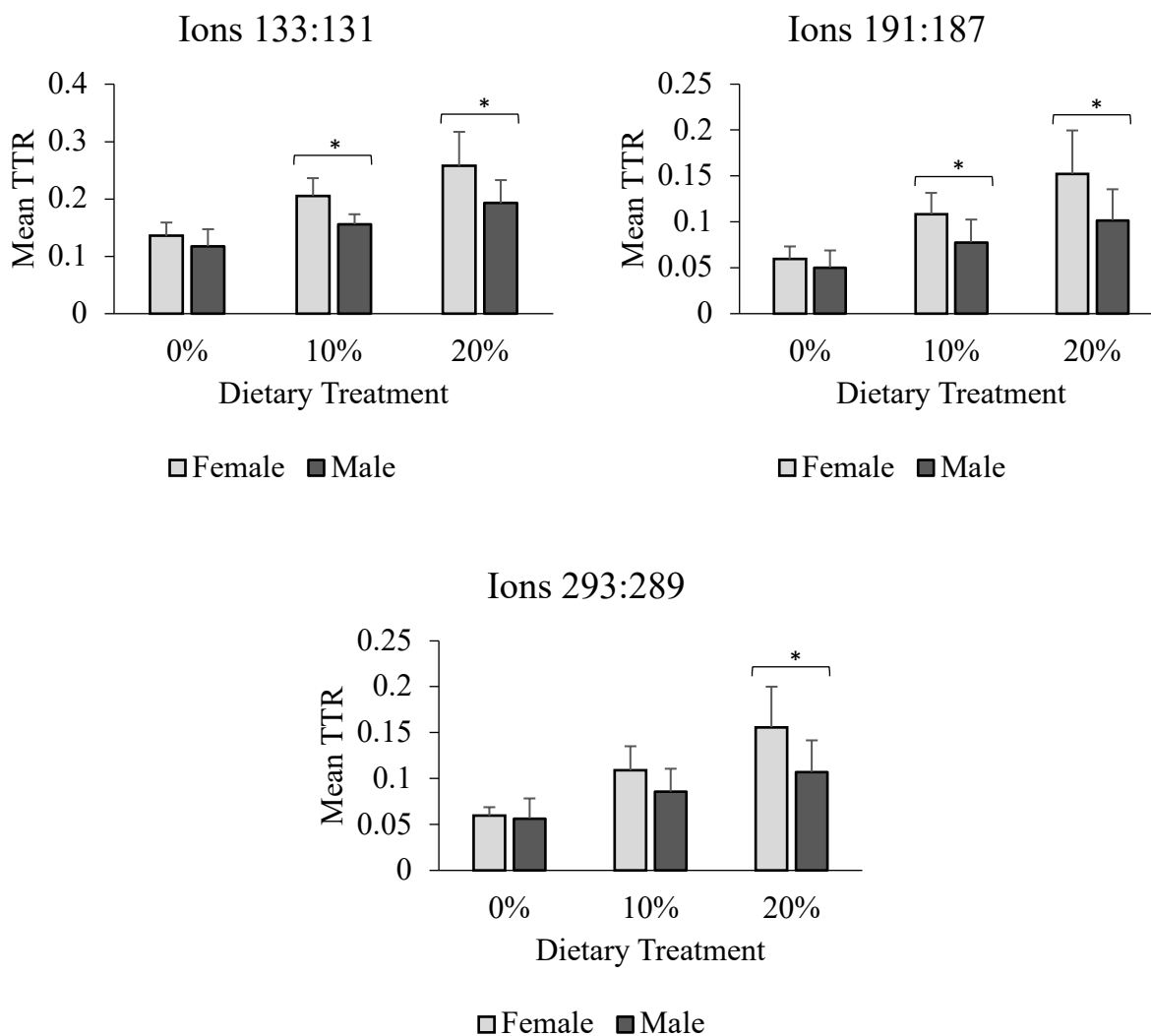


**Figure A.14: Effect of sex by diet on mean glucose TTR for various ions at T = 30 minutes in FE2 mice**

Bars represent mean  $\pm$  standard deviations in percent. For analysis of mean TTR: n=7 for 20% females; n=8 for 0% females, 10% females, 10% males, 20% males; n=9 for 0% males. A two-way ANOVA followed by Tukey's Post-hoc test ( $p < 0.05$ ) was used to test for dietary treatment effect. Additionally, Student T-Test ( $p < 0.05$ ) was used to test for within diet effects.

\* denotes statistical differences in mean TTR between sex within the same dietary treatment.

0%, 0% fructose; 10%, 10% fructose; 20%, 20% fructose

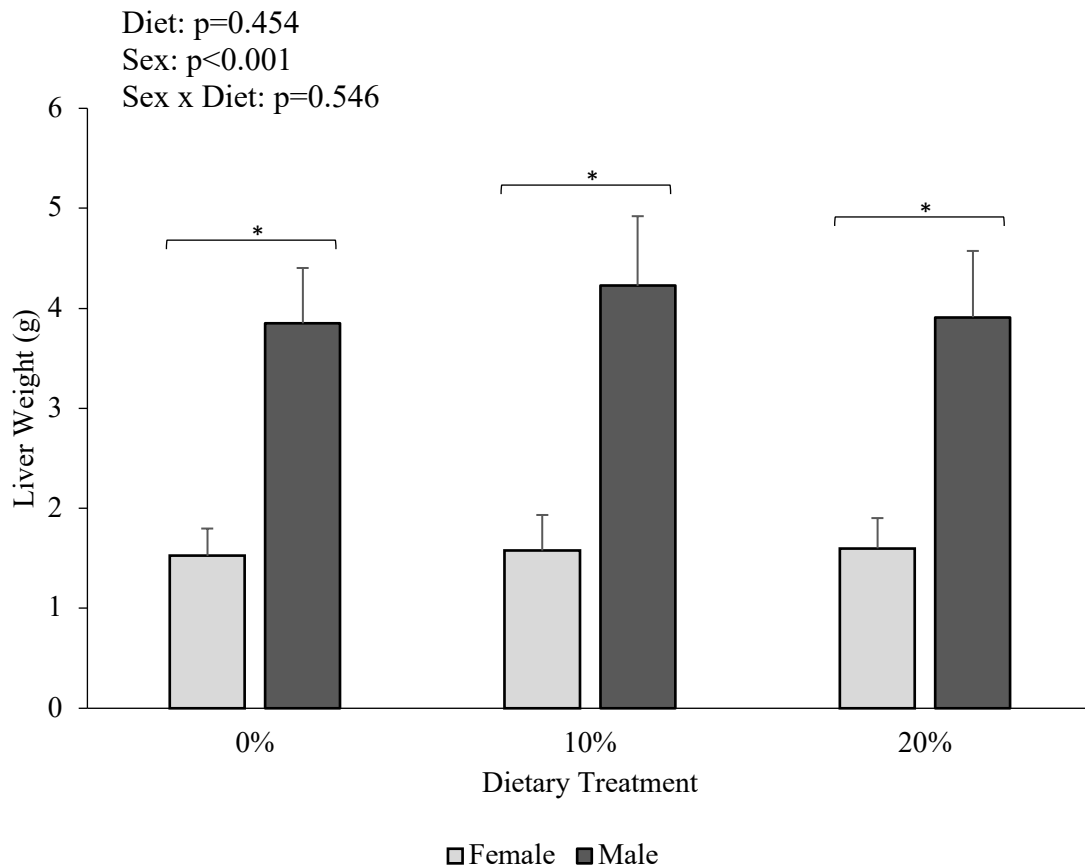


**Figure A.15: Effect of sex by diet on liver weight of FE2 mice**

Bars represent mean  $\pm$  standard deviations in grams. For analysis of liver weight:  $n=8$  for 0% female, 20% female, 10% male;  $n=9$  for 10% female, 0% male, 20% male. A two-way ANOVA followed by Tukey's Post-hoc test ( $p < 0.05$ ) was used to test for sex by diet effects.

Additionally, Student T-Test ( $p < 0.05$ ) was used to test for within diet effects.

\* denotes statistical differences in liver weight between sex within the same dietary treatment.

0%, 0% fructose; 10%, 10% fructose; 20%, 20% fructose

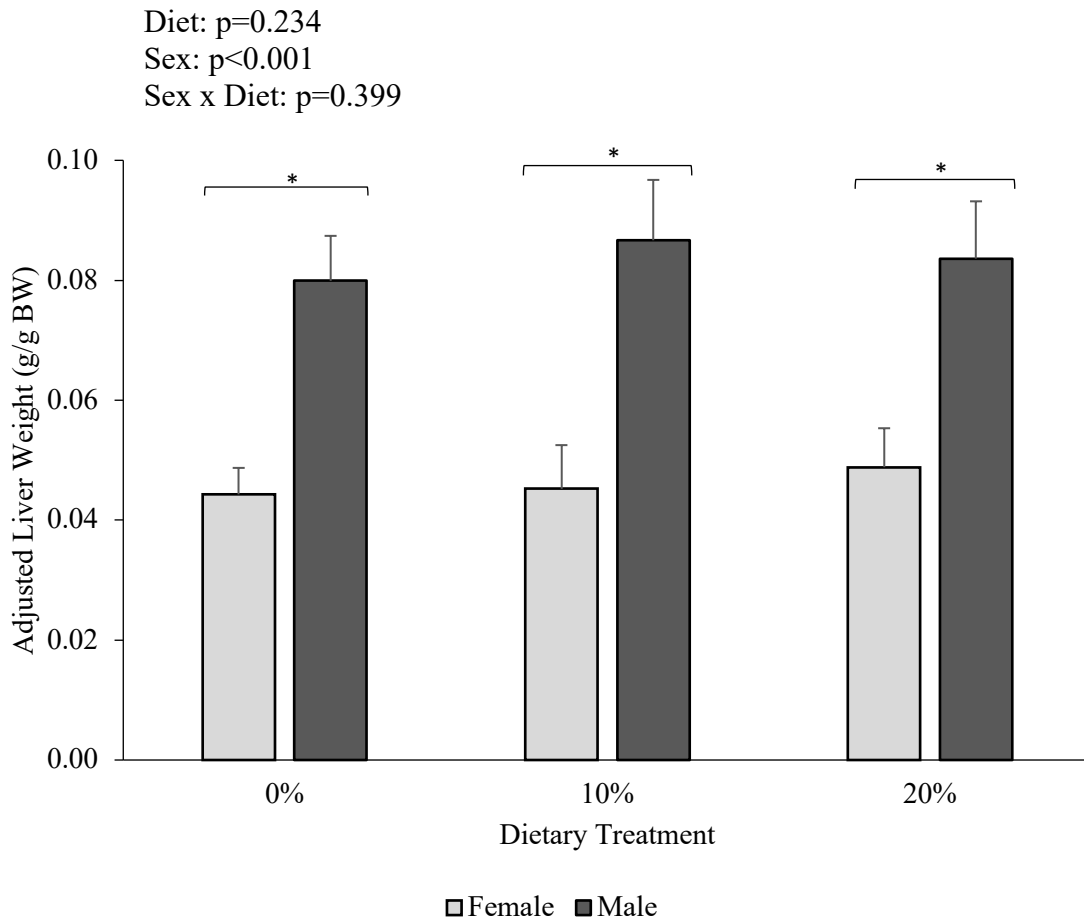


**Figure A.16: Effect of sex by diet on adjusted liver weight of FE2 mice**

Bars represent mean  $\pm$  standard deviations in percent body weight (g/g body weight). For analysis of adjusted liver weight:  $n=8$  for 0% female, 20% female, 10% male;  $n=9$  for 10% female, 0% male, 20% male. A two-way ANOVA followed by Tukey's Post-hoc test ( $p < 0.05$ ) was used to test for sex by diet effects. Additionally, Student T-Test ( $p < 0.05$ ) was used to test for within diet effects. \* denotes statistical differences in adjusted liver weight between sex within the same dietary treatment.

0%, 0% fructose; 10%, 10% fructose; 20%, 20% fructose

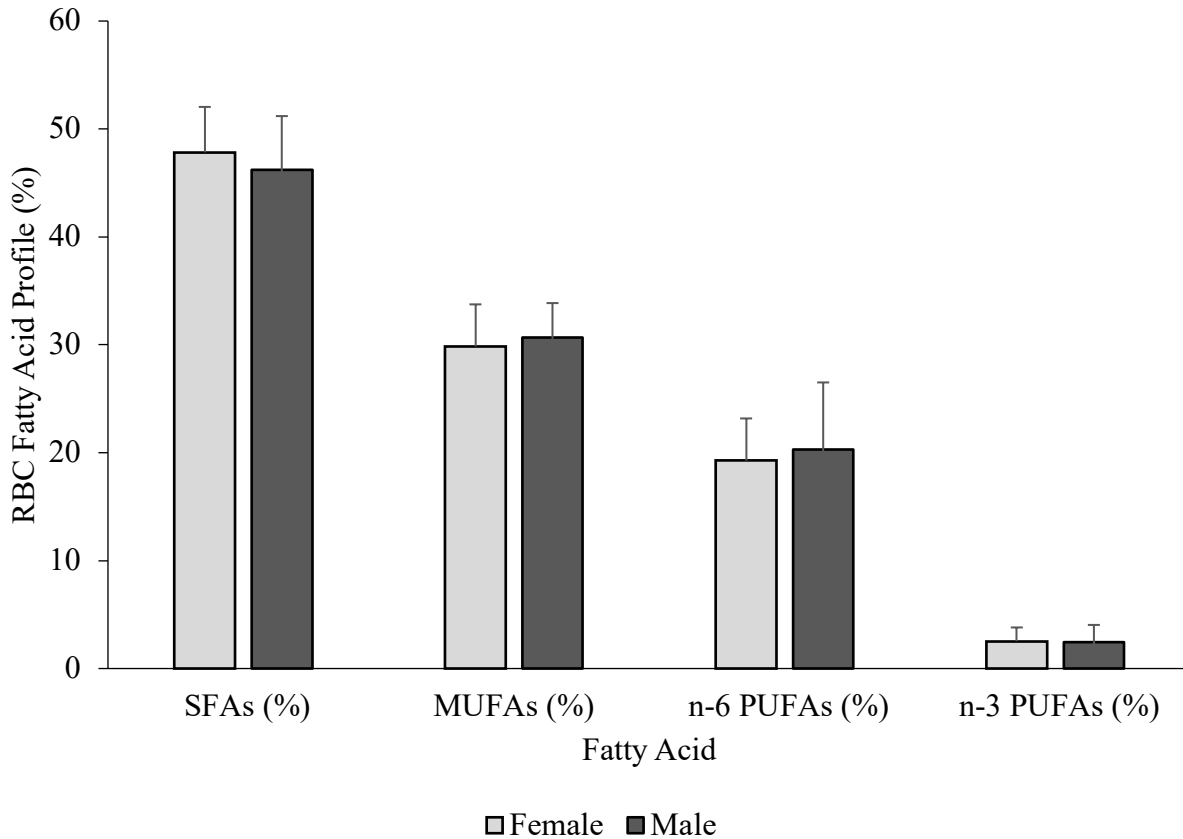


**Figure A.17: Effect of sex on RBC lipid profile of FE2 mice**

Bars represent mean  $\pm$  standard deviations in percent. For analysis of RBC lipid profile, n=26 for females and n=27 for males. Two-way ANOVA followed by Tukey's Post-hoc test ( $p < 0.05$ ) was used to test for sex by diet effects. No differences were determined between sexes or sex by diet interactions.

Diet: SFAs,  $p=0.240$ ; MUFAs,  $p=0.883$ ; n-6 PUFAs,  $p=0.349$ , n-3 PUFAs,  $p=0.818$

Sex: SFAs,  $p=0.212$ ; MUFAs,  $p=0.415$ ; n-6 PUFAs,  $p=0.481$ , n-3 PUFAs,  $p=0.880$

Sex x Diet: SFAs,  $p=0.977$ ; MUFAs,  $p=0.485$ ; n-6 PUFAs,  $p=0.640$ , n-3 PUFAs,  $p=0.741$

0%, 0% fructose; 10%, 10% fructose; 20%, 20% fructose; MUFAs; monounsaturated fatty acids; n-6 PUFAs, omega-6 polyunsaturated fatty acids; n-3 PUFAs, omega-3 polyunsaturated fatty acids

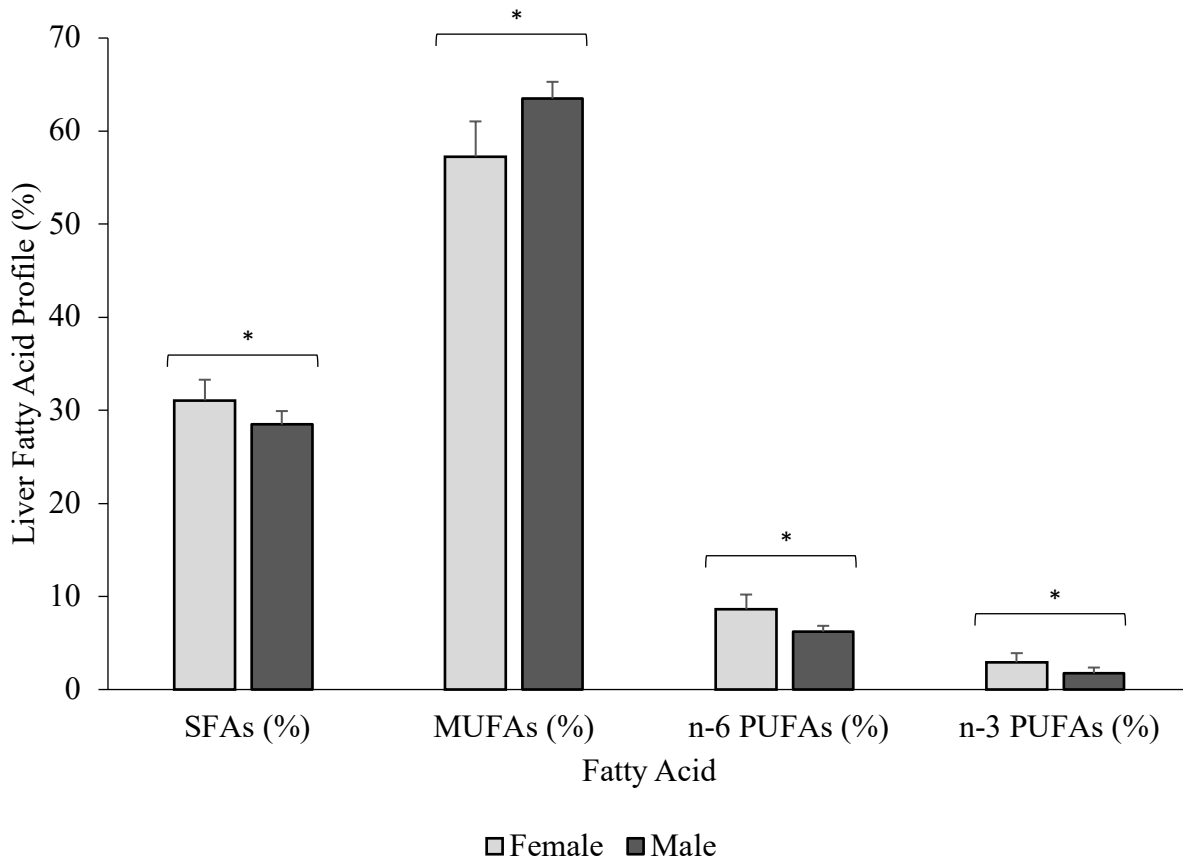


**Figure A.18: Effect of sex on liver lipid profile of FE2 mice**

Bars represent mean  $\pm$  standard deviations in percent. For analysis of liver lipid profile, n=26 for females and n=27 for males. Student T-test ( $p < 0.05$ ) was used to test for differences between sexes. \* over each class of FA (e.g. SFA) denotes statistical significance between females and males.

Diet: SFAs,  $p=0.390$ ; MUFAs,  $p=0.414$ ; n-6 PUFAs,  $p=0.567$ , n-3 PUFAs,  $p=0.718$

Sex: SFAs,  $p < 0.001$ ; MUFAs,  $p < 0.001$ ; n-6 PUFAs,  $p < 0.001$ , n-3 PUFAs,  $p < 0.001$

Sex x Diet: SFAs,  $p=0.951$ ; MUFAs,  $p=0.839$ ; n-6 PUFAs,  $p=0.515$ , n-3 PUFAs,  $p=0.463$

MUFAs; monounsaturated fatty acids; n-6 PUFAs, omega-6 polyunsaturated fatty acids; n-3 PUFAs, omega-3 polyunsaturated fatty acids

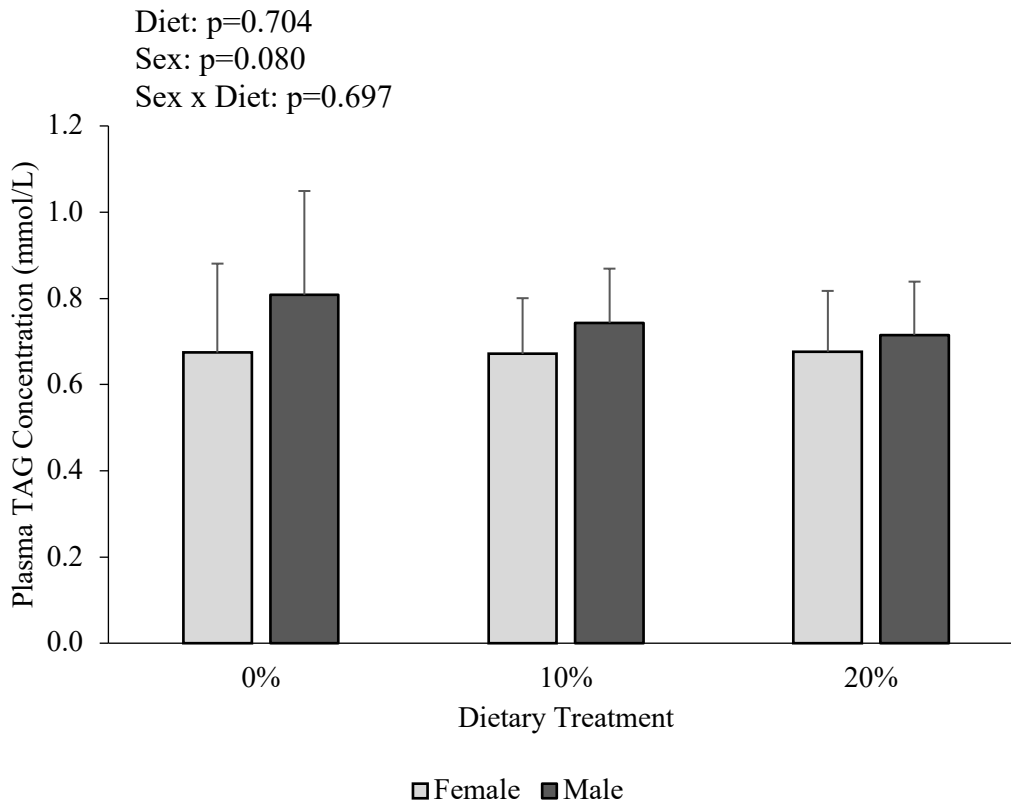


**Figure A.19: Effect of sex by diet on mean plasma TAG concentrations of FE2 mice**

Bars represent mean  $\pm$  standard deviations in mmol/L. For analysis of plasma TAG

concentrations: n=8 for 0% female, 20% female, 10% male; n=9 for 10% female, 0% male, 20% male. A two-way ANOVA followed by Tukey's Post-hoc test ( $p < 0.05$ ) was used to test for sex by diet effects. No differences were determined between sex within the same dietary treatment or within the same sex across dietary treatment.

0%, 0% fructose; 10%, 10% fructose; 20%, 20% fructose

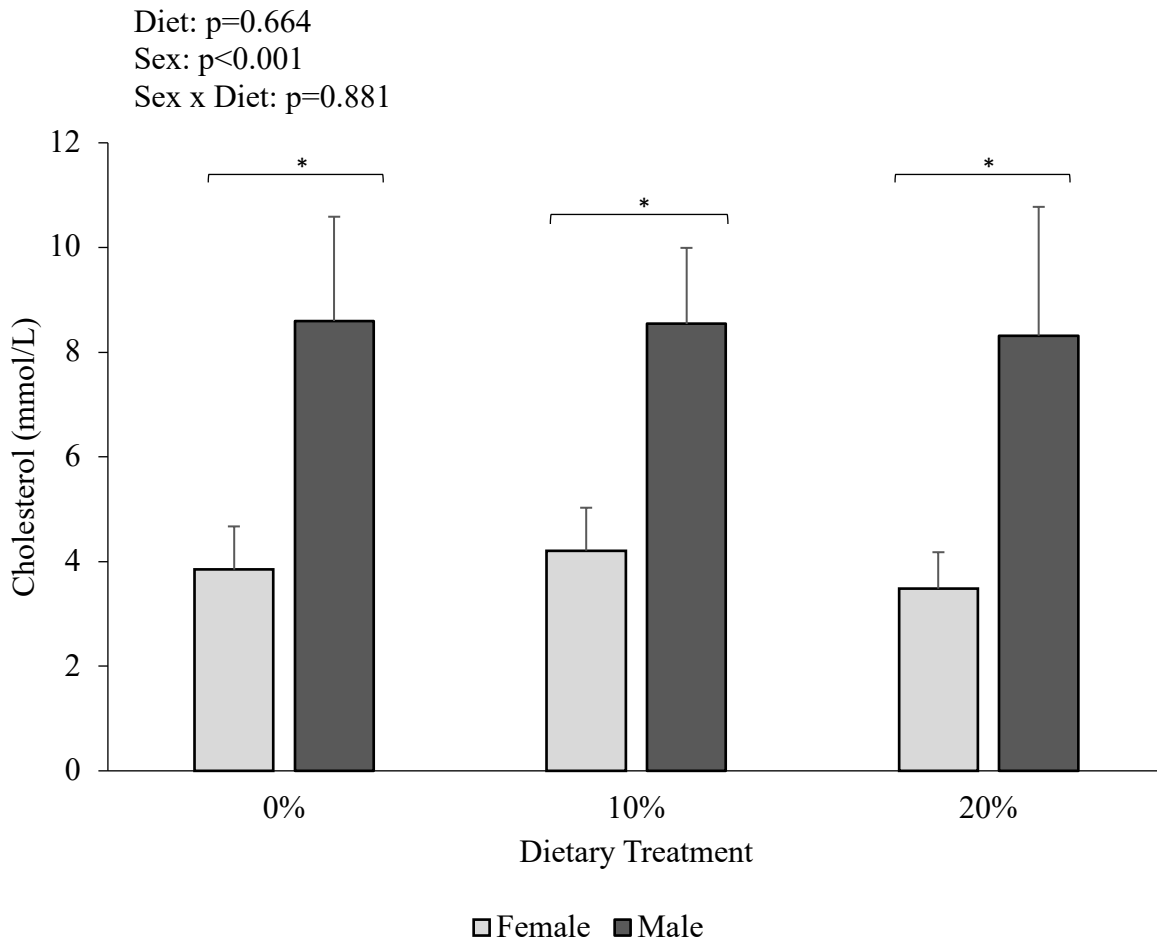


**Figure A.20: Effect of sex by diet on mean total plasma cholesterol of FE2 mice**

Bars represent mean  $\pm$  standard deviations in mmol/L. For analysis of total plasma cholesterol:  $n=8$  for 0% female, 20% female, 10% male;  $n=9$  for 10% female, 0% male, 20% male. A two-way ANOVA followed by Tukey's Post-hoc test ( $p < 0.05$ ) was used to test for sex by diet effects. Additionally, Student T-Test ( $p < 0.05$ ) was used to test for within diet effects.

\* denotes statistical differences in total plasma cholesterol concentrations between sex within the same dietary treatment.

0%, 0% fructose; 10%, 10% fructose; 20%, 20% fructose

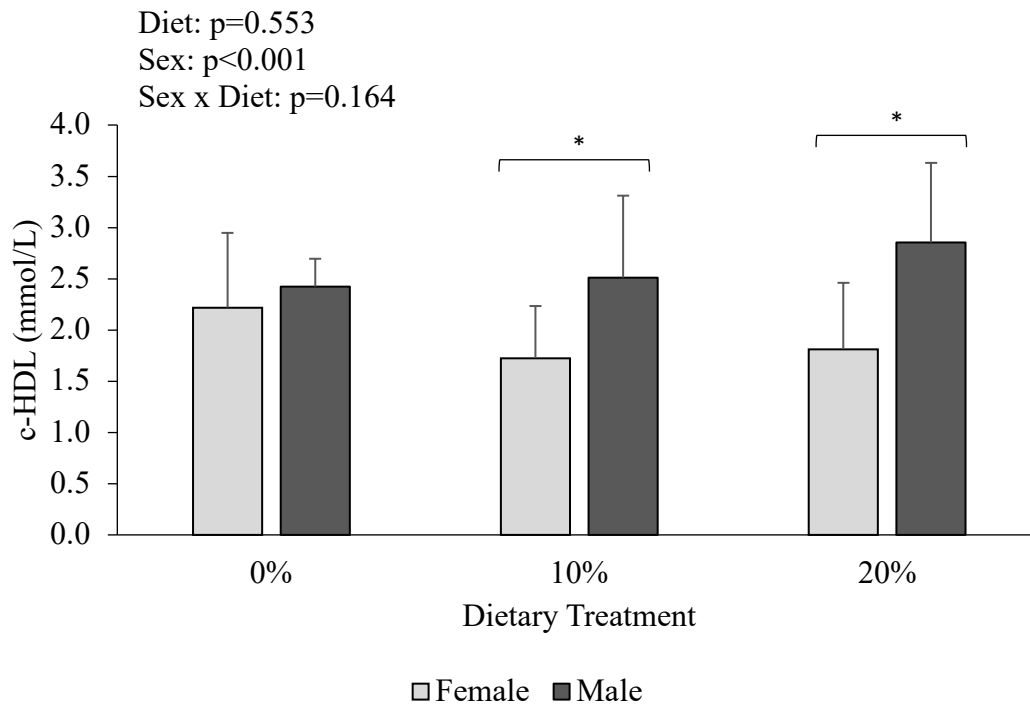


**Figure A.21: Effect of sex by diet on mean plasma c-HDL cholesterol concentrations of FE2 mice**

Bars represent mean  $\pm$  standard deviations. For analysis of plasma c-HDL cholesterol concentrations:  $n=8$  for 0% female, 20% female, 10% male;  $n=9$  for 10% female, 0% male, 20% male. A two-way ANOVA followed by Tukey's Post-hoc test ( $p < 0.05$ ) was used to test for sex by diet effects. Additionally, Student T-Test ( $p < 0.05$ ) was used to test for within diet effects. \* denotes statistical differences ( $p < 0.001$ ) in mean plasma c-HDL cholesterol concentrations between sex within the same dietary treatment.

0%, 0% fructose; 10%, 10% fructose; 20%, 20% fructose

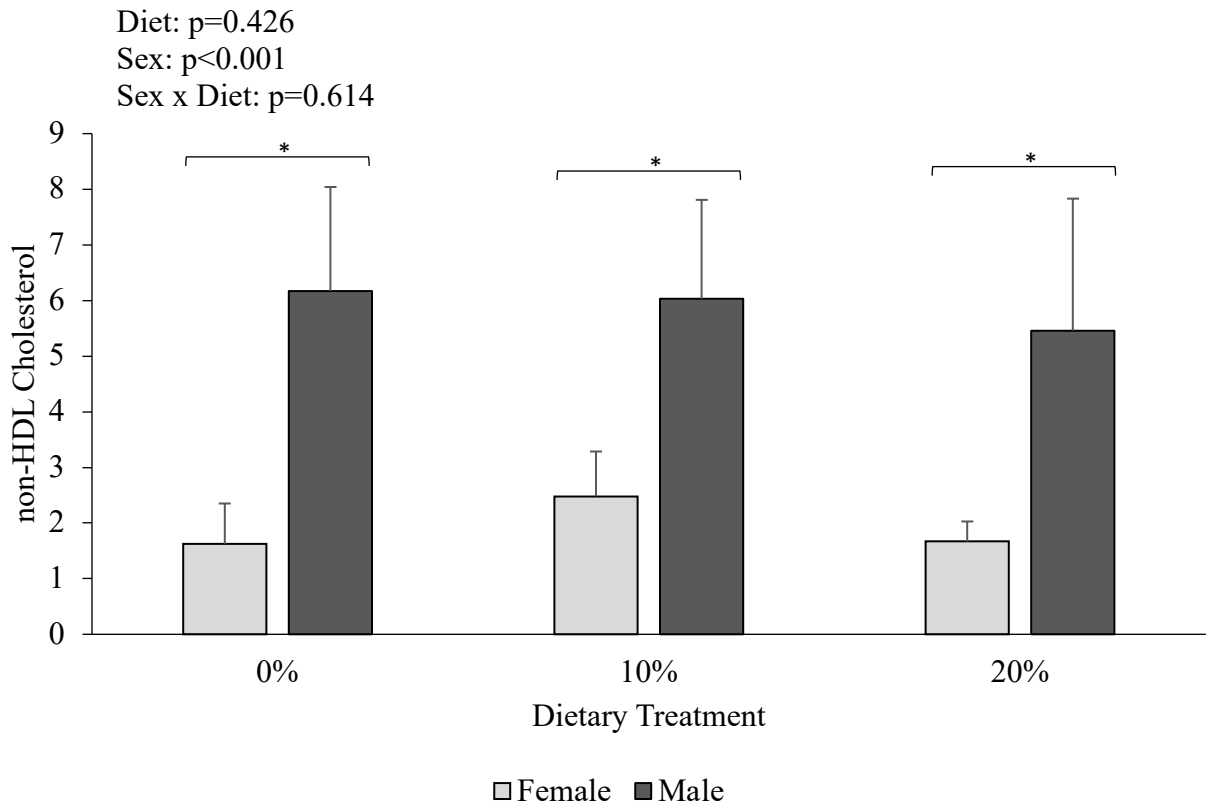


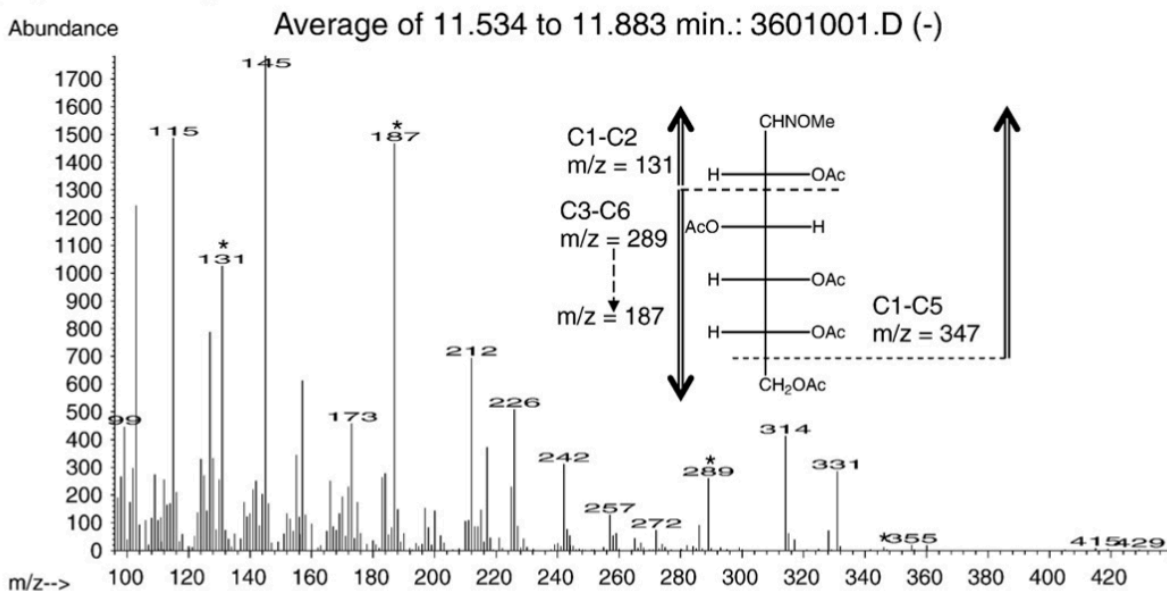
**Figure A.22: Effect of sex by diet on mean plasma non-HDL cholesterol concentrations of FE2 mice**

Bars represent mean  $\pm$  standard deviations in mmol/L. For analysis of plasma non-HDL cholesterol concentrations:  $n=8$  for 0% female, 20% female, 10% male;  $n=9$  for 10% female, 0% male, 20% male. A two-way ANOVA followed by Tukey's Post-hoc test ( $p < 0.05$ ) was used to test for sex by diet effects. Additionally, Student T-Test ( $p < 0.05$ ) was used to test for within diet effects. \* denotes statistical differences ( $p<0.001$ ) in non-HDL cholesterol concentrations between sex within the same dietary treatment.

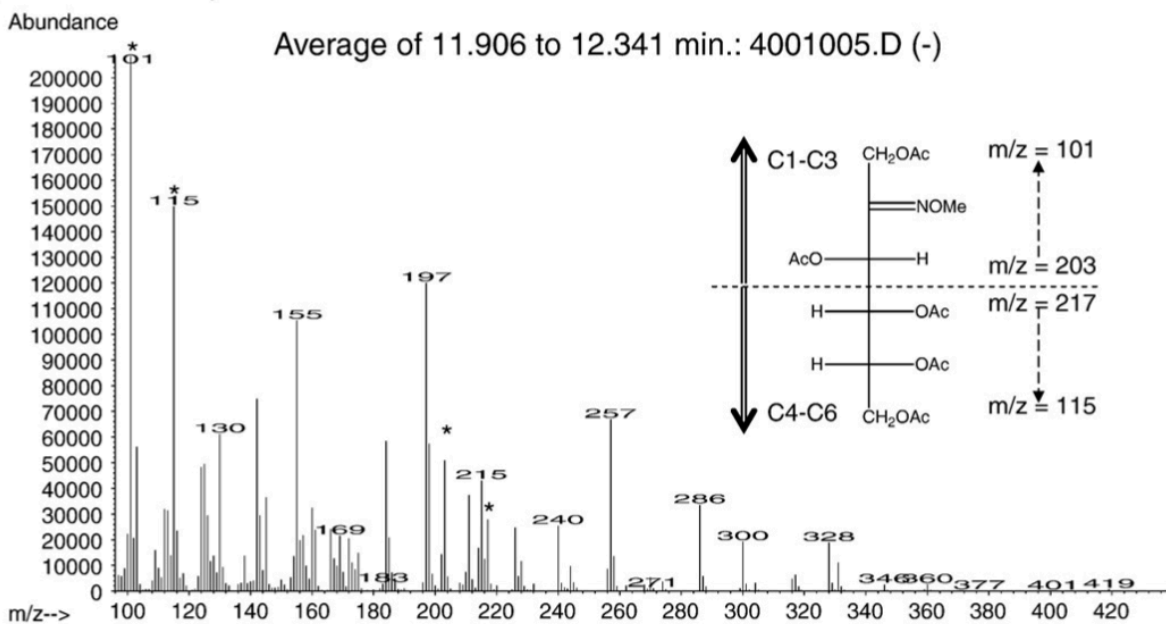
0%, 0% fructose; 10%, 10% fructose; 20%, 20% fructose

**Appendix XIII: Isotopomer analysis of fragments formed by carbon-carbon bond cleavage of D-glucose-MOA and D-fructose-MOAs demonstrated by Wahjudi et al. (Wahjudi et al., 2010)**

**a) D-glucose-MOA EI spectra**



**b) D-fructose-MOA EI spectra**



**Appendix XIV: Mass spectra fragmentation pattern of (A) D-glucose-MOA and (B) D-fructose-MOA as demonstrated by Wahjudi et al. (Wahjudi et al., 2010)**

Methyloxime-peracetate	Fragments observed	Isotopomer <i>m/z</i> values			
		D-Glucose	[1,2- <sup>13</sup> C <sub>2</sub> ] D-glucose	[U- <sup>13</sup> C <sub>6</sub> ] D-glucose	[6- <sup>13</sup> C <sub>1</sub> ] D-glucose
Glucose	C1–C6	<i>m/z</i> = <i>m</i>	<i>m/z</i> = <i>m</i> +2	<i>m/z</i> = <i>m</i> +6	<i>m/z</i> = <i>m</i> +1
	C1–C5	347 ( <i>m</i> )	349 ( <i>m</i> +2)	352 ( <i>m</i> +5)	347 ( <i>m</i> )
	C1–C2	131 ( <i>m</i> )	133 ( <i>m</i> +2)	133 ( <i>m</i> +2)	131 ( <i>m</i> )
	C3–C6	289 ( <i>m</i> )	289 ( <i>m</i> )	293 ( <i>m</i> +4)	290 ( <i>m</i> +1)
Fructose		D-Fructose	[1,2,3- <sup>13</sup> C <sub>3</sub> ] D-fructose	[U- <sup>13</sup> C <sub>6</sub> ] D-fructose	
	C1–C6	<i>m/z</i> = <i>m</i>	<i>m/z</i> = <i>m</i> +3	<i>m/z</i> = <i>m</i> +6	
	C1–C3	101 ( <i>m</i> )	104 ( <i>m</i> +3)	104 ( <i>m</i> +3)	
	C1–C3	203 ( <i>m</i> )	206 ( <i>m</i> +3)	206 ( <i>m</i> +3)	
	C4–C6	115 ( <i>m</i> )	115 ( <i>m</i> )	118 ( <i>m</i> +3)	
	C4–C6	217 ( <i>m</i> )	217 ( <i>m</i> )	220 ( <i>m</i> +3)	